Study of the JAK/STAT signaling pathway in adaptation to therapeutic inhibition in gastrointestinal stromal tumors

Daniel Fernando Pilco Janeta

Study of the JAK/STAT signaling pathway in adaptation to therapeutic inhibition in gastrointestinal stromal tumors

Daniel Fernando Pilco Janeta

Ph.D. Thesis

Universitat Autònoma de Barcelona

VHIO VALL D'HEBRON Instituto de Oncología

Doctoral Program in Medicine

Department of Medicine

Doctoral Thesis:

Study of the JAK/STAT signaling pathway in adaptation to therapeutic inhibition in gastrointestinal stromal tumors

Author:

Daniel Fernando Pilco Janeta, M.D.

Thesis supervisors:

César Serrano García, M.D., Ph.D.

Joan Carles Galcerán, M.D., Ph.D.

Academic tutor:

Josep Tabernero Caturla, M.D., Ph.D.

2023

Universitat Autònoma de Barcelona

VHIO VALL D'HEBRON Instituto de Oncología

DEDICATORIA

A mis abuelos **Manuel Pilco** y **Manuela Janeta**, quienes soñaban con una generación de jóvenes libres mediante el acceso a una educación gratuita, donaron sus tierras y fundaron la primera escuela en una comunidad indígena del Ecuador. Ese sueño se cumplió con uno de sus nietos, que creció junto a ellos y recorrió diferentes latitudes hasta alcanzar el mayor grado académico.

AGRADECIMIENTOS

En estos 4 años he tenido la fortuna y el honor de compartir con muchas personas que me han ayudado a lograr este noble sueño, el de convertirme en médico científico. Han sido años llenos de estudio, trabajo y sacrificios, y para alcanzar esta meta siempre he contado con la mano amiga que me ha permitido completar esta etapa de mi carrera.

En primer lugar, quisiera agradecerle al Dr. **César Serrano** por haberme acogido en su laboratorio del Vall d'Hebron Instituto de Oncología (VHIO) y permitirme desarrollar mi tesis doctoral bajo su mentoría, César siempre recordaré aquel sábado de junio 2018 en Chicago, cuando te pregunté por la posibilidad de hacer el doctorado contigo y amablemente me acompañaste durante todo el proceso, gracias por toda tu ayuda, paciencia y dedicación, espero que nuestra amistad siga fortalecida y mantengamos nuestra relación de amigos igual de cercana y que sepas que siempre estaré agradecido por todo. Al Dr. **Joan Carles**, también agradecerle el haber aceptado ser mi co-director de tesis y haber aportado a mi desarrollo académico. Al Dr. **Josep Tabernero** agradecerle por haber aceptado ser mi tutor de tesis y por haberme brindado todo el apoyo en la realización del presente trabajo.

Al Dr. **Jonathan Fletcher**, por acogerme durante mi último año de tesis en su laboratorio en la Escuela de Medicina de Harvard y enseñarme a tener una perspectiva traslacional, por compartir su enfoque del mundo de la ciencia conmigo, y por brindarme valiosos consejos.

A mis amigos del laboratorio, a **Alfonsi**, por enseñarme tantas cosas y acompañarme en la transición inicial de la clínica al laboratorio, a **David** por esas charlas de bioinformática tan estimulantes, a **Iván** y **Jordi** por estar siempre dispuestos a ayudarme, a **Philipp** por su paciencia y buen humor ante aquellos experimentos que resultasen complejos de llevar a cabo.

A mi Esposa, **Myriam De la Cruz**, mi compañera de vida, con quien voy de la mano alcanzando nuestros sueños comunes.

A mi amado hijo **Daniel Alejandro**, quien acaba de nacer y ya ha cautivado mi corazón por completo. Esta tesis es una muestra de todo el esfuerzo y dedicación que he puesto en mi carrera, y también de todo el amor y compromiso que siento hacia ti como mi hijo. Espero que algún día puedas leerla y sentirte inspirado a perseguir tus propios sueños con la misma pasión que yo he perseguido los míos.

En toda esta etapa, pese a la distancia geográfica, siempre estuvieron a mi lado, mi madre **Rosita Pilco**, quien me ha dado todo y me ha inculcado los valores como la empatía, la disciplina, la pasión por el estudio y a nunca rendirme hasta alcanzar cada sueño. Mis hermanas: **Tatiana**, **Tamialy** y **Daisy**, con los consejos de todas ustedes he llegado hasta aquí y continuaré con afán por el camino ya emprendido.

ABBREVIATIONS

AJCC	American Joint Committee on Cancer
AKT	Akt Murine Thymoma Viral Oncogene Homolog
ATP	Adenosine triphosphate
CD34	Cluster of differentiation 34
CDKN2A	Cyclin Dependent Kinase Inhibitor 2A
CML	Chronic myeloid leukemia
CTCL	cutaneous T-cell lymphoma
DMSO	Dimethyl Sulfoxide
EMA	European Medicines Agency
EUS	Endoscopic ultrasound
EUS	Endoscopic ultrasound
FBS	Fetal Bovine Serum South America
FDR	False discovery rate
FGF	Fibroblast growth factor
FGFR	Fibroblast growth factor receptor
FNA	Fine needle aspiration
GIST	Gastrointestinal Stromal Tumor
GSEA	Gene set enrichment analysis
HBSS	Hank’s balanced salts solution
HBSS	Hank’s balanced salts solution

HPFs	high-power fields
ICC	Interstitial cells of Cajal
IM	Imatinib
IMDM	Iscove's modified Dulbecco's Medium
MAPK	Mitogen-activated protein kinase
MDM2	Mouse double minute 2 homolog
mPFS	median progression-free survival
mTOR	Mammalian target of rapamycin
NGS	Next generation sequencing
ORR	overall response rate
p-AKT	Phoshorylated Akt
PCR	Polymerase chain reaction
PDGFRA	Platelet-derived growth factor receptor alpha
PDK1	Pyruvate Dehydrogenase Kinase 1
PFS	Progression-free survival
PI3K	Phosphatidylinositol 3-kinase
PIAS	Protein inhibitors of activated STAT proteins
PIAS	Protein inhibitors of activated STAT proteins
PIP2	Phosphatidylinositol 4,5-bisphosphate
PIP3	phosphatidylinositol (3,4,5)-trisphosphate
PLCG1	Phospholipase C gamma 1
pS6	Ribosomal protein phosphor serine 235/236

PSEA	Protein set enrichment analysis
PTEN	Phosphatase and tensin homolog
PTMs	post-translational modifications
PTMs	Post-translational modifications
RNA-seq	RNA sequencing
RTK	Receptor tyrosine kinase
SCF	Stem cell factor
SCF	stem cell factor
SH2	Src homology 2
shRNA	Short hairpin RNA
SOCS	Suppressors of cytokine signaling
SOCS	Suppressors of cytokine signaling
STAT1	Signal transducer and activator of transcription 1
STAT3	Signal transducer and activator of transcription 3
STS	Soft tissue sarcoma
SU	Sunitinib
TGFB	Transforming growth factor-beta
TKI	Tyrosine kinase inhibitor
TP53	Tumor protein 53
UICC	Union for International Cancer Control
VEGF	Vascular endothelial growth factor
VEGFR	Vascular endothelial growth factor receptor

Table of Contents

SUMMARY

GIST relies on KIT/PDGFRA signaling for tumor growth and proliferation, and therapeutic targeting of these kinases with first-line imatinib or related tyrosine kinases inhibitors (TKI) significantly improves GIST patients' outcomes. However, most patients eventually progress to these therapies due to the polyclonal expansion of subpopulations containing secondary resistance mutations in KIT. Therefore, the development of novel therapeutic strategies in TKI-resistant GIST is an unmet clinical need. PI3K/mTOR signaling pathway is critical in GIST biology throughout the entire course of the disease, including TKI-resistant GIST. Nevertheless, therapeutic inhibition of the PI3K/mTOR pathway in GIST has only shown modest clinical benefit. Therefore, we hypothesize that an unbiased assessment of the cellular adaptations to the therapeutic inhibition of the PI3K/mTOR pathway in GIST will pinpoint vulnerabilities that can be exploited therapeutically.

To this end, we used three clinically representative models of GIST, two imatinib-sensitive and one imatinib-resistant. In this thesis we first demonstrated that after the expected antiproliferative effect of PI3K/mTOR suppression decreases over time due to the activation of JAK/STAT pathway. We further dissected essential targets in the JAK/STAT pathway and uncovered transcriptomic and proteomic changes involving FGFR1-mediated activation of JAK/STAT pathway in response to PI3K/mTOR inhibition. Finally, we explored combination strategies to overcome this therapeutic adaptation to maximize the activity of PI3K/mTOR inhibition in GIST.

RESUMEN

Los tumores del estroma gastrointestinal (GIST) se basa en la señalización de KIT/PDGFRA para el crecimiento y la proliferación tumoral, y el uso de terapias dirigidas como tratamiento de primera línea contra estas cinasas como imatinib o los inhibidores de tirosina cinasas (TKI) relacionados, mejora significativamente los resultados de los pacientes con GIST. Sin embargo, la mayoría de los pacientes eventualmente progresan a estas terapias debido a la expansión policlonal de subpoblaciones que contienen mutaciones de resistencia secundaria en KIT. Por lo tanto, existe una necesidad clínica no cubierta para desarrollar nuevas estrategias terapéuticas en los GIST resistentes a TKI. La vía de señalización de PI3K/mTOR es fundamental en la biología de los GIST durante todo el curso de la enfermedad, incluidos los GIST resistentes a los inhibidores de la tirosina quinasa. Sin embargo, la inhibición terapéutica de la vía PI3K/mTOR en GIST solo ha demostrado un modesto beneficio clínico. Por lo tanto, planteamos la hipótesis de que una evaluación imparcial de las adaptaciones celulares a la inhibición terapéutica de la vía PI3K/mTOR en GIST podría identificar vulnerabilidades que puedan ser explotadas terapéuticamente.

Para ello, utilizamos tres modelos clínicamente representativos de GIST, dos sensibles a imatinib y uno resistente a imatinib. En esta tesis, primero demostramos que después del efecto antiproliferativo esperado de PI3K/mTOR, la supresión disminuye con el tiempo debido a la activación de la vía JAK/STAT. Además, identificamos dianas esenciales en la vía JAK/STAT y descubrimos cambios transcriptómicos y proteómicos relacionados con la activación de la vía JAK/STAT mediada por FGFR1 en respuesta a la inhibición de PI3K/mTOR. Finalmente, exploramos estrategias de combinación para superar esta adaptación terapéutica y maximizar la actividad de inhibición de la vía de PI3K/mTOR en GIST.

INTRODUCTION

1. INTRODUCTION

The Gastrointestinal Stromal Tumor (GIST) is a rare type of cancer that affects the gastrointestinal tract or nearby structures within the abdomen. GIST is a histological subtype of soft tissue sarcoma (STS). The medical term "sarcoma" is derived from the Ancient Greek and literally means fleshy tumor (sarcoma) (oma). Sarcomas are rare malignant tumors that arise from mesenchymal, non-epithelial tissues derived from the embryonic mesodermal layer (1).

The term "stromal tumors" was first described by Mazur and Clark (2) in 1983 and Schaldenbrand and Appleman in 1984 (3).

GISTs were defined as a distinct subtype of sarcoma in the 1990s, thanks to the advent of different immunohistochemical markers, mainly CD34 and CD117 (KIT), which allowed a better molecular characterization of this disease. Subsequently, the expression of CD34 and KIT in these tumors was evaluated and compared with the expression in the interstitial cells of Cajal (ICC), the intestinal pacemaker cells located in the circular muscle layer of the intestine. The discovery of the ICC, also co-expressing KIT and CD34, led to the conclusion that these ICC cells correspond to the origin of GIST (4). The reverse transcriptase-polymerase chain reaction of *KIT* clones demonstrated activation mutations in the juxtamembrane domain of the *KIT* gene (in exons 9, 11, 13, or 17), resulting in constitutive activation of this receptor tyrosine kinase (RTK).

Approximately 85% of GIST are associated with mutations in KIT, which is an oncogenic driver located as a transmembrane receptor for a growth factor called stem cell factor (SCF).

Oncogenic mutations in KIT lead to SCF-independent activation, followed by constitutive activation of downstream KIT signaling pathways, which in turn trigger cell division and proliferation.

The discovery of KIT in 1998 by Hirota and colleagues (5) as an oncogenic driver provided a therapeutic target for the treatment of GIST. Heinrich and colleagues (6) found shortly thereafter mutations in the platelet-derived growth factor receptor alpha (*PDGFRA*) gene as alternative pathogenesis in GIST without *KIT* gene mutation.

In 2001, the first patient with metastatic GIST refractory to multiple types of therapy was reported to be treated with imatinib, which is a small-molecule tyrosine kinase inhibitor (TKI) with highly specific and potent activity against the KIT RTK. This treatment induced an early, rapid, and sustained response (7), which was also supported by preclinical data (8,9). This case provided proof of principle that targeted inhibition of KIT with imatinib was associated with a clinical improvement in the disease and allowed a better understanding of GIST biology and therapeutics. Afterward, different phase I, II and III clinical trials evaluating the efficacy of imatinib have achieved promising results, marking a significant milestone in the development of targeted therapies for GIST. These trials demonstrated imatinib's safety and effectiveness in treating GIST patients. Nearly 70% of the patients achieved disease control, with a median progression-free survival (PFS) of 20 to 24 months (10–12).

These findings demonstrate the potential for this treatment to provide long-term benefits for GIST patients. The remarkable therapeutic efficacy of imatinib in GIST patients coupled with accurate diagnoses using the expression of KIT resulted in the subsequent approval of imatinib in this indication by the Food and Drug Administration (FDA) in February 2002 (10). In 2006, Sunitinib, a multi-target TKI with activity against KIT, PDGFR, vascular endothelial growth factor (VEGF) receptor (VEGFR), and FLT-1/KDR, also received FDA approval for the treatment of patients who are refractory or intolerant to imatinib (13).

In 2013, the DFA approved Regorafenib, a multikinase inhibitor that blocks the activity of multiple protein kinases, including those involved in the regulation of tumor angiogenesis (VEGFR-1, VEGFR -2, and VEGFR -3, and TIE2), oncogenesis (KIT, RET, RAF-1, BRAF, and BRAFV600E), and the tumor microenvironment (PDGFR and FGFR), Demetri et al (14), demonstrated that Regorafenib can provide a significant improvement in PFS compared with placebo in patients with metastatic GIST after progression on standard treatments (imatinib or sunitinib).

In the last years, we have faced significant advancements in drug development against GIST. Ripretinib and avapritinib are two drugs recently approved by the FDA and the European Medicines Agency (EMA) as targeted therapy to treat GIST patients. On the one hand, ripretinib is a switch control inhibitor with broad anti-KIT/PDGFRA activity. It has been approved as a ≥4th-line treatment in GIST after progression to all standard therapies (15). Avapritinib, on the other hand, is a highly specific type I tyrosine kinase inhibitor (TKI) against the multi-resistant PDGFRA D842V mutation (16). This approval

marked an important landmark in the field of GIST treatment providing a much-needed therapeutic option for GIST patients.

Over the last two decades, significant new insights have been made regarding of our understanding of the pathogenesis and treatment of GIST, since throughout this time we have managed to the identify the cell of origin, determine a targeted genetic alteration, and discover different drugs to treat patients with GIST. Future advances require an understanding of the molecular biology when the approved TKIs lose their effectiveness, opening opportunities for the search for new treatments.

1.1 Epidemiology and clinical- features of GIST

1.1.1 Epidemiology

GISTs are the most common mesenchymal neoplasms affecting the gastrointestinal tract, mesenchymal tumors represent about 1% of primary gastrointestinal cancers (17–19). GISTs are rare tumors, with an estimated unadjusted incidence of about 1-2/100.000 cases per year (20,21).

It has been estimated that there are 3.300 to 6.000 new GIST cases per year in the United States (22) and in Spain the annual incidence of GIST is 1.24 cases/100.000 inhabitants/year (23). It has an equally distribution across all geographic and ethnic groups and men and women are equally affected. Most patients present between the ages of 50 and 80 (24).

1.1.2 Clinical features

GIST occur frequently in the stomach (60%), small intestine (25%), rectum (5%) and esophagus (3%) (25), but it can be diagnosed anywhere along the GI tract (26,27) Figure 1.

There are no clinical nor pathognomonic signs or symptoms suggestive of GIST diagnosis, and the clinical presentation of these patients varies depending on the anatomic location of the tumor together with tumor size and aggressiveness. The most common presentation of GIST is GI bleeding, which may be acute, presenting as hematemesis or melena, or chronic and results in anemia; tumor rupture can cause an acute abdomen. (28,29). Other clinical symptoms include fatigue, dysphagia, satiety (22).

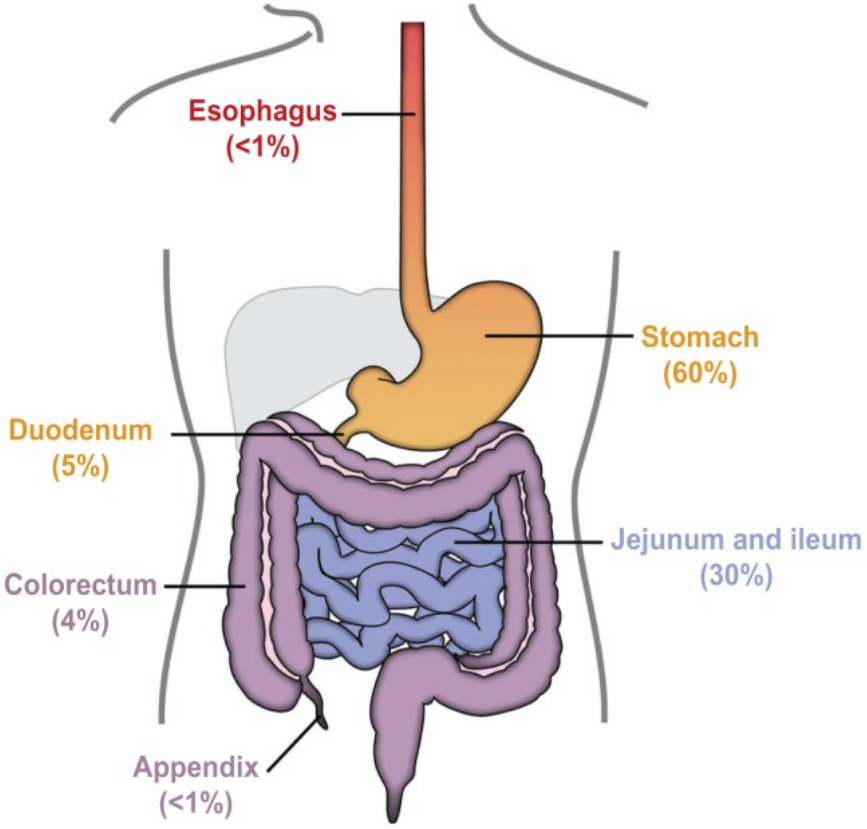

Figure 1. Primary GIST anatomic locations and relative frequencies (30).

1.2 Diagnosis

The standard approach for a definitive diagnosis of GIST requires tissue acquisition via endoscopic ultrasound (EUS)-guided FNA (31). EUS-guided FNA (EUS-FNA) biopsy of primary site is preferred over percutaneous biopsy due to the risk of tumor hemorrhage and intra-abdominal tumor dissemination. Percutaneous image-guided biopsy may be appropriate for confirmation of metastatic disease.

Pathologically, the diagnosis of GIST relies on morphology, immunohistochemical staining for KIT, DOG1, and/or CD34 and molecular genetic testing to identify *KIT* and/or *PDGFRA* mutations are useful in the diagnosis of GIST (32).

Macroscopic features

GISTs are well-circumscribed tumors most commonly arising in the muscularis propria of the GI tract. The tumor size varies; for high-risk GIST, the median tumor size is 8.9 cm (33). These tumors have a fleshy pink or tan-white cut surface with hemorrhagic foci, central cystic degenerative changes, or necrosis.

Microscopic features

The size of GISTs varies from 1 to 40 cm (mean ~5 cm). Microscopically, GISTs are composed mostly by spindle cells (~70%), but they can have an epithelioid (20%) or mixed morphology (10%). In the spindle cell pattern (Fig. 2A) the cells are elongated and arranged in short fascicles and whorls.

In the epithelioid pattern (Fig. 2B) the cells are round with eosinophilic cytoplasm. In some cases, multinucleated cells may also be present (Fig. 2C). In both patterns stromal modifications can be seen, such as perivascular hyalinization, and hyaline material that seem to create a trabecular pattern. Small bowel GISTs may contain skeinoid fibers (eosinophilic aggregates of extracellular collagen) (34).

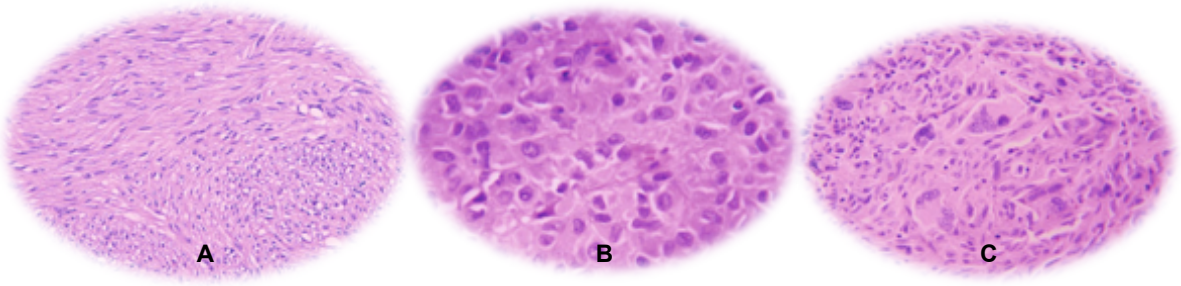

Figure 2. Hematoxylin-eosin-stained sections. **A** GIST characterized by spindle cells with ovoid or elongated nuclei and with mildly eosinophilic fibrillar cytoplasm. A number of intracytoplasmic vacuoles can be seen. The cells are mostly monomorphic, with only mild atypia. **B** GIST with rounded epithelioid cells and with eosinophilic cytoplasm. **C** GIST with large pleomorphic cells (35).

Pathology report include anatomic location, size, and an accurate assessment of the mitotic rate measured in the most proliferative area of the tumor and reported as the number of mitoses in 50 high-power fields (HPFs) (equivalent to 5 mm^2 of tissue).

For an accurate diagnosis of GIST, it is essential that morphological examination must be complemented with immunohistochemical staining for the KIT receptor (CD117). Approximately 95% of GISTs stain positive for KIT, and the expression pattern is typically cytoplasmic, with membranous or perinuclear expression seen less frequently (17,36). The presence of KIT expression leading to the diagnosis of GIST has

therapeutic implications, making it a valuable biomarker for diagnosis and treatment. Other significant immunohistochemical markers include CD34, a protein expressed on mesenchymal cells and identified as positive in up to 70% of GISTs (37,38). More recently, anoctamin 1 (DOG1) is part of the routine panel of immunohistochemistry that allows a more accurate diagnosis of GIST. DOG1 is a calcium-activated chloride channel protein encoded by the ANO1 gene. It is an essential component of the intercellular calcium signaling pathway, which plays a crucial role in several physiological processes, such as nerve conduction and smooth muscle contraction. DOG1 is essential for the functioning of ICC. More than 95% of GISTs show diffuse cytoplasmic and membranous expression of DOG1. DOG1 has been identified as a valuable marker to confirm GIST KIT negatives, as it is present in most cases. (39–41) . Other markers less commonly expressed include smooth muscle actin (25%), and desmin (less than 5%) (29).

Molecular analysis of GIST is crucial to identify mutations in the *KIT* and *PDGFRA* genes. It is generally performed through polymerase chain reaction (PCR) or targeted exome next-generation sequencing (NGS). KIT and PDGFRA mutational analysis add useful prognostic information and determines the most appropriate type and dose of targeted therapy. In addition, identifying KIT and PDGFRA mutations can help in cases of GIST negative for KIT and DOG1 and dedifferentiated GIST that are difficult to diagnose (4,17,6).

1.3 Staging evaluation of risk of progression

The American Joint Committee on Cancer (AJCC)–Union for International Cancer Control (UICC) established TNM staging criteria for the GIST staging system but it is rarely used, given the natural history of GISTs. On the contrary, several risk classifications have been proposed to assess the risk of relapse of a localized disease. The spectrum of clinical/biological behavior of GIST ranges from “no risk” to “high risk” clinically aggressive tumors associated with widespread dissemination. Most GIST have low mitotic activity. Risk stratification is performed by counting the number of mitoses in a 5 mm^2 area, which correlates to a variable number of high-power fields depending on the microscope used. The mitotic count is incorporated with primary tumor site and tumor size to determine risk of disease progression, based on data obtained from two large studies (Table 1) (29).

Table 1. Prediction of risk according to size, mitotic index, and location of the primary tumor (NIH-Fletcher criteria for GIST risk assessment).

Tumor size (cm)	Mitotic Index (x 50 HPF)	Primary Tumor Locations			
		Stomach	Duodenum	Jejunum / ileus	Straight
≤ 2	≤ 5	Very low	Very low	Very low	Very low
> 2 ≤ 5		Very low	Low	Low	Low
> 5 ≤ 10		Low	Intermediate	Insufficient Data	Insufficient Data
> 10		Intermediate	High	High	High
≤ 2	> 5	-	High		High
> 2 ≤ 5		Intermediate	High	High	High
> 5 ≤ 10		High	High	High	High
> 10		High	High	High	High

1.4. Treatment of GIST

1.4.1 Surgery

In GIST, surgery is indicated as the initial therapy in patients with localized and non-metastatic disease, while it requires to be discussed in patient-by-patient basis and for locally advanced and metastatic disease. The goal of this type of treatment is complete macroscopic resection, with an intact pseudocapsule and negative microscopic

margins (42). This primary resection is possible in 86% of cases (25). Since the lymph node metastasis are rare in GIST, it is not necessary to perform lymph node dissection if it is not clinically affected.

1.4.2 Targeted Therapy

TKIs have revolutionized the management of GIST. Gain-of-function mutations in KIT are the key oncogenic driver event (4), present in over 80% of GISTs and leading to constitutive, ligand-independent activation of the KIT receptor and its downstream pathways, ultimately increasing cell proliferation and inhibiting apoptosis (43). Since KIT activation occurs in the majority of cases of GIST, KIT inhibition has emerged as the primary therapeutic modality along with surgery for the treatment of GIST (42). Currently, there are five drugs approved by the FDA to inhibit KIT: imatinib, sunitinib, regorafenib, avapritinib and ripretinib, which are the standard-of-care treatment options for GIST patients (Table 2).

Table 2. FDA- and EMA-Approved Tyrosine Kinase Inhibitors for unresectable or metastatic GIST (44).

TKI	Mutation targeted	Treatment line	ORR (%)	Stable disease at 12 weeks (%)	mPFS (months)	Reference
Imatinib	KIT/PDGFR	First	68.1	15.6	24.0	Demetri et al (10)
Sunitinib	KIT/PDGFR	Second	6.8	53.0	5.6	Demetri et al (13)
Regorafenib	KIT/PDGFR	Third	4.5	53.0	4.8	Demetri et al (14)
Ripretinib	KIT/PDGFR	Fourth or more	9.4	47.0	6.3	Blay et al (15)
Avapritinib	PDGFRA D842V	Any	91.0	98.0	34.0*	Heinrich et al (16)

1.4.2.1 Imatinib

Imatinib mesylate is a TKI that revolutionized the treatment of GIST in 2002. Imatinib exerts its action by targeting the BCR-ABL oncoproteins and other protein kinases, including KIT and PDGFR (7).

The efficacy of imatinib in GIST was evaluated in 147 metastatic patients in a clinical trial conducted by Demetri and colleagues in 2002. Results demonstrated that 53.7% of patients had partial responses to treatment and 27.9% had stable disease (10). These results provided evidence of this treatment's potential efficacy in managing GIST. It is approved as a first-line treatment for unresectable, metastatic, or recurrent GIST. Median overall survival rates have shifted from less than 12 months to more than 5 years since the advent of imatinib therapy (12).

Studies have shown that a 400 mg/day starting dose of imatinib is safe and effective in inducing a response (9). Dose escalation to 800 mg/d is a reasonable option for patients progressing on 400 mg/d (45).

Imatinib could also be administered as a neoadjuvant treatment to reduce the tumor volume for patients with large primary GIST that cannot be removed without the risk of unacceptable morbidity (46).

While surgery is the primary treatment option for GIST, it does not guarantee a disease control. To ensure optimal patient outcomes, adjuvant treatment with imatinib is recommended for at least three years for those patients with high-risk disease.

1.4.2.2 Sunitinib

Sunitinib is a multitargeted TKI inhibitor that effectively targets KIT and PDGFRA, among several other kinases, and induce objective responses and control progressive disease in patients with imatinib-resistant GIST. Sunitinib has been proven effective against GIST, with a median progression-free survival (mPFS) of 5.6 months and an overall response rate (ORR) of 6.8%. In January 2006, sunitinib received FDA approval for the treatment of GIST after disease progression on or intolerance to imatinib. Sunitinib has also been found to be more effective in SDH-deficient GIST, providing a potential alternative for patients lacking mutations in KIT or PDGFRA (13,47).

1.4.2.3 Regorafenib

Regorafenib is a multi-kinase inhibitor with potential activity targeting KIT, PDGFR, and VEGFR. In a randomized clinical trial, it was seen that the median overall survival rate with regorafenib was 4.8 months, which was significantly longer than the 0.9 months in the placebo group. Furthermore, the ORR for regorafenib was 4.5%, confirming that regorafenib is an effective therapeutic option for GIST patients. In light of these results, the FDA has approved for the treatment of patients with locally advanced, unresectable, or metastatic GIST previously treated with imatinib and sunitinib (42).

1.4.2.4 Ripretinib

Ripretinib (DCC-2618) is an innovative type II TKI specifically designed to target a broad spectrum of primary and secondary drug-resistant mutations in GIST. It works by binding to both: the switch pocket and the activation loop of KIT and PDGFRA, locking them in an inactive conformation. The results of the INVICTUS study, a double-blind, randomized, placebo-controlled, phase III trial, were recently published with remarkable outcomes. With a median PFS rate of 6.3 months and the objective response rate of 9.4%, ripretinib achieved unprecedented success in GIST patients, leading to FDA approval in the fourth line of treatment and beyond for advanced or metastatic GIST (15).

1.4.2.5 Avapritinib

Avapritinib (BLU-285) is a highly potent and selective type I kinase inhibitor of KIT and PDGFRA that has demonstrated promising activity in the treatment of GIST patients harboring the PDGFRA D842V mutation. The phase I NAVIGATOR trial evaluated the safety and efficacy of avapritinib as a single-agent therapy for advanced GIST patients, showing remarkable activity, with an overall response rate of 88%, a median duration of response (mDOR) of 27.6 months and a 12 months PFS rate of 91%. Due to the significant results achieved, avapritinib has been approved by the FDA for metastatic PDGFRA D842V mutant GIST treatment, establishing the first successful TKI in this subset of patients with PDGFRA D842V mutation (16,48).

1.4.2.6 Other TKIs

The use of other TKIs with KIT/PDGFRA inhibitory activity has been widely tested in advanced and metastatic gastrointestinal stromal tumors, but without regulatory approval for this indication (Table 3). These drugs have been shown to reduce tumor size, slow down progression and improve overall survival in patients with GISTs. However, due to the lack of regulatory approval for this indication, further studies are necessary to properly assess their safety and efficacy in the treatment of GISTs.

Table 3: Tyrosine kinase inhibitors with KIT/PDGFRA inhibitory activity tested in advanced and metastatic gastrointestinal stromal tumors, but without regulatory approval for this indication (44).

Drug	Clinical Trial	Setting Treatment Line	ORR (%)	mPFS (mo)	Phase
Avapritinib	Kang (2021)	Third/fourth	17	4.2	III-R
Cabozantinib	Schöffski (2020)	Third	14	5.5	II
Dasatinib	Schuetze (2018)	Second or more	4	2.9	II
Dovitinib	Kang (2013)	Third or more	3	3.6	II
	Joensuu (2017)	Third or more	5	4.6	II
Masitinib	Adenis (2014)	Second	NA	3.7	II
Nilotinib	Montemurro (2009)	Third or more	10	2.8	II
	Sawaki (2011)	Third	3	3.7	II
	Cauchi (2012)	Third or more	0	2.0	II
	Reichardt (2012)	Third	< 1	3.6	III-R
Pazopanib	Ganjoo (2014)	Second or more	0	1.9	II
	Mir (2016)	Second or more	0	3.4	II-R
	Eriksson (2021)	Third/fourth	3	4.5	II

Ponatinib	George (2022)	Second or more	8	4.3	II
Sorafenib	Kindler (2011)	Second or more	13	5.2	II
	Park (2012)	Third or more	13	4.9	II

1.5 Molecular Biology of GIST

GISTs most likely originate from the ICC (4,49). ICC are pacemaker-like intermediates between the GI autonomic nervous system and smooth muscle cells regulating GI motility and autonomic nerve function (50). ICC or their stem cell-like precursors can differentiate into smooth muscle cells if KIT signaling is disrupted (51).

A large majority of GISTs (95%) express KIT receptor tyrosine kinase, which is expressed by the ICCs (22). Approximately 80% of GISTs have a mutation in the gene encoding the KIT receptor tyrosine kinase; another 5% to 10% of GISTs have a mutation in the gene encoding the related PDGFRA receptor tyrosine kinase (6,36). About 10% to 15% of GISTs have no detectable KIT or PDGFRA mutations (wild-type GIST).

Gain-of-function mutations in receptor tyrosine kinases KIT or PDGFRA are the main drivers of GIST survival and proliferation. KIT and PDGFRA mutations are mutually exclusive. Most of the primary KIT mutations occur in the juxtamembrane domain encoded by *KIT* exon 11 and some are detected in the extracellular domain encoded by exon 9 (52). And less frequently KIT mutations have also been identified in the tyrosine kinase domain (exon 13 and exon 17) (53). The majority of the PDGFRA mutations affect exon 18 in the tyrosine kinase domain 2. Few mutations also occur in exon 12 (juxtamembrane domain) and exon 14 (tyrosine kinase domain 1), although

they are rare (54). *KIT* exon 11 mutations are most common in GISTs of all sites, whereas *KIT* exon 9 mutations are specific for intestinal GISTs and PDGFRA exon 18 mutations are common in gastric GISTs (52) (Figure 3).

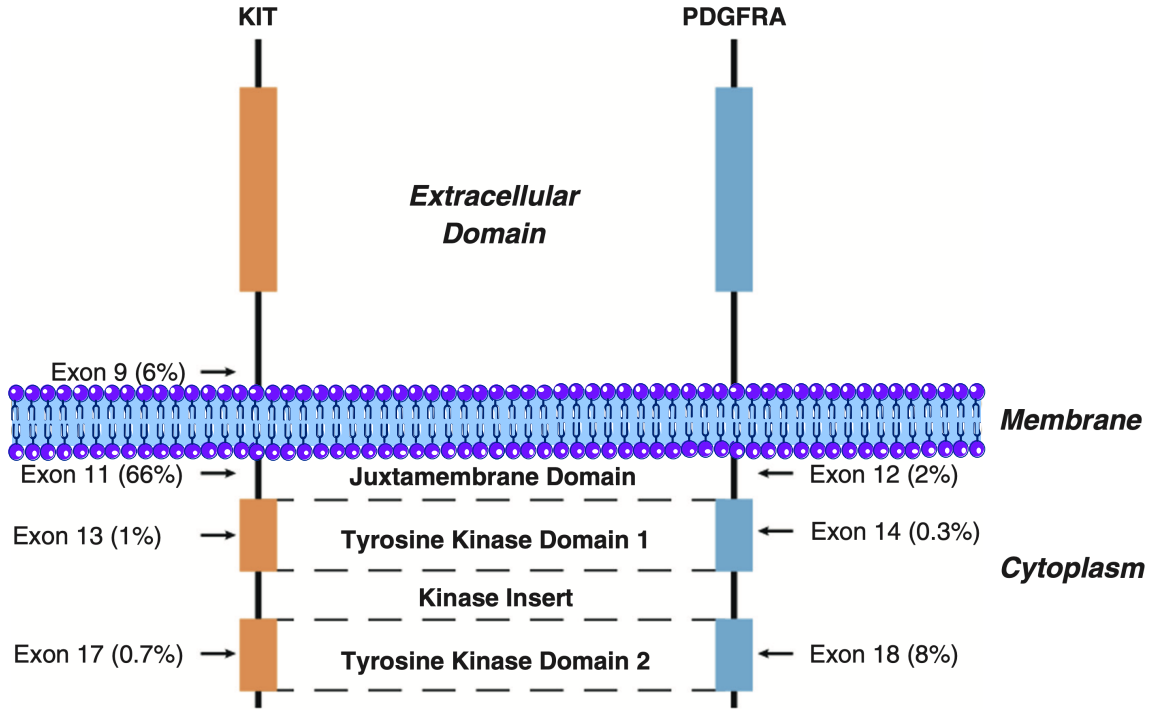

Figure 3. Distribution of mutations in GIST prior to treatment with systemic therapy. Schematic of KIT and PDGFRA showing the relative percentage of mutations in various exons and domains present in primary GIST (55)

Constitutive activation of any of these receptor tyrosine kinases plays a central role in the pathogenesis of GIST (4,6). The proper identification of GIST with genotyping is very important because of the availability of specific, molecular-targeted therapy with KIT/PDGFRA tyrosine kinase inhibitors (TKI), such as imatinib mesylate (13,14,56).

Primary and Secondary Resistance

Five small molecule inhibitors against KIT and PDGFRA currently hold regulatory approval: imatinib, sunitinib, regorafenib, ripretinib, and avapritinib. While imatinib is the first-line therapy for unresectable and/or metastatic GIST, sunitinib is used for patients with progression on imatinib, and regorafenib and ripretinib as third- and fourth-line of treatment, respectively. Despite the success of imatinib with the vast majority of KIT/PDGFRA-mutant GIST, certain molecular variants show little or no response to imatinib. Treatment resistance against KIT and PDGFRA inhibitors like imatinib is classified into primary and secondary.

Primary resistance: is defined as disease progression within the first six months after initiating the therapy. Approximately 10% of GIST patients are reported to have primary resistance. Different clinical trials have identified a strong correlation between genotyping and resistance to imatinib. Specifically, the probability of primary resistance to imatinib in *KIT* exon 11, *KIT* exon 9, and wild-type GISTs is 5%, 16%, and 23%, respectively (57,58)

Additionally, a group of GISTs with PDGFRA exon 18 mutations, particularly the D842V substitution being the most common alteration, involves complete resistance to imatinib.

Secondary resistance: it is established for those GIST patients who acquired resistance after an initial benefit from imatinib of at least more than six months (59). Unfortunately, 85-90% of these patients will eventually become resistant to the treatment, usually within the first three years. It is established that acquired mutations

in KIT or PDGFRA account for most secondary resistance, and these mutations commonly occur in the same gene and allele as the primary oncogenic driver mutation (60–63).

Secondary mutations occurring in the KIT kinase domain are distributed in exons 13 (39%) and 14 (11%) (correspond to the ATP binding domain) and exons 17 and 18 (41%) (correspond to the activation loop domains). Mutations in these exons prevent drug binding to the receptor, thereby conferring resistance (64). These secondary mutations are responsible for the resistance to tyrosine kinase inhibitors in 90% of cases (65).

Other secondary resistance or adaptive mechanisms have been described and involve the fibroblast growth factor receptor (FGFR) signaling pathway (66). In particular, FGF2 is overexpressed in imatinib-resistant GIST cells and imatinib-resistant GIST tumor samples (67,68). Furthermore, in the complex crosstalk between tyrosine kinases, the interaction of FGF2 with FGFR1 and FGFR3 restored MAPK signaling during imatinib treatment (68).

Other molecular alterations in GIST tumor progression or resistance include PI3K/mTOR and RAS/MAPK pathways that are important for the activity of KIT, regardless of the type of primary and secondary mutations. Both pathways are involved in KIT downstream signaling interacting directly with PI3K and GRB2 signaling mediators; Imatinib resistance can be produced by activating the PI3K/mTOR pathway, which is an essential pathway for GIST proliferation and survival

(69–71) . Furthermore, the RAS/MAPK pathway is a key regulator of cell growth and survival. Dysregulation of this pathway, through mutations in RAS and RAF or inactivation of NF1, can replace the KIT-initiated oncogenesis serving as tumor stimulators or fortifying resistance to imatinib or other TKIs (72–74).

1.6 PI3K/AKT/mTOR pathway in GIST

The PI3K/mTOR pathway is a critical signaling pathway that is widely dysregulated in cancer. It can be disrupted through various mechanisms, ranging from loss or inactivation of the tumor suppressor PTEN to mutation or amplification of PI3K, as well as oncogenic activation of tyrosine kinase upstream growth factor receptors and/or PI3K downstream oncogenes that overall promote cell proliferation, survival and tumorigenesis (75–77).

The significance of the constitutive activation of KIT is explained by the biological relevance that it has in GIST for the activity of the signaling pathways dependent on KIT. KIT activation leads to PI3K/mTOR pathway constitutive signaling (Figure 4) (55). PI3K is directly activated by KIT, which converts PIP2 into PIP3, leading the binding of PDK1 and AKT kinases to the cell membrane. This process results in the activation of GSK-3B, mTOR, S6K and other effectors, and leads to cell survival, increased protein synthesis and translation control (70,71).

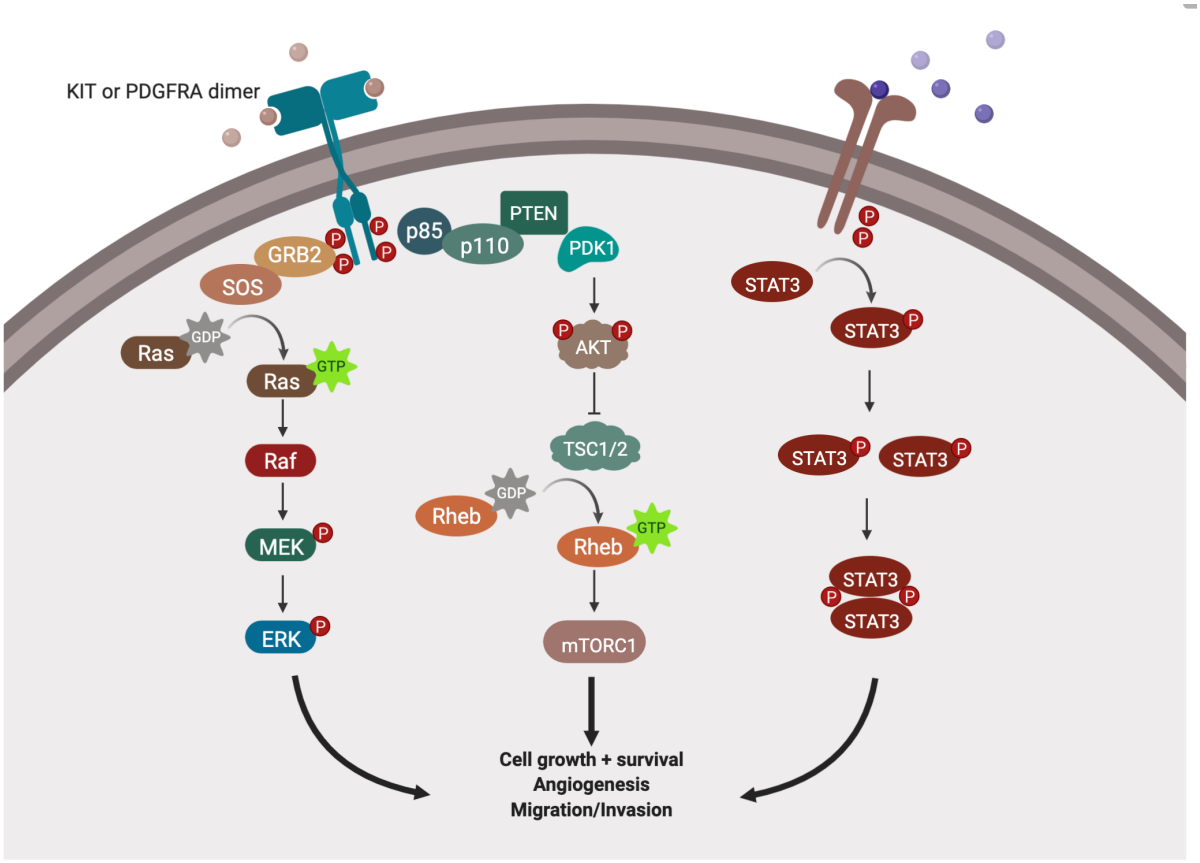

Figure 4. Signaling in KIT/PDGFRA-mutated and WT GIST (39). Molecular triggers and intracellular pathways involved in GIST pathogenesis. GISTs can hinge upon alterations of one of the following: KIT, PDGFRA, neurofibromin, BRAF or SDH. Additionally, exceptional defects of RAS or phosphatidylinositol 3-Kinase (PIK3CA) have been signaled in GISTs, although together with one of the other "classical" triggers. In the figure, KIT and PDGFRA activation initiate a downstream signaling involving multiple pathways: RAS/RAF/MEK/ERK (MAPK) (left); PI3K/AKT/mTOR (center) and JAK/STAT3 (right), stimulating oncogenic gene transcription or protein synthesis. In NF1-associated GISTs, tumoral inactivation of the WT neurofibromin impairs its RAS inhibiting effect, resulting in the activation of MAPK cascade downstream to KIT and PDGFRA. Created with BioRender.

The addiction that GIST has to the oncogenic signaling of KIT and consequently, to the pathways activated by KIT, makes KIT-downstream pathways an attractive target to investigate novel therapeutic strategies. Evaluations using *in-vitro* and *in-vivo* GIST models, as well as human GIST clinical specimens, demonstrate that PI3K/mTOR is

an essential oncogenic signaling pathway in GIST (69,70). This pathway is constitutively activated by KIT (or oncogenic PDGFRA), thereby increasing cell proliferation and survival (69,78,79). Targeted PI3K/mTOR pathway inhibition in cancer has been evaluated in various clinical trials and has shown clinical success in hormone-dependent breast cancer and certain hematological neoplasms, thus obtaining approval in these indications. FDA-approved anti PI3K agents include Alpelisib, a selective inhibitor class I PI3K p110α that is indicated in combination with Fulvestrant for patients with HR-positive, HER2-negative, PIK3CA-mutated, Advanced or Metastatic Breast Cancer (80); Idelalisib, a PI3Kδ inhibitor approved for the treatment of relapsed chronic lymphocytic leukemia (CLL) and for the treatment of relapsed indolent B-cell malignancies (81,82); Copanlisib, a pan-class I PI3K inhibitor was approved by FDA for the treatment of relapsed follicular lymphoma (83,84); Duvelisib is a PI3Kδ/PI3Kγ inhibitor approved by FDA for patients with relapsed or refractory chronic lymphocytic leukemia (CLL) or small lymphocytic lymphoma (SLL) after at least two prior therapies (85,86).

The potential of PI3K inhibitors as novel therapeutic agents in the treatment of GIST has been studied in recent years. Early preclinical studies have evaluated the effect of PI3K inhibitors achieving strong antiproliferative and proapoptotic effects in imatinib-sensitive and -resistant GIST models, both as monotherapy and in combination with imatinib (69,70,78,87).

Contrary to expectations, the clinical benefit of targeting the PI3K/mTOR pathway in GIST has been limited. In a phase I clinical trial evaluating the PI3K/mTOR inhibitor

GDC-0980 in GIST, disease control was prolonged by a median of only 1.4 to 3.5 months. The placebo arm in patients with similarly advanced and multi-resistant GIST shows apparent disease control of less than one month (88). Another clinical trial evaluated the efficacy of imatinib in combination with everolimus, an mTOR inhibitor, for the treatment of metastatic GIST. In this study, cohort 1 showed a response rate of 0%, while cohort 2 showed a slightly higher ORR of 2%. Additionally, the median PFS was 1.9 and 3.5 months for cohorts 1 and 2, respectively (89). Furthermore, a phase Ib clinical trial combining Imatinib and buparlisib, a PI3K inhibitor, was conducted on 60 patients with advanced GIST refractory to imatinib and sunitinib. This trial failed to generate objective responses and was not developed further (90). Therefore, therapeutic inhibition of PI3K/mTOR in GIST patients is associated with limited clinical benefit.

The complex network of PI3K/mTOR signaling involves a multitude of feedback loops, and interconnections with several other signaling pathways together with compensatory feedbacks, thus providing ample opportunities for modulation and adaptation in treated cancer cell conditions. This adaptive mechanisms have been addressed in various cancer models, including breast cancer, where adaptive resistance is an important mechanism of resistance to PI3K/mTOR inhibition and involves upregulation of upstream regulators that includes RTKs such as HER3, INSR, and IGF-1R, as well as IRS-1, and SRC (91–93). Furthermore, a compensatory JAK2/STAT5 activation has been shown to contribute to the resistance mechanism of

PI3K/mTOR pathway suppression, reversing this effect with dual-targeted inhibition of both pathways (94).

In addition to solid tumors, resistance to TKIs, such as first-line imatinib, is also often observed in chronic myeloid leukemia (CML). Although the vast majority of CML patients initially respond to imatinib, resistance to this targeted therapy eventually occurs in a subset of these patients (95). Point mutations and chromosomal aberrations can activate alternative cellular signaling pathways like JAK/STAT, which can contribute to imatinib resistance (95,96). The role of the JAK/STAT pathway has been described in many types of cancer (97,98), but particularly it has been explored in CML with resistance to imatinib, where the reactivation of the JAK/STAT pathway is seen in resistant disease (99–101). Together, potentially, analogous biological findings could be found in GIST.

Like in these cancer models, alternative adaptive mechanisms may compensate in GIST for PI3K/mTOR signaling inhibition and therefore diminish the expected therapeutic effect. Based on prior data , one of the compensatory pathways could be JAK/STAT signaling activation in adaptative mechanish of resistance to PI3K/mTOR inhibition. In order to optimize treatment strategies in GIST, it is essential to understand how and why these adaptive mechanisms are activated.

1.7 JAK/STAT pathway in Cancer

The JAK/STAT pathway was discovered through the study that linked interferon-responsive genes to signal transduction (102,103). The JAK/STAT pathway plays a

central role in cell proliferation, differentiation, survival, and embryological processes. Pathological activation of the JAK-STAT pathway due to genetic mutations, amplifications, or polymorphisms can lead to constitutive or persistent activation of the pathway and affect cancer development (104).

The JAK family includes JAK1, JAK2, JAK3, and TYK2 and the STAT family includes STAT1, STAT2, STAT3, STAT4, STAT5a, STAT5b and STAT6 (105,106).

The canonical JAK/STAT signaling pathway activation follow the classical signaling models where a given ligand, usually cytokines such as interferons or interleukins, binds to the extracellular domain of a transmembrane receptor (e.g. cytokine receptor, IFN-α/β and IFN-γ) and triggers a cascade of phosphorylation reactions (107) (Figure 5). These reactions include phosphorylation of the JAK kinases, activated JAKs phosphorylate the receptor cytoplasmic domains that create docking sites for Src homology 2 (SH2)-containing signaling proteins. Among the substrates of tyrosine phosphorylation are members of the signal transducers and activators of transcription family of proteins (STATs) (108,109). STAT phosphorylation leads to nuclear localization, subsequent DNA binding, and gene regulation. The regulation on this pathway is given by several families of phosphatases remove the phosphate groups from JAK and STAT. Protein inhibitors of activated STAT proteins (PIAS) inhibit STAT-DNA binding, control the cellular location of STAT, and facilitate posttranslational modifications of STAT. Suppressors of cytokine signaling (SOCS) are competitive inhibitors of STAT receptor binding and also act as ubiquitin ligases that target components of the pathway for proteosomal degradation. STATs positively regulate

the transcription of SOCS genes, creating a negative feedback loop that imposes a good level of control on the pathway (Figure 5) (110).

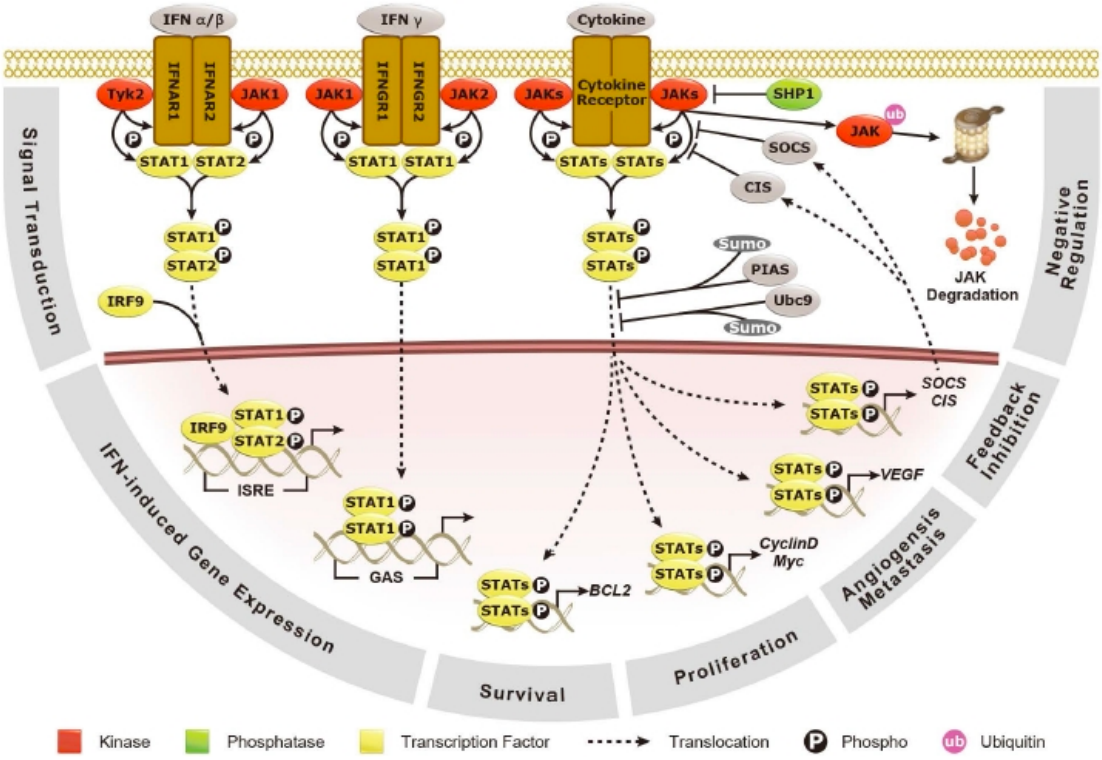

Figure 5. The JAK–STAT pathway. A schematic representation of the Janus kinase (JAK)–signal transducer and activator of transcription (STAT) pathway. The activation of JAKs after cytokine stimulation results in the phosphorylation of STATs, which then dimerize and translocate to the nucleus to activate gene transcription (111).

The BCR/ABL fusion protein, which is a hallmark of CML, leads to the activation of downstream signaling pathways such as RAS/MAPK, PI3K/mTOR, and JAK/STAT. Similarly, different RTKs and cytokine receptors activate these three signaling pathways. This same analogy could also be occurring in GIST where these critical signal transduction cascades could frequently be hyper-activated as a consequence of gain-of-function mutations in their limbs, loss-of-function mutations or deletions in negative regulators, or activation of upstream proteins or receptors. Furthermore, the

JAK/STAT signaling pathway has been reported in GIST, highlighting STAT1 and STAT3 activation in most primary GIST (70). In addition, the KIT inhibition with imatinib reduced STAT1 and STAT3 phosphorylation in imatinib-sensitive and -resistant GIST models (69). Further investigation into this direction is needed to comprehend the intricate mechanisms of adaptative resistance in GISTs.

1.8 High-throughput multi-omics technologies for characterization of signaling pathways

Advances in omics technologies have revolutionized the field of precision oncology. We have achieved the personalization of medicine at an extraordinarily detailed molecular level by harnessing the power of high-throughput technologies such as genomics, transcriptomics, proteomics, and metabolomics.

In recent years, our understanding of transcriptomics has achieved substantial progress. RNA sequencing (RNA-Seq) utilizes the capabilities of high-throughput sequencing methods to gain insight into a cell's transcriptome. The transcriptome comparison helps to discover which genes are differentially expressed in different cell populations or in response to different treatment conditions. In the context of cancer, this method represents an opportunity to dissect the complexity and heterogeneity of tumors and discover new biomarkers or therapeutic strategies (112).

An important limitation of genomic and transcriptomic profiling studies is that the data obtained are only indirect measurements of cell states, but do not reflect protein

changes. These data do not reveal changes in post-translational modifications (PTMs), including protein phosphorylation and degradation (113).

While genomic and transcriptomic data are necessary and beneficial, they alone cannot provide a comprehensive understanding of cancer biological processes. To improve this knowledge, proteomics plays a vital role in cancer research in the post-genomic era.

Mass spectrometry has opened a new era in proteomic characterization. With its fast and relatively deep capabilities, it has revolutionized the way we can study the structure and function of proteins. High-throughput proteomic profiling generates novel information on various tumors and shows promise for a new era of proteomics-driven precision medicine. In this coming era, high-resolution, systems-level investigations of proteins and their post-translational modifications will undoubtedly facilitate more precise targeted therapies against cancer (114). Consequently, modern proteomics has a plethora of potential applications in the discovery of new signaling pathways in cancer and pharmacological exploration (113). Consequently, new projects like the Human Proteome Project have emerged (115).

However, each individual technology has a limited capability to capture the full biological complexity of cancer. The integration of multiple technologies has emerged as an approach to provide a more comprehensive view of biology and disease (116,117). Hence, throughout this thesis, we have specifically taken advantage of the integration of transcriptomic and proteomic data to elucidate new mechanisms involved in the adaptive resistance of GIST.

As we have described earlier, GIST depends on the oncogenic signaling of KIT and PDGFRA, and therefore, patients with GIST have significant responses with imatinib and with other TKIs with activity against these receptors. However, most patients end up progressing to these therapies due to the polyclonal expansion of subpopulations that contain various types of secondary resistance mutations in KIT and PDGFRA, and which cannot be completely suppressed with any TKI. Therefore, it is imperative to develop new therapeutic strategies in GIST resistant to TKI, regardless of the type of secondary mutation. Both the primary and secondary mutations in KIT/PDGFRA share the same signaling pathways. Therefore, there is a strong rational to inhibit the PI3K/mTOR pathway in GIST, an essential pathway for the survival and proliferation of GIST. However, the collective evidence shows that therapeutic inhibition of the PI3K/mTOR pathway in GIST produces little clinical benefit, likely due adaptation through yet unknown compensatory mechanisms.

The Sarcoma Translational Research Laboratory at VHIO has generated transcriptomic data (RNAseq) in several cellular models with single-agent inhibition of PI3K/mTOR in order to study the relevance of this pathway and the impact of it inhibition on the molecular biology and therapeutics of GIST (118).

Therefore, the proposal of our study is to determine and validate molecules/signaling pathways in the biology of GISTs with a critical role in the adaptation to targeted therapies.

HYPOTHESIS &

RESEARCH OBJECTIVES

2. HYPOTHESIS

Previous studies have demonstrated the biological relevance of PI3K/mTOR signaling in GIST throughout the entire course of the disease. However, therapeutic inhibition of the PI3K/mTOR pathway in GIST has only shown modest benefit in patients. Therefore, we hypothesize that an unbiased assessment of the cellular adaptations resulting from the targeted inhibition of PI3K/mTOR signaling in GIST will identify vulnerabilities that can be exploited therapeutically to provide clinical benefit to GIST patients.

3. OBJECTIVES

Main Objective:

Investigate the critical node and signaling pathway in the adaptative resistance to therapeutic inhibition of PI3K/mTOR inhibition in gastrointestinal stromal tumors to develop more effective combination therapies to overcome therapeutic resistance.

Secondary objectives:

1. Identification and functional validation *in silico* and *in vitro* of critical nodes and signaling pathways potentially involved in the adaptation to targeted therapies in GIST.
2. Determination of the biological relevance of the signaling nodes identified in objective 1.

3. Validation of drug-strategies against essential targets in adaptive pathways to maximize GIST response to PI3K/mTOR inhibition.

MATERIALS & METHODS

4. MATERIALS AND METHODS

4.1 Human GIST cell lines and cultures

GIST-T1: is an imatinib-sensitive GIST cell line established from an untreated metastatic GIST containing a homozygous 57 bp deletion in *KIT* exon 11 (119).

GIST882: is an imatinib-sensitive human cell line established from an untreated GIST with a primary homozygous missense mutation in *KIT* exon 13, encoding a K642E mutant KIT oncoprotein (120).

GIST-T1/670: is an imatinib-resistant GIST cell line derived from GIST-T1 through imatinib pressure. GIST-T1/670 has the same primary *KIT* exon 11 mutation, and has a secondary ATP pocket mutation in the exon 14 (T670I) (121).

The cells were grown at 37 °C in presence of 5% CO2 and in medium: Iscove's modified Dulbecco's Medium (IMDM) from Invitrogen (Ref: 12440053) and RPMI 1640 from Invitrogen (Ref: 21875-091) supplemented with 15% Fetal Bovine Serum South America (FBS) from Invitrogen (Ref: 10500064), Invitrogen Antibiotic/Antimitotic (Ref: 15240-062), Invitrogen Fungizone B 500 ul/100 mL (Ref: 15290-018), Invitrogen Gentamicin 10 mg/mL (Ref: 15710-049) and 1% L-Glutamine from Lab Clinics (Ref.: X0550-100).

4.2 Reagents

Imatinib, sunitinib, GDC-0980, and BEZ-235 were purchased from LC Laboratories (Woburn, MA, USA); Fludarabine and LY2874455 were purchased from Selleck Chemicals (Houston, TX).

4.3 Immunoblot

Preparation of whole-cell lysates was done as described previously (122). Electrophoresis was carried out in 10% polyacrylamide gels and transferred to nitrocellulose membranes. Bands were detected by incubating with Immobilon Forte Western HRP Substrate (Millipore-MERK KGaA) and captured by chemiluminescence with Amersham Imager 600 (GE Healthcare Life Science).

Table 4: Primary antibodies

Antibodies	Company	Dilution	Blocking (NFM)	Source /Isotype	Cat #	Molecular Weight (kDa)
STAT1 Tyr701	Cell Signaling	1:1000	5%	rabbit	9167	91
STAT1 Ser727	Cell Signaling	1:1000	5%	rabbit	9177	91
Total STAT1	Zymed	1:500	3%	mouse	33-1400	91
STAT3 Tyr705	Cell Signaling	1:1000	5%	rabbit	9131	79, 86
Total STAT3	Zymed	1:1000	3%	mouse	13-7000	89
FGFR-1 Tyr653/654	Cell Signaling	1:1000	5%	mouse	3476	120-145
Total FGFR1	Cell Signaling	1:1000	5%	rabbit	9740	97, 120, 145
KIT Tyr703	Cell Signaling	1:1000	5%	rabbit	3073	145, 160
Total KIT	Dako	1:2000	5%	rabbit	A4502	145, 160
AKT Ser473	Cell Signaling	1:1000	5%	rabbit	9271	60

Total AKT	Cell Signaling	1:1000	5%	rabbit	9272	60
S6 Ser235/236	Cell Signaling	1:1000	5%	rabbit	2211	32
Total S6	Cell Signaling	1:500	5%	mouse	2317	32
PARP Cleaved Asp214	Cell Signaling	1:1000	5%	rabbit	9541	89
PCNA	Santa Cruz	1:500	1%	mouse	sc-56	36
Cyclin A	Santa Cruz	1:500	5%	mouse	sc-271682	54
Actin	Sigma	1:1000	5%	mouse	A4700	42

4.4 Viability assays

Cell viability studies were carried out using Cell Titer-Glo luminescent assay from Promega, in which the luciferase catalyzed luciferin/ATP reaction provides an indicator of cell number. For these studies, cell lines were plated in triplicates at 5,000 (GIST-T1 and GIST-T1/670) and 10,000 (GIST882) cells per well in a 96-well flat-bottomed plate (Falcon), and then incubated for 3 (GIST-T1 and GIST-T1/670) or 6 days (GIST882) with reagents at different concentrations or DMSO. The Cell Titer-Glo luminescence assay was measured with Infinite 200 Pro Microplate Luminometer (Tecan Trading AG) and the data were normalized to the DMSO control group. All experiments were performed in triplicates.

4.5 Apoptosis induction assay

Apoptosis induction studies were performed by measuring caspase-3 and caspase-7 activity with the Caspase-Glo 3/7 Assay Kit (Promega) according to the manufacturer's protocol. Cells were plated in triplicates in 96-well flat-bottomed plates at 5,000 (GIST-T1 and GIST-T1/670) and 10,000 (GIST882) cells per well. After 24-hour culture, medium was replaced with fresh medium (with or without respective drugs) and apoptosis was measured according to the manufacturer's instructions at 24 hours (GIST-T1, GIST-T1/670) and 48 hours (GIST882) with Infinite 200 Pro Microplate Luminometer (Tecan Trading AG). All experiments were performed in triplicates.

4.6 Flow cytometry

Annexin V/PI

GIST cells were cultured in 6-well plates. After indicated time-points of drug incubation, 1×10^6 cells were resuspended in Hank's balanced salts solution (HBSS) from Thermo Fisher Scientific and incubated with annexin V-FITC antibody (Ref.: 550475, BD Bioscience, NJ, US) for 15 min in the dark at RT. Then, cells were incubated with propidium iodide (10 µg/ml final concentration) for 5 min RT and immediately analyzed by flow cytometry with BD FACSCelesta™ from BD Bioscience.

4.7 5-Bromodeoxyuridine assay

Cell proliferation studies were carried out using BrdU Cell Proliferation ELISA Assay (Roche) according to the manufacturer's protocol. For these studies, cell lines were

seeded in triplicates at 10,000 (GIST-T1 and GIST-T1/670) and 15,000 (GIST882) cells per well in a 96-well tissue culture plate (Sigma-Aldrich) and were incubated in media containing drugs and DMSO for 48 hours. 5-bromodeoxyuridine (BrdU) was added and incubation was continued for 24 hours. Assay plates were measured with Infinite 200 Pro Microplate Luminometer (Tecan Trading AG).

4.8 Plasmids

STAT1 shRNA knock-down

pLKO.1 constructs against STAT1 (sh*STAT1* shRNA1: TRCN0000280021, targeting CTGGAAGATTTACAAGATGAA and sh*STAT1* shRNA2: TRCN0000280024, targeting CCCTGAAGTATCTGTATCCAA were purchased from Sigma-Aldrich (Merck KGaA, Darmstadt, Germany). pLKO.1 shControl (targeting CCTAAGGTTAAGTCGCCCTCG) was purchased from Addgene. Lentiviruses were generated by co-transfecting shSTAT1 hairpin constructs or pLKO.1 shControl with psPax2 and psMDG2 (Addgene) into 293T cells using Polyethyenimine (PEI) MW40000 (Polyscience, Warrington, PA, USA). GIST-T1 and GIST-T1/670 cell lines were infected with shSTAT1 or shControl and selected with puromycin (1ug/mL). All the experiments were performed within the first 5 passages post-infection.

4.9 Transcriptomics Study

RNA extraction

Total RNA was isolated using Qiashredder (Qiagen, Hilden, Germany) and purified using the RNeasy Mini Kit (Qiagen, Hilden, Germany). Both procedures were

performed according to the manufacturer's specification. The purification included a DNase treatment using the RNase free DNase Set (Qiagen, Hilden, Germany). The yield and purity of the RNA was measured photometrically.

RNA sequencing

The quality control for quantity and quality of the total RNA was done using the Qubit® RNA HS Assay (Life Technologies) and RNA 6000 Nano Assay on a Bioanalyzer 2100 (Agilent). The RNASeq libraries were prepared using TruSeq®Stranded mRNA LT Sample Prep Kit (Illumina Inc., Rev.E, October 2013) and sequenced on HiSeq 4000 (Illumina) in paired-end mode (2x76bp), following the manufacturer's protocol. Raw reads were pre-processed and the quality was assessed with FastQC. Reads were mapped to the Ensembl GRCh38 human genome reference and the annotation from Gencode version 25 using STAR version 2.5.2a, allowing the default ratio of mismatches in a read pair, keeping only alignments with valid splice junctions, mapping to no more than 20 loci and a minimum overhang of 8 for spliced alignments. Gene quantification was performed with RSEM version 1.2.28, using the same gene model used before to guide the aligner, and handling overlapping reads as suggested in the default options. For the differential expression analysis, we used R version 4.0.2 and limma with voom transformation to normalize, transform, and model RNA-Seq data. A design including one term combining the treatment and timepoint, blocking for the cell line, was used for testing the differences in gene expression between the treatment combining the two drugs at 24 hours and the baseline expression at 0 hours, after subtraction of the specific effects at 24h of the drugs administered alone. Also,

analyses for each cell line separate from the others were done in parallel, using the same design (without blocking) and contrast of interest. P-values were adjusted by Benjamini & Hochberg (FDR), and genes with FDR <0.01 and a fold change in expression of at least 2 were considered differentially expressed. The molecular signatures from MSigDB were used to identify enrichment of known gene sets, namely KEGG, GO biological processes (GOBP), hallmarks gene sets and oncogenic signatures, using a GSEA analysis implemented in the package clusterProfiler.

4.10 Proteomics Study

Cell lysis and protein extraction.

Cell pellets (GIST-T1 and GIST-T1/670 treated with GDC-0980 versus DMSO) were transferred to a 50 mL falcon tube with 10 ml of lysis buffer (7M urea, 2M thiourea, 30 mM Tris.HCl, pH=8.5, 4% CHAPS) plus phosphatase inhibitors (1M NaF, 0.1M Na3VO4), and were sonicated using a probe sonicator (VCX 150; Sonics & Materials Inc. USA) with 5 cycles of 20 seconds of ultrasound bursts, followed by 10 seconds of cooling intervals, while keeping the tube ice-cooled. Then, lysed samples were centrifuged 20 min at 4000 rpm and the supernatants were collected. Proteins were then precipitated by addition of trichloroacetic acid to a final concentration of 20% TCA plus 5 volumes of acetone. Samples were kept overnight at -20ºC and then centrifuged for 10 min at 9500 rpm at 4ºC (Sorvall Legend XTR, Thermo Fisher scientific co.). The supernatants were removed by aspiration and pellets were resuspended in 4 mL of 8M urea 50 mM ammonium bicarbonate plus phosphatase inhibitors. Total protein

content was quantified using RCDC kit (Bio-Rad), and 25 mg of each sample was taken for tryptic digestion.

Trypsin digestion.

Samples were first reduced with DTT by addition of freshly prepared 700 mM DTT solution to a final concentration of 10 mM, for 1h at rt. Next, they were carbamidomethylated with iodoacetamide (IAA), by addition of the required volume of freshly prepared 700 mM IAA to obtain a final concentration of 30mM in the sample. Alkylation was allowed to proceed for 30 min at rt in the dark, and then the reaction was quenched by addition of N-acetyl-L-cysteine to a final concentration of 35 mM, followed by incubation for 15 min at rt in the dark. Samples were then diluted with 50 mM ammonium bicarbonate to a final concentration of 1M Urea, and then trypsin (*Worthington Biochemical*) was added in a ratio of 1:10 (w/w), and the mixture was incubated overnight at 37 °C. The reaction was stopped with formic acid to a final concentration of 0.5%. Each of the sample digests was concentrated and purified by chromatography through a reverse-phase Sep-Pak column (*HLB Plus 225mg, Oasis*). Columns were initially equilibrated with 3 ml of ACN followed by 3 ml of 0.1% TFA. Then sample was loaded in the column, followed by a washing step with 3 ml of 0.1% TFA. Finally, sample was eluted with 2 ml of 50% ACN 0.1% TFA. These digests were stored in the freezer at -20ºC. until further processing or LC-MS analysis. 1 mg of each of the digests was used for total proteome analysis by LC-MS.

Phosphopeptide enrichment using titanium dioxide.

Phosphopeptide enrichment on titanium dioxide was performed according to Thingholm and Larsen (123),with some modifications. 150 mg of each sample was used for enrichment. TiO_2 beads at 0.80mg/µl were previously equilibrated in 1M glycolic acid, 80% ACN and 1% TFA. Peptides were diluted in 60% ACN with 1% TFA and added to 0.9 mg TiO_2. The suspension was incubated during 20 min at rt, with end-over-end rotation for phosphopetide binding. The mixture was then centrifuged at 13000 rpm and supernatant containing non-phosphorylated peptides was discarded. TiO_2 beads with bound phosphopeptides were loaded on previously prepared stage tips (made using two high performance Empore C18 extraction disks in a pipette tip). After two successive washes with 150 mL 60% ACN and 1% TFA, bound phosphopeptides were eluted first with 30 mL 5% NH_4OH and then with 30 mL 10% NH_4OH with 25% ACN. The combined fractions of eluted phosphopeptides were evaporated, resuspended in 50 mL 0.1% FA and stored at -20ºC until further analysis. 20% of the enriched sample was loaded for the LCMS analysis.

Tyrosine phosphopeptide enrichment.

Phoshotyrosine peptide affinity enrichment was performed using PTMScan kit Phospho-Tyrosine Rabbit mAb (P-Tyr 1000) (Cell Signaling), using a fraction of each protein digest corresponding to 20 mg of total protein. The peptide mixture was first evaporated to dryness, resuspended in 1.4 mL IAP buffer (PTMScan® IAP Buffer, 50mM MOPS/NaOH pH=7.2, 50mM Na_2HPO_4, 50mM NaCl), and clarified by centrifugation for 5 min at 10,000 g at 4°C . Tubes were cooled on ice. The antibody-bead slurry (PTMScan® Rabbit mAb P-Tyr-1000) was centrifuged at 2,000 g for 30

sec. and supernatant was discarded. Antibody beads were washed four times with 1 ml of PBS and centrifuged 30 sec. at 2,000 g after each wash. Then, beads were resuspended in 40 µl of PBS. Next, peptide solution was transferred into the vial containing anti P-Tyr antibody beads and incubated on an end-to-end rotator for 2 h at 4°C. Then, samples were centrifuged at 2,000 g for 30 sec and the supernatants were separated and kept at -80°. Beads were then washed three times with IAP buffer by adding 1 ml of IAP buffer, mixing by inverting the tube 5 times and then centrifuging for 30 sec at 2,000 G. Supernatants were discarded. This step was repeated two times. Next, three more washes with 1 ml of HPLC water were performed, following the same steps as above. After the last washing step, supernatant was completely removed from the beads. Next, 55 µl of 0.15% TFA were added to the beads to elute phospho-peptides bound to the Ab-beads. Elution was allowed to proceed for 10 min at room temperature, with gently mixing every 2-3 min. After centrifugation for 30 sec at 2,000 g the supernatant was transferred to a new 2 ml Eppendorf tube. A second elution step was performed with additional 50 µl 0.15% TFA. The supernatant from this second elution was combined with the previous one. The phosphor tyrosine peptide enriched solutions were finally purified on reverse phase C18 micro columns (*Omix C-18 10µl, Varian)* and kept at -20ºC until further analysis. 20% of the enriched sample was loaded for the LCMS analysis.

Liquid chromatography-Mass spectrometry analysis (LC-MS)

For LC-MS/MS analysis peptide mixtures were diluted in 3% ACN, 1% FA and the sample was loaded to a 300 µm × 5 mm Pep-Map C18 (Thermo Scientific) at a flow rate of 15 µl/min using a Thermo Scientific Dionex Ultimate 3000 chromatographic system (Thermo Scientific). Peptides were separated using a C18 analytical column (NanoEase MZ HSS T3 column, 75 µm × 250 mm, 1.8 µm, 100Å, Waters) with a 210 min run for Total Proteome samples, comprising four consecutive steps, first 3 min of isocratic gradient at 3%B, from 3 to 35% B in 180 min, from 35 to 50% B in 5 min, from 50 to 85% B in 1 min, followed by isocratic elution at 85 % B in 5 min and stabilization to initial conditions (A= 0.1% FA in water, B= 0.1% FA in CH3CN), and with a 120 min run for TiO2 and p-Tyr samples, comprising four consecutive steps, first 3 min of isocratic gradient at 3%B, from 3 to 35% B in 90 min, from 35 to 50% B in 5 min, from 50 to 85% B in 1 min, followed by isocratic elution at 85% B in 5 min and stabilization to initial conditions (A= 0.1% FA in water, B= 0.1% FA in CH3CN). Flow rate was 250 nL/min and the column was kept at 40 ºC. The column outlet was directly connected to an Advion TriVersa NanoMate (Advion) fitted on an Orbitrap Fusion Lumos™ Tribrid (Thermo Scientific). The mass spectrometer was operated in a data-dependent acquisition (DDA) mode. Survey MS scans were acquired in the orbitrap with the resolution (defined at 200 m/z) set to 120,000. The lock mass was user-defined at 445.12 m/z in each Orbitrap scan. The top speed (most intense) ions per scan were fragmented in the HCD cell and detected in the orbitrap at 30000 resolution. Quadrupole isolation was employed to selectively isolate peptides of 350-1700 m/z. The predictive automatic gain control (pAGC) target was set to 4e5. The maximum

injection time was set to 50ms for MS1 and 70ms for MS2 scan. Included charged states were 2 to 7. Target ions already selected for MS/MS were dynamically excluded for 15 s. The mass tolerance of this dynamic exclusion was set to ±2.5 ppm from the calculated monoisotopic mass. Spray voltage in the NanoMate source was set to 1.7 kV. RF Lens were tuned to 30%. Minimal signal required to trigger MS to MS/MS switch was set to 5000 and activation Q was 0.250. The spectrometer was working in positive polarity mode and singly charge state precursors were rejected for fragmentation.

Protein identification and quantitative differential analysis.

Progenesis ® QI for proteomics software v3.0 (Nonlinear dynamics, UK) was used for MS data analysis using default settings. The LC-MS runs were automatically aligned to an automatically selected reference sample Alignments were then manually supervised. Only features within the 400 to 1,600 m/z range, 45 to 190 min retention time, for total proteome, or 30-105 min for phosphopeptide analysis, and with positive charges between 2 to 4 were considered for identification and quantification. Peak lists (mgf files) were generated using Progenesis and loaded to Proteome Discoverer v2.1 (Thermo Fisher Scientific) for protein identification. Proteins were identified using Mascot v2.5 (Matrix Science, London UK) to search the SwissProt database (taxonomy restricted to human proteins). MS/MS spectra were searched with a precursor mass tolerance of 10 ppm, fragment tolerance of 0.02 Da, trypsin specificity with a maximum of 2 missed cleavages, cysteine carbamidomethylation set as fixed

modification and methionine oxidation as variable modification for total proteome analysis, plus phospho (S/T) and phosphor (Y) as variable modifications for phosphopeptide analysis. Significance threshold for the identifications was set to $p<0.05$, minimum ions score of 20.

4.11 Bioinformatics tools

Gene Set Enrichment Analysis (GSEA):

GSEA is a method to identify classes of genes or proteins that are over-represented in a large set of genes or proteins, and may have an association with disease phenotypes (http://software.broadinstitute.org/gsea/index.jsp). The method uses statistical approaches to identify significantly enriched or depleted groups of genes. Transcriptomics technologies and proteomics results often identify thousands of genes which are used for the analysis (124).

Venny 2.0

To generate de Venn diagram, we used an open software called Venny 2.0 (http://bioinfogp.cnb.csic.es/tools/venny/), it allows for three sets in a graph mode. It was used in comparative genomics, for the visualization of results, discovering correlations and trends in our transcriptomic datasets.

HiPathia

The HiPathia method was applied for the computation of signal transduction along signaling pathways from transcriptomic data (http://hipathia.babelomics.org/). The method is based on an iterative algorithm which is able to compute the signal intensity

passing through the nodes of a network by taking into account the level of expression of each gene and the intensity of the signal arriving to it. It also provides a new approach to functional analysis allowing to compute the signal arriving to the functions annotated to each pathway. It is a free open-source software (125).

Protein Set Enrichment Analysis (PSEA)

A functional enrichment analysis web tool (http://www.webgestalt.org/) was used to perform statistical significance tests based on molecular signatures, which effectively integrate protein functional category information with statistical tests of proteomics data (126).

4.12 Statistical Analysis

For GSEA analysis, the significantly related genes were defined with an adj. $P < .05$ and FDR < 0.25. Statistical, bioinformatic analysis and graphical plotting were conducted by the free R software, version 3.6.0 (https://www.r-project.org/), packages as gplot2, heatmap.plus, RColorBrewer, and pheatmap were used for differential expression gene data analysis and ggpubr, magrittr, ggbarplot for differential signal data analysis.

Statistical significance for apoptosis and proliferation assays was calculated by two-way ANOVA followed by a Tukey's multiple comparison test for *in vitro* proliferation studies and by one-way ANOVA followed by a Tukey's multiple comparison test in experiments with more than one condition. * ≤ 0.05, ** ≤ 0.005, *** ≤ 0.001, **** 0.0001.

RESULTS

5. RESULTS

5.1. KIT downstream PI3K/mTOR signaling pathway is essential for the survival and proliferation of GIST cells.

To investigate how PI3K/mTOR contributes to the survival and proliferation of GIST cells, we undertook cell-response assays in three cell lines, including GIST models with clinically representative primary and secondary KIT mutations. For suppression of the PI3K/mTOR pathway, we used selective inhibitors (GDC-0980 and BEZ-235) compared with imatinib for sensitive models (GIST-T1, GIST882) and sunitinib for the resistant subline (GIST-T1/670) as internal positive controls. We first found in short-time functional studies that suppression of the PI3K/mTOR pathway led to a decrease in cell viability (Figure 6), showing IC50s with GDC-0980 within the nanomolar range for GIST-T1, GIST882, and GIST-T1/670 of 311,9 nmol/L, 212,5 nmol/L, 173,6 nmol/L respectively (Table 5). These cell viability results were comparable with those obtained with a second PI3K/mTOR inhibitor, BEZ-235, thus confirming the relevance of this pathway downstream KIT in GIST regardless the type of primary or secondary mutations. Furthermore, a slight but statistical significant increase in apoptosis induction (Figure 7) showed that GDC-0980 is effective in triggering cell death among all GIST cell lines, although apoptosis induction was more patent after upstream KIT inhibition using TKIs imatinib and sunitinib. These functional effects were corroborated through kinase inhibition studies (Figure 8): drug on-target effect was shown after PI3K/mTOR pathway inhibition with GDC-0980, and after KIT blockade with imatinib

or sunitinib, leading to a decrease in the expression of KIT-downstream AKT and S6 phosphorylation in both cases, and only to a decrease in KIT phosphorylation in the latter.

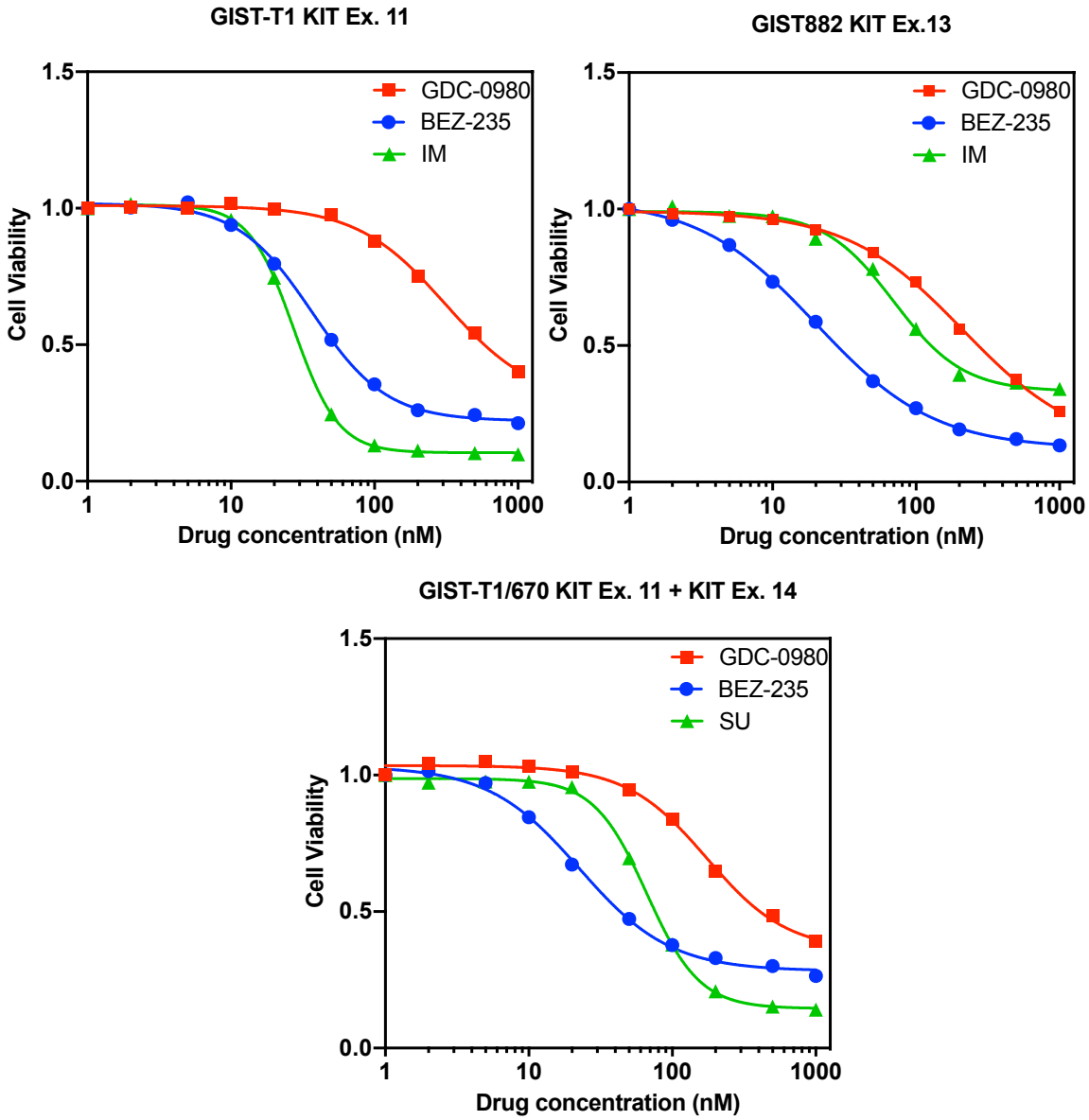

Figure 6. Cell viability assay in GIST cell lines.

In vitro cell viability assays performed in three GIST cell lines imatinib-sensitive (GIST-T1 and GIST882) and imatinib-resistant (GIST-T1/670) to imatinib. The PI3K/mTOR pathway was suppressed with GDC-0980 and BEZ-235, imatinib (IM) and sunitinib (SU) were used as a control for sensitive and resistant models respectively. Cell viability was measured by Cell Titer-Glo assay.

In order to demonstrate if this inhibitory effect on the PI3K/mTOR pathway is sustained over time, we performed a proliferation study using a longer time point. Here, and unlike short-term evidences, the effect observed was cytostatic comparing PI3K/mTOR suppression with KIT suppression, where the effect was rather cytotoxic (Figure 9). Taken together, these observations led us to hypothesize that the long-term absence of anti-proliferative effect could be due to the emergence of an adaptive mechanism developed by GIST cells that ultimately produced primary resistance after the suppression of critical KIT-downstream PI3K/mTOR pathway.

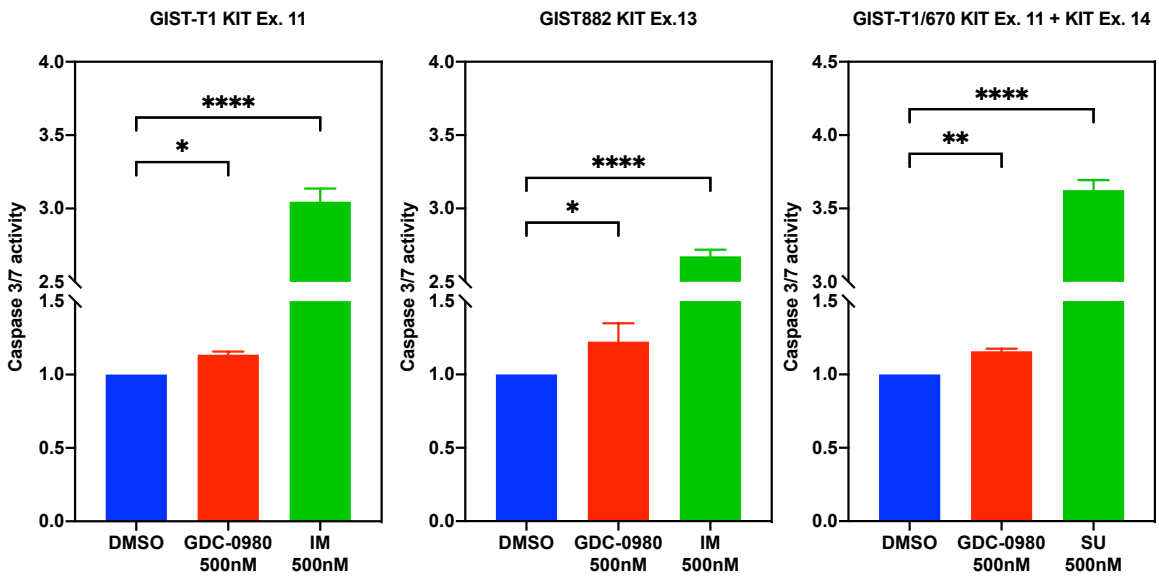

Figure 7. Apoptosis assay in GIST cell lines.

Apoptosis studies measured by caspase 3/7 activity in GIST cell lines after incubation of GDC-0980, imatinib and sunitinib at the indicated concentrations (nM). All conditions were performed in triplicates. Differences between treatments were considered to be significant with a p-value, * ≤ 0.05; ** ≤ 0.005; *** ≤ 0.001; **** ≤ 0.0001.

Table 5: IC50 values from cell viability studies represented in the Figure 6

Drug	IC50 (nM)		
	GIST-T1	GIST882	GIST-T1/670
GDC-0980	311,9	212,5	173,6
BEZ-235	36,73	20,1	22,53
Imatinib	27,35	69,9	-
Sunitinib	-	-	66,42

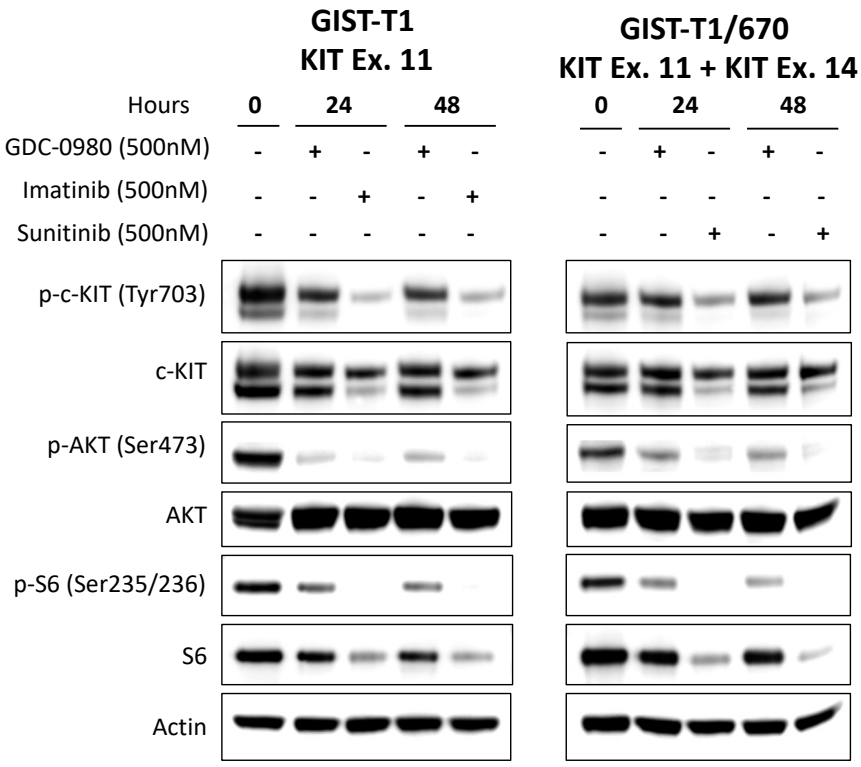

Figure 8. Immunoblot in GIST cell lines after KIT and PI3K/mTOR suppression.
Kinase inhibition studies at 24 and 48 hours in GIST-T1 and GIST-T1/670 using the same treatment concentrations as in Figure 7.

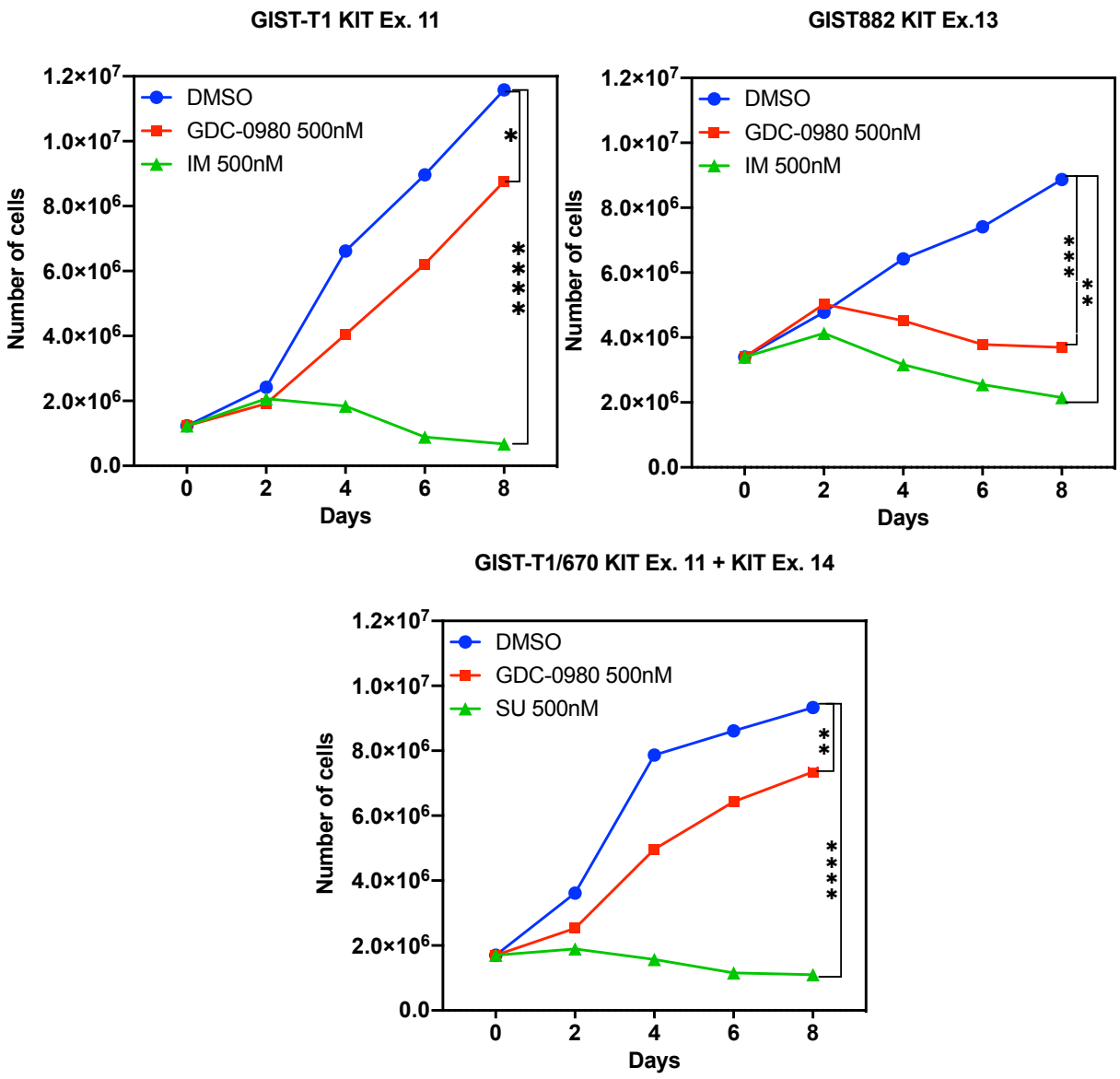

Figure 9. Proliferation assay in GIST cell lines.

8-day cell proliferation studies (raw cell count) in the two imatinib-sensitive cell lines, GIST-T1 and GIST882, and in the imatinib-resistant cell line GIST-T1/670; drug conditions: DMSO, GDC-0980 500nM, imatinib 500nM and sunitinib 500 nM. Differences between treatments were considered to be significant with a p-value, * ≤ 0.05; ** ≤ 0.005; *** ≤ 0.001; **** ≤ 0.0001.

5.2. JAK/STAT signaling pathway plays a critical role in the adaptative resistance to PI3K/mTOR suppression in GIST.

In order to study the specific molecules and/or signaling pathways potentially responsible for the therapeutic adaptation to the targeted suppression of the PI3K/mTOR pathway, we carried out transcriptomic studies in the three GIST cell lines treated with GDC-0980 for 24 hours. We performed gene set enrichment analysis (GSEA) to identify the pathways that are differentially expressed in the three GIST cell lines. Among all pathways found significantly dysregulated, cancer-relevant signaling alterations were found, such as P53, Notch, Cell Cycle, RIG-I-like receptor, and Toll-like receptor signaling pathways were found differentially expressed in at least one cell line. Interestingly, in the gene set enrichment analysis (GSEA), significant activation of the JAK/STAT signaling pathway was found across all studied cell lines after short-term (24 hours) of PI3K/mTOR pathway inhibition (Figure 10 A and B). This activation was given fundamentally by the upregulation of STAT1 and STAT3 (Figure 11). In addition, a landscape of the gene expression of all members of the JAK/STAT pathway showed that 47,4 % of genes were upregulated in the three GIST cell lines after 24 hours of suppression with GDC-0980. The shared genes between the three GIST cell lines were: JAK1, JAK2, JAK3, STAT1, STAT2, STAT3, STAT5A, STAT6, CBLB, CISH, CLCF1, CREBBP, EP300, GHR, IL10RB, IL12A, IL13RA1, IL13RA2, IL15, IL15RA, IL6ST, IRF9, OSMR, PIAS1, PIAS4, PIK3CA, PIM1, SOCS1, SOCS3, SOCS7, SOS, 1, SOS, 2, SPRED2, SPRY1, SPRY2, and STAM2. Most of these upregulated genes are known to be involved in the canonical JAK/STAT pathway

activation (Figure 12 A and B). Moreover, we wanted to confirm the GSEA results using a different bioinformatic tool named HiPathia. HiPathia is a bioinformatic methodology used for transcriptomic data analysis and visualization, with a special focus on the directionality of each single node within a given pathway (125). We performed signaling pathways analysis of circuits and subcircuits and, consistently with prior findings, we also identified the activation of JAK/STAT signaling after suppression with GDC-0980. The node that was most commonly and significantly upregulated was STAT1 (Figure 13 A, B, and C). When the analysis was extended using the same HiPathia method for STAT3, we found the same pattern of upregulation identified in STAT1 compared to the DMSO in all GIST cell lines (Figure 14).

In order to confirm our bioinformatics findings, we performed validation studies with Western blot, which showed the increased phosphorylation levels of STAT1 and STAT3 after 24 but mainly after 48 hours of the PI3K/mTOR suppression, assessed by the reduction of phospho-AKT levels (Figure 15). This pattern was shared in all studied GIST cell lines, thereby confirming GSEA and HiPathia findings.

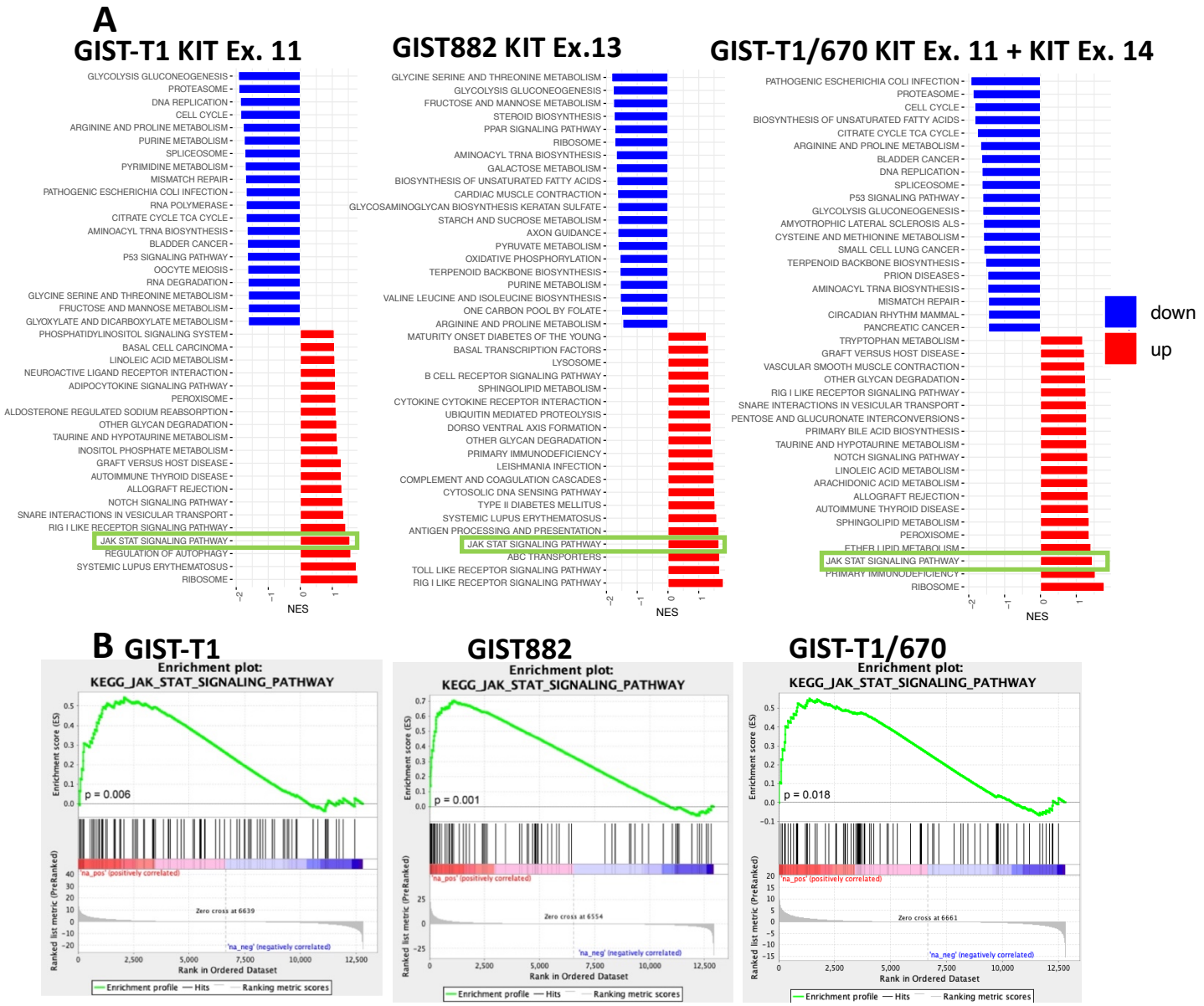

Figure 10. Gene Set Enrichment Analysis (GSEA) in GIST cell lines.

GSEA analysis in GIST cell lines after the suppression with GDC-0980 for 24 h. Horizontal bar plot represents 40 highly enriched pathways from KEGG (A). Enrichment plot represents the significance of JAK/STAT pathway in GSEA with positive and negative correlation (B).

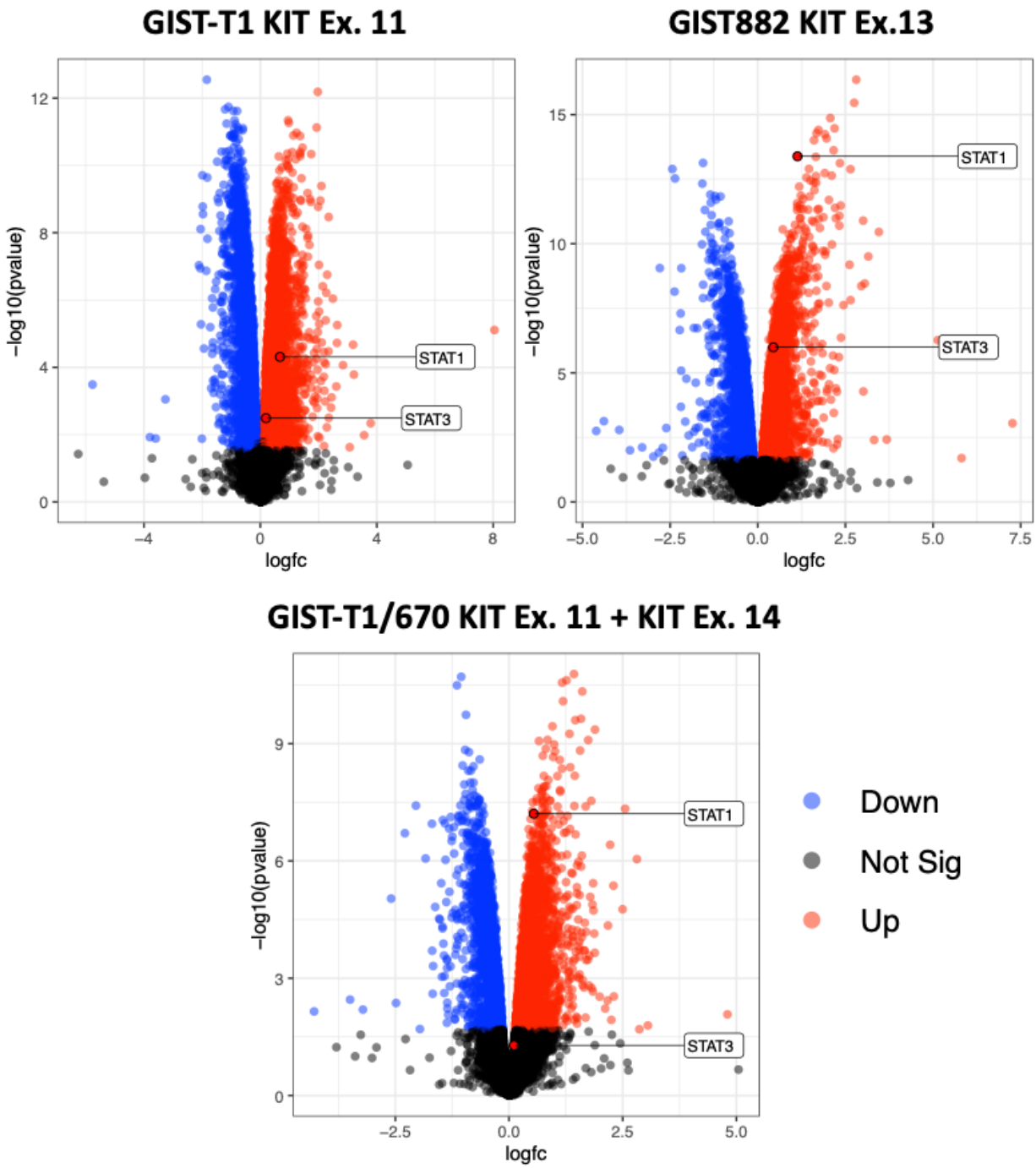

Figure 11. Volcano plot of differentially expressed genes in GIST

Transcriptomic analysis representation by a volcano plot. The log2 FC indicates the mean expression level for each gene. Each dots represents one gene. After 24 hours of GCD-0980 500nM administration, black dots represent no significant DEGs, the blue dots represent down-regulated genes and red dots represent up-regulated genes.

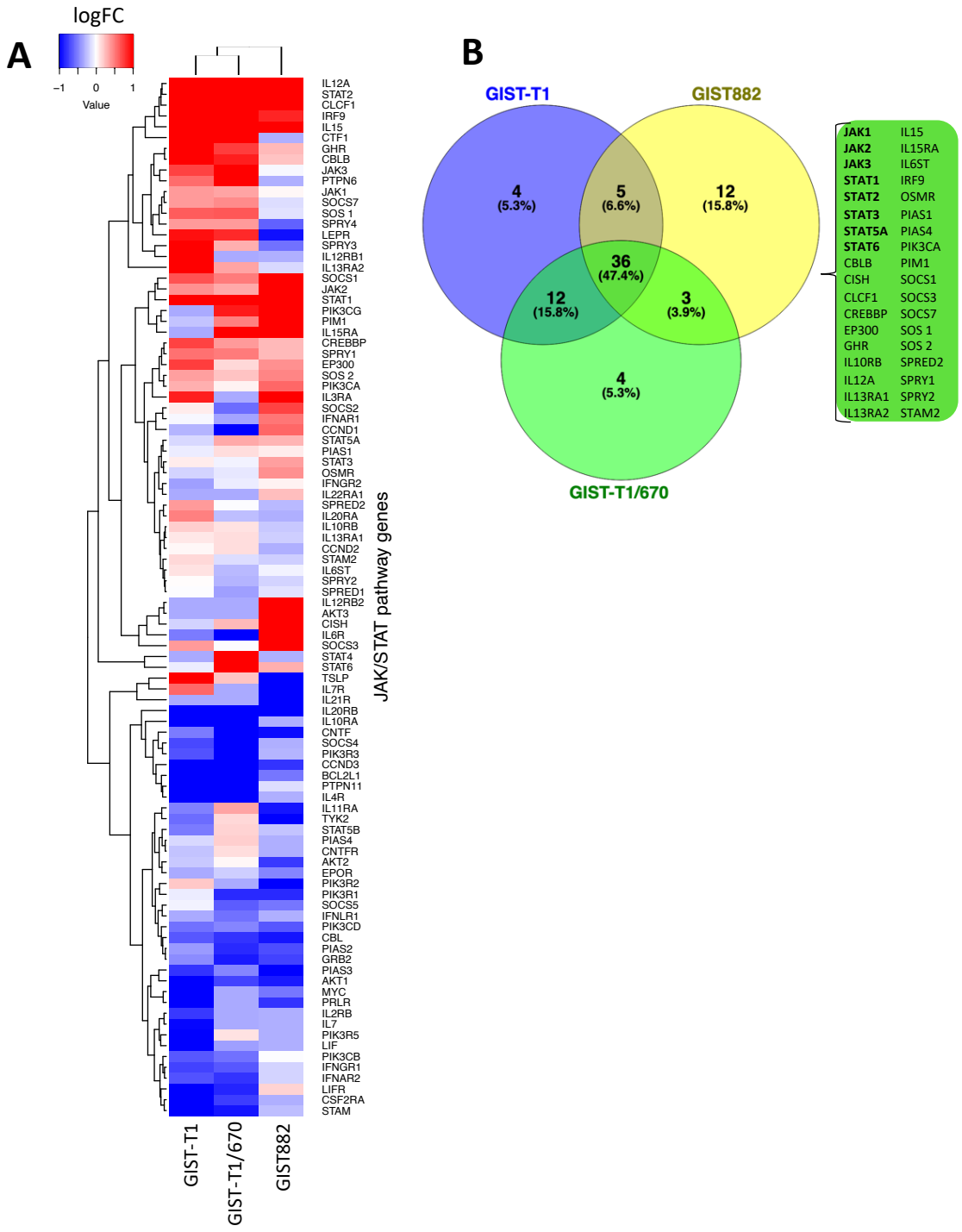

Figure 12. The JAK/STAT pathway differentially expressed genes in GIST

Heatmap of JAK/STAT pathway genes in GIST cell lines after 24H of GDC-0980 500nM (A). Venn diagram common upregulated JAK/STAT genes among GIST cell lines after PI3K/mTOR suppression (B)

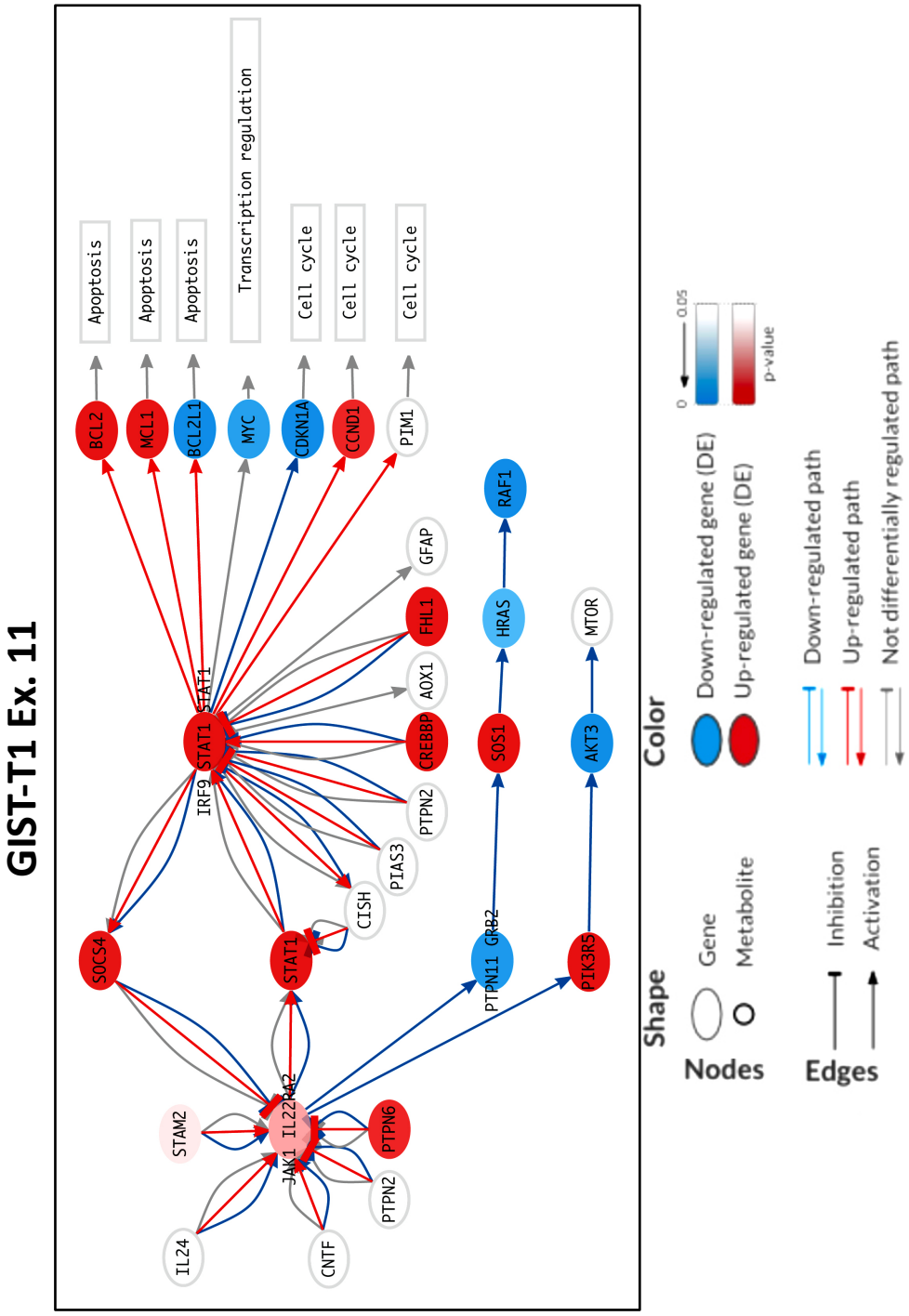

Figure 13. A) HiPathia analysis in GIST

JAK/STAT pathways showing signaling circuits differentially activated after the GIST-T1 cells were treated with GDC-0980 500nM 24H. Effector nodes and functions affected have been enhanced for clarity. Blue arrows indicate down-activation and red arrows up-activation.

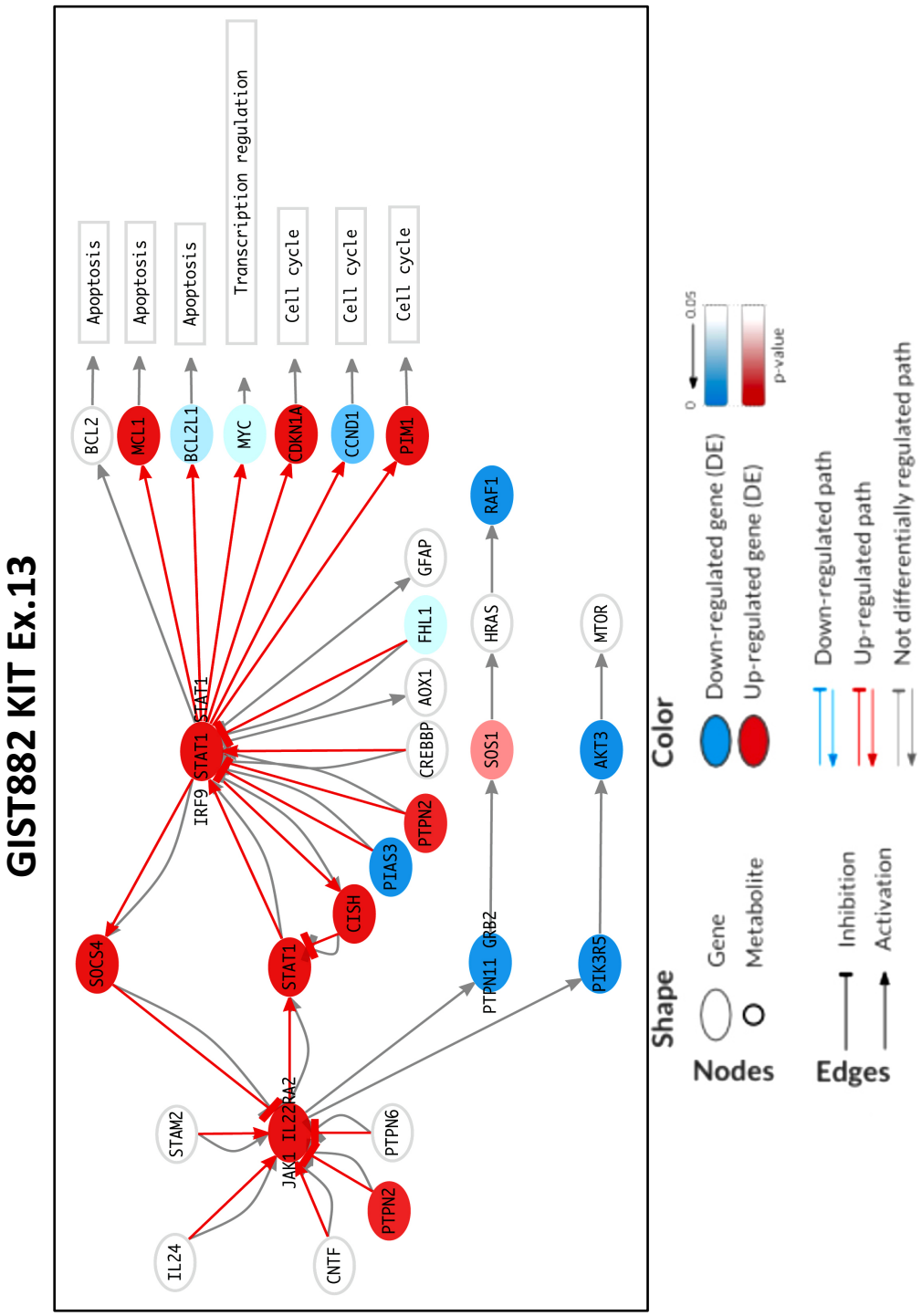

Figure 13. B) HiPathia analysis in GIST

JAK/STAT pathways showing signaling circuits differentially activated after the GIST882 cells were treated with GDC-0980 500nM 24H. Effector nodes and functions affected have been enhanced for clarity. Blue arrows indicate down-activation and red arrows up-activation.

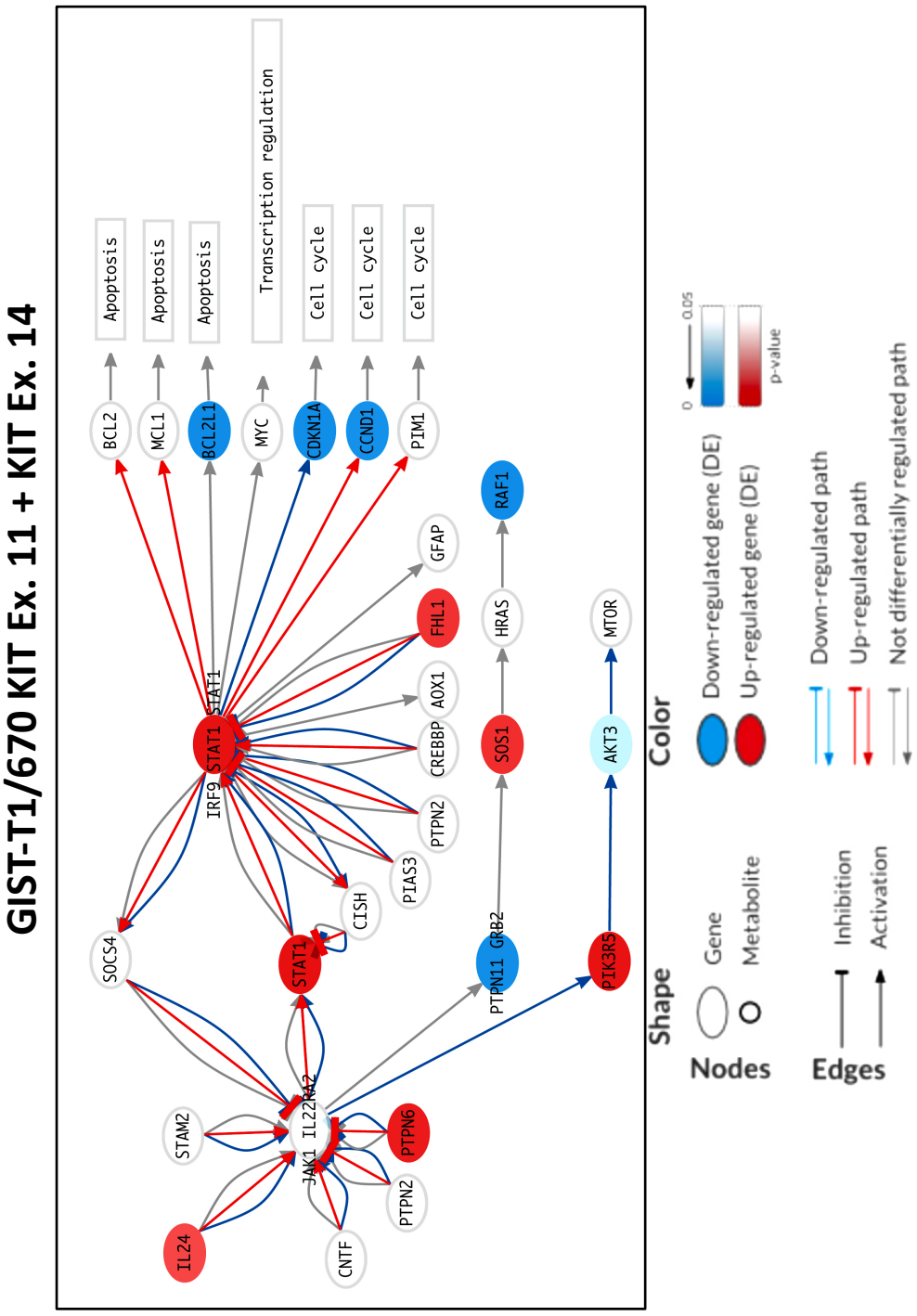

Figure 13. C) HiPathia analysis in GIST

JAK/STAT pathways showing signaling circuits differentially activated after the GIST-T1/670 cells were treated with GDC-0980 500nM 24H. Effector nodes and functions affected have been enhanced for clarity. Blue arrows indicate down-activation and red arrows up-activation.

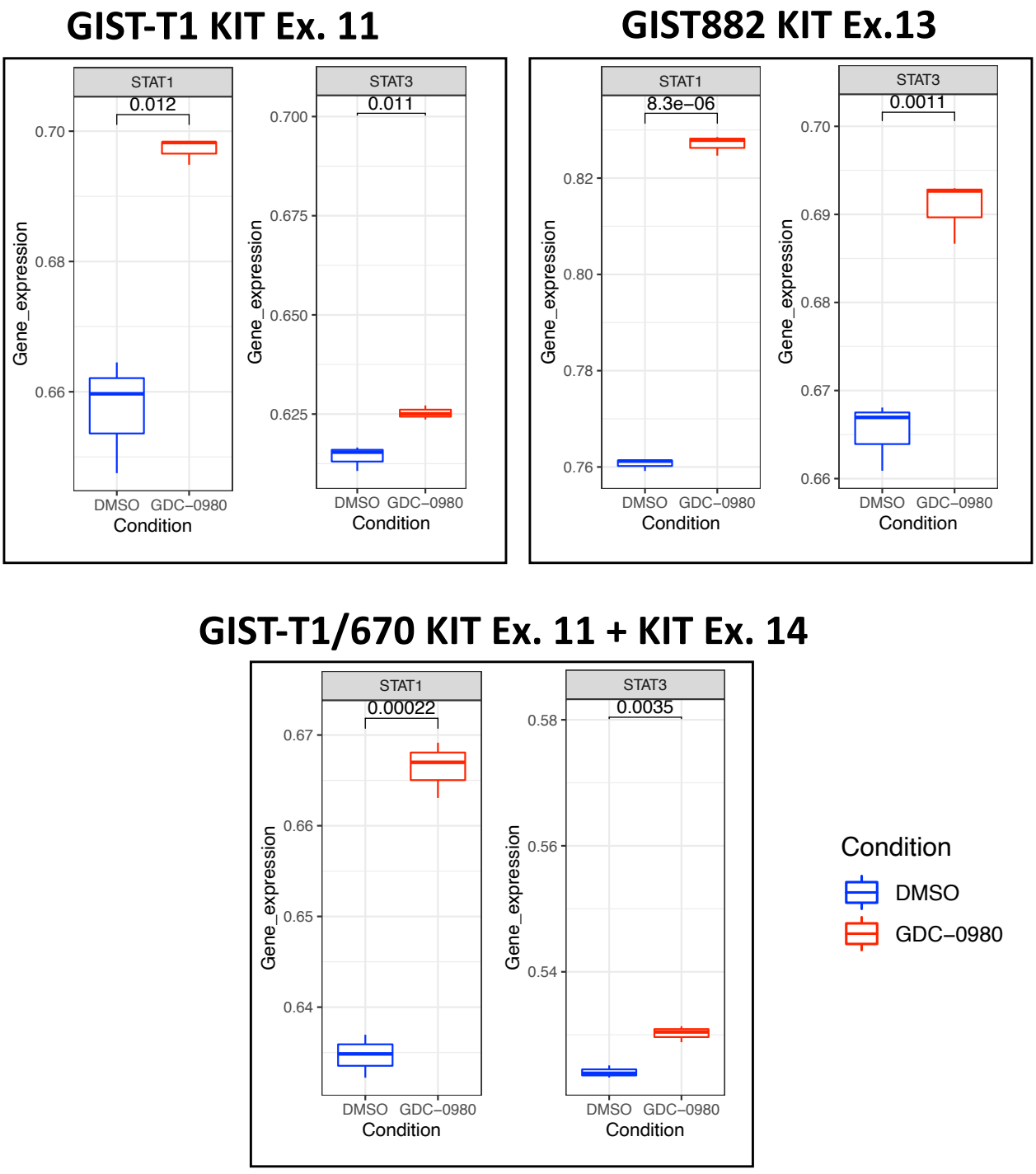

Figure 14. Boxplot of High-throughput Pathway Analysis including STAT1and STAT3 expression after 24 hours of PI3K/mTOR pathway suppression.

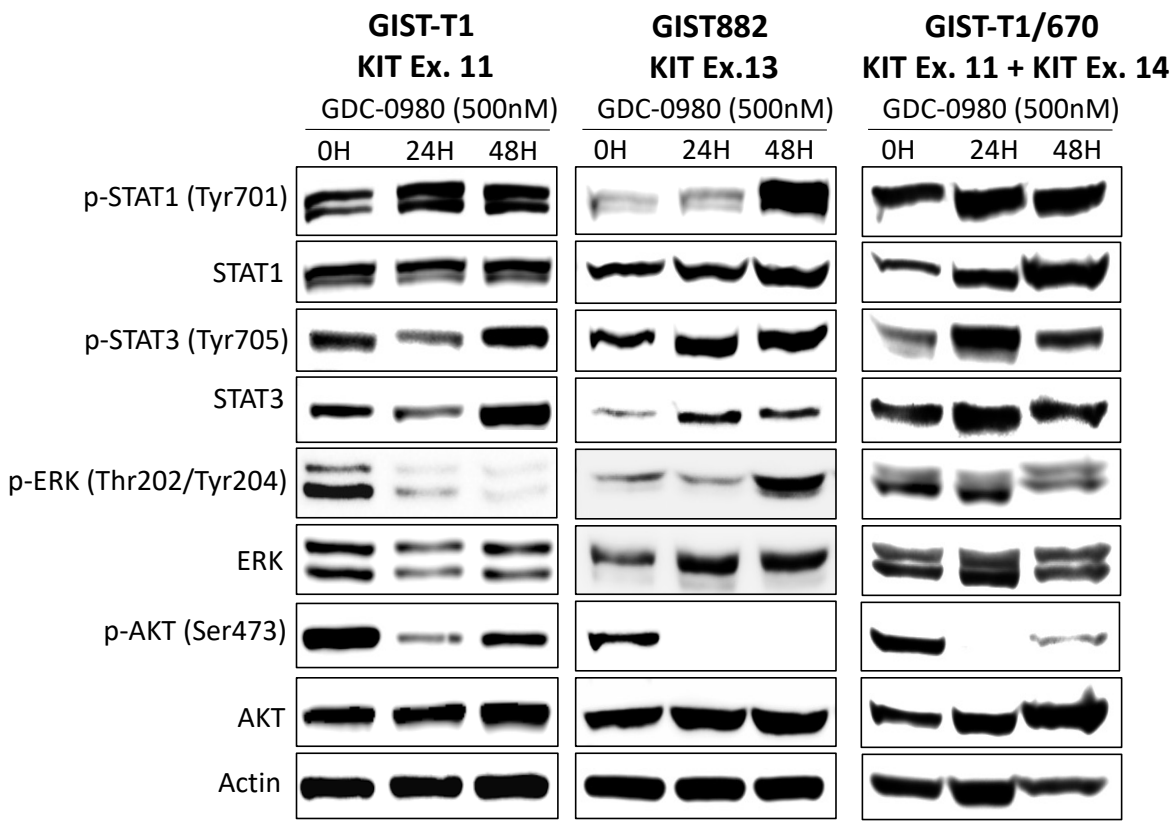

Figure 15. Immunoblot in GIST cell lines after PI3K/mTOR suppression with GDC-0980. Time points and doses are indicated in the figure.

5.3 Combined inhibition of STAT1 and PI3K/mTOR reduces cell viability, proliferation, and induces apoptosis in GIST cell lines.

To further understand the biological role and the therapeutic potential of the JAK/STAT pathway upon PI3K/mTOR signaling abrogation in GIST, we first investigated whether combined PI3K/mTOR and JAK/STAT pathways blockage could result have anti-proliferative and/or pro-apoptotic consequences. To this end, we first performed STAT1 knockdown using two different shRNAs, followed by the pharmacological suppression of the PI3K/mTOR pathway with GDC-0980 at 24 and 48 hours. This was undertaken in imatinib-sensitive GIST-T1 and in the imatinib-resistant subline GIST-

T1/670. In STAT1 shRNA-silenced cells, the absence of JAK/STAT rebound upon PI3K/mTOR inhibition with GDC-0980 resulted in decreased levels of Cyclin A and PCNA, two well-known proliferation markers in GIST. Furthermore, we observed an increase in Cleaved PARP, as a marker of apoptosis (Figure 16). These anti-proliferative and pro-apoptotic effects firstly observed in western blot in at least one time point, were also confirmed in apoptosis and cell proliferation assays, as shown in Figure 17 and Figure 18, respectively. Importantly, we observed that the absence of JAK/STAT signaling rebound due to shRNA knockdown after PI3K/mTOR pathway blockade with GDC-0980 treatment led to a sustained anti-proliferative effect in *in vitro* experiments. (Figure 18).

Similar synergistic effects obtained with shRNA knockdown of STAT1 were found after pharmacological suppression with fludarabine, a chemotherapeutic agent with off-target inhibitory activity against STAT1. Fludarabine treatment achieved a reduction in the phosphorylation levels of STAT1, mainly in the imatinib-sensitive GIST models (GIST-T1 and GIST882). The co-treatment with fludarabine (STAT1 inhibition) and GDC-0980 (PI3K/mTOR inhibition) resulted in apoptosis induction in all GIST cell models, as assessed by cleaved PARP (Figures 19). In addition, we observed a higher apoptosis induction in the combination strategy, confirmed by the increased activity of caspase 3/7 in all GIST cell lines (Figure 20). Together, the collective data suggests that JAK/STAT pathway does not have any obvious relevant role under normal conditions in GIST (constitutive activation of KIT and KIT downstream pathways). However, JAK/STAT seems to exert essential regulation of cell proliferation and

evasion of apoptosis as a consequence of the blockade of PI3K/mTOR signaling. Suppression of both pathways leads to a significant induction of apoptosis and decreased proliferation of GIST. Therefore, our results point out that the compensatory activation of the JAK/STAT pathway can be the oncogenic mechanism potentially responsible for the therapeutic adaptation to PI3K/mTOR targeted inhibition in GIST, thereby explaining their failure in clinical trials.

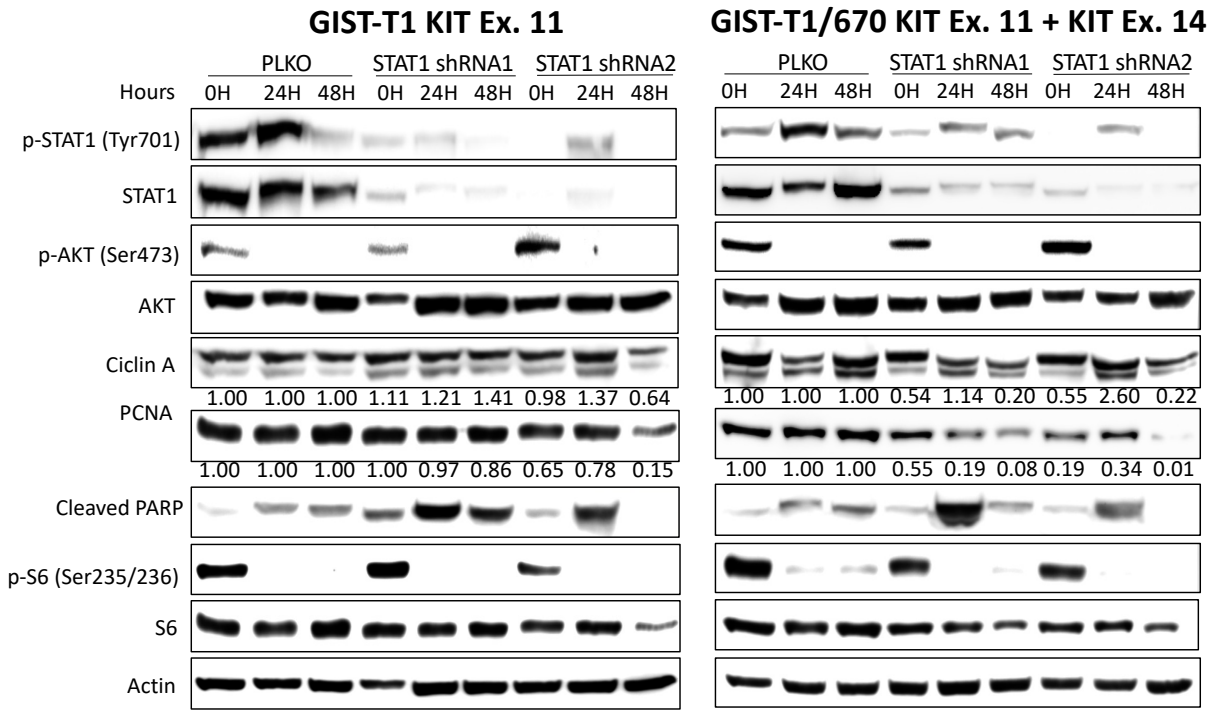

Figure 16. Knockdown of STAT1 in GIST cell lines and treated with GDC-0980.

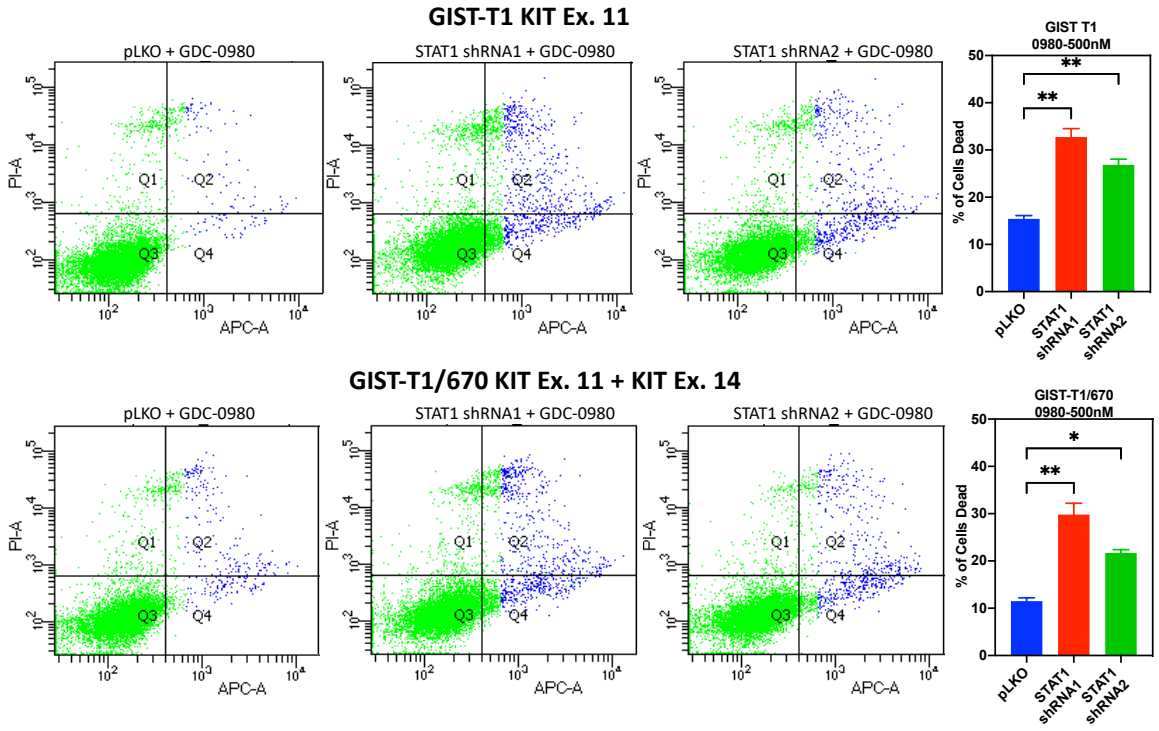

Figure 17. Apoptosis assay in GIST

Anexin V after STAT1 shRNA and PI3K/mTOR suppression in GIST cell lines. GIST cells infected with shSTAT1 were treated with GDC-0980 (500nM) for 48 h. Cell death was measured by propidium iodide (PI) and Annexin V staining (right panel). The bar

plots (left) show the quantification of the percentage of apoptosis induction in STAT1 knockdown versus pLKO. Differences between treatments were considered to be significant with a p-value, * ≤ 0.05; ** ≤ 0.005; *** ≤ 0.001; **** ≤ 0.0001.

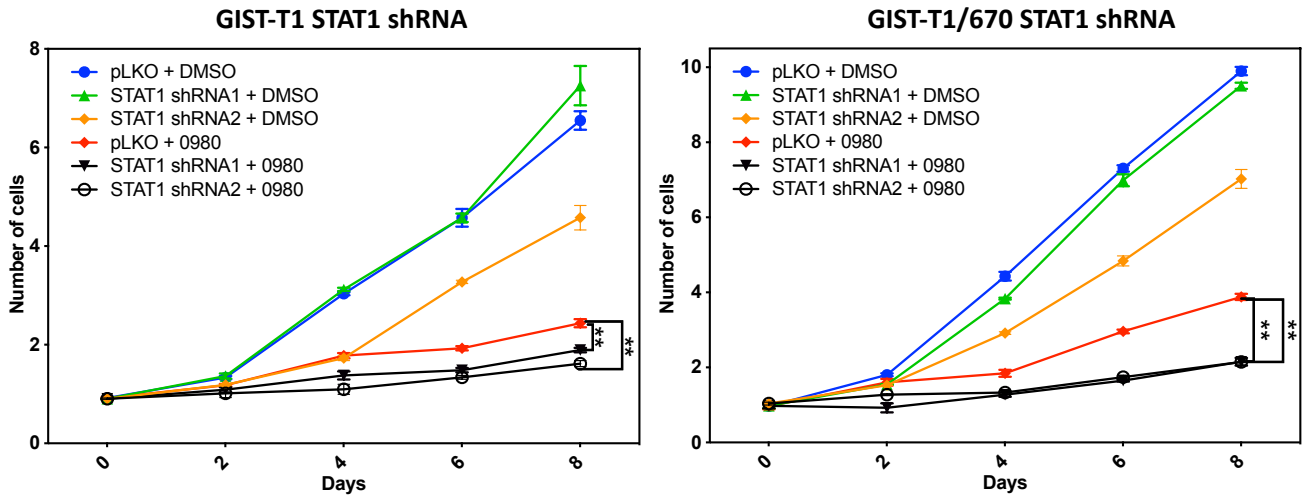

Figure 18. Proliferation assay in GIST.

Proliferation assay after STAT1 knockdown and PI3K/mTOR suppression in GIST cell lines. GDC-0980 dose: 500nM. Differences between treatments were considered to be significant with a p-value, * ≤ 0.05; ** ≤ 0.005; *** ≤ 0.001; **** ≤ 0.0001.

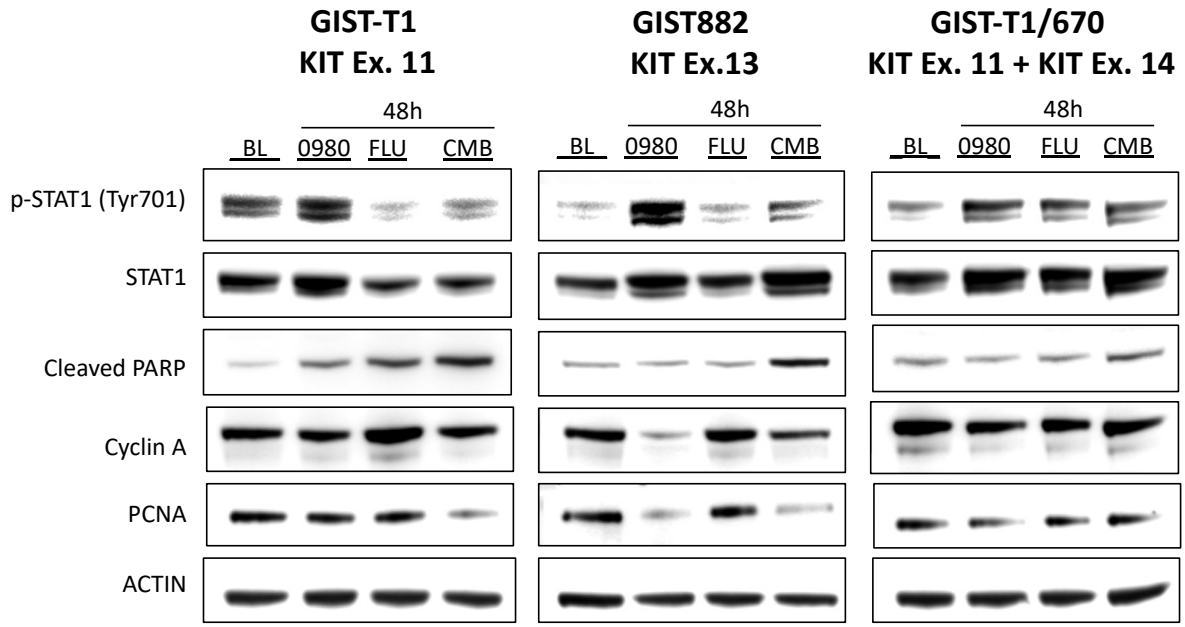

Figure 19. Immunoblot suppressing STAT1 with Fludarabine 50uM and PI3K/mTOR with GDC-0980 500nM 48h in GIST cell lines

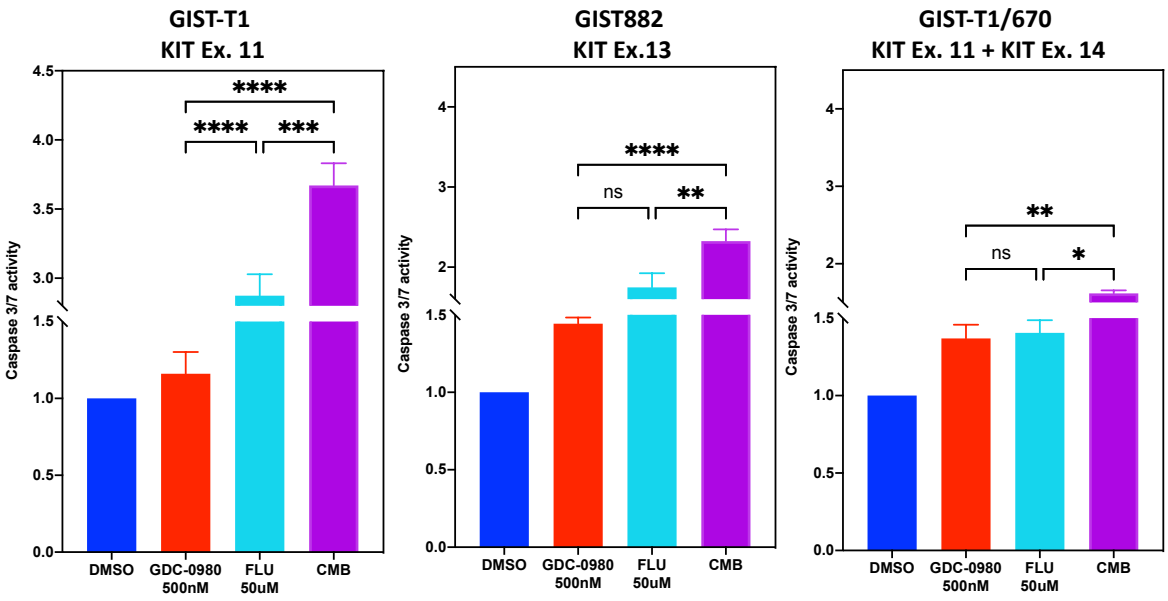

Figure 20. Apoptosis assay suppressing STAT1 with Fludarabine and PI3K/mTOR pathway in GIST cell lines. Doses are expressed in the figure. Differences between treatments were considered to be significant with a p-value, * ≤ 0.05; ** ≤ 0.005; *** ≤ 0.001; **** ≤ 0.0001.

5.4. Proteomics study reveals new candidates for JAK/STAT pathway upstream suppression in GIST.

To gain further insight into the molecular mechanisms leading to the crosstalk between JAK/STAT and PI3K/mTOR pathways upon the inhibition of the latter, we conducted a high-throughput proteomic study to define in an unbiassed manner potential candidates. For this purpose, we selected two GIST models, one imatinib-sensitive (GIST-T1) and one imatinib-resistant (GIST-T1/670), which were incubated in the absence or presence of GDC-0980 500 nM for 48 hours. We identified and quantified a total of 4.051 proteins and 5.075 peptides (Figure 20). In order to identify critical dysregulated proteins, we performed a protein set enrichment analysis (PSEA). The fold changes of proteins increased or decreased in both GIST cell models upon GDC-

0980 treatment was compared to untreated controls and analyzed through PSEA. Several biological processes were shown to be enriched, being the most interesting the spliceosome, and pathways in cancer (upregulated), and focal adhesion and metabolic pathways (underregulated) (Figure 21 A). Several genes potentially related to the JAK/STAT pathway explained the enrichment in “pathways in cancer”. The enrichment score for this pathway was mainly given enriched proteins such as FGFR1, TGFB1, MSH3, STAT2, PLCB4, and STAT1 (Figure 21 B).

Because total FGFR1 increase was found to be one of the top upregulated proteins, we analyzed the phospho-proteome data to farther address activation of pathways. Indeed, phospho-proteome and correlative western blot studies found an increase in FGFR1 phosphorylation followed by the downstream phosphorylation of STAT1, STAT3, SHP2, and PLCG1 (Figure 22).

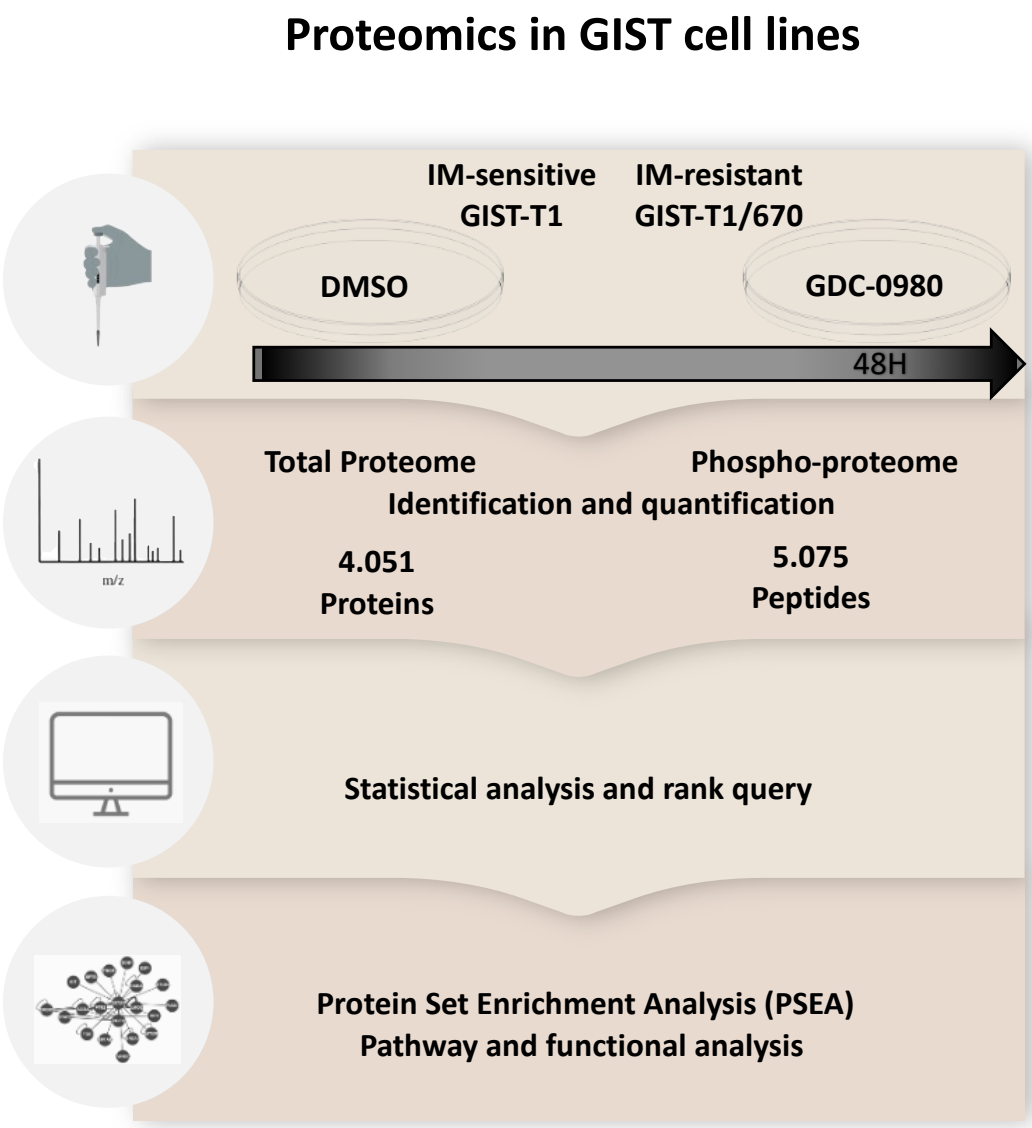

Figure 20. Proteomics in GIST cell lines

Two GIST imatinib-sensitive (GIST-T1) and imatinib-resistant (GIST-T1/670) GIST cell lines were treated for 48H with GDC-0980 500 nM and compared with untreated cells at baseline. Mass spectrometry analysis were focused on the total proteome and phopho-proteome for identification of proteins/peptides regulated by PI3K/mTOR KIT-downstream pathway.

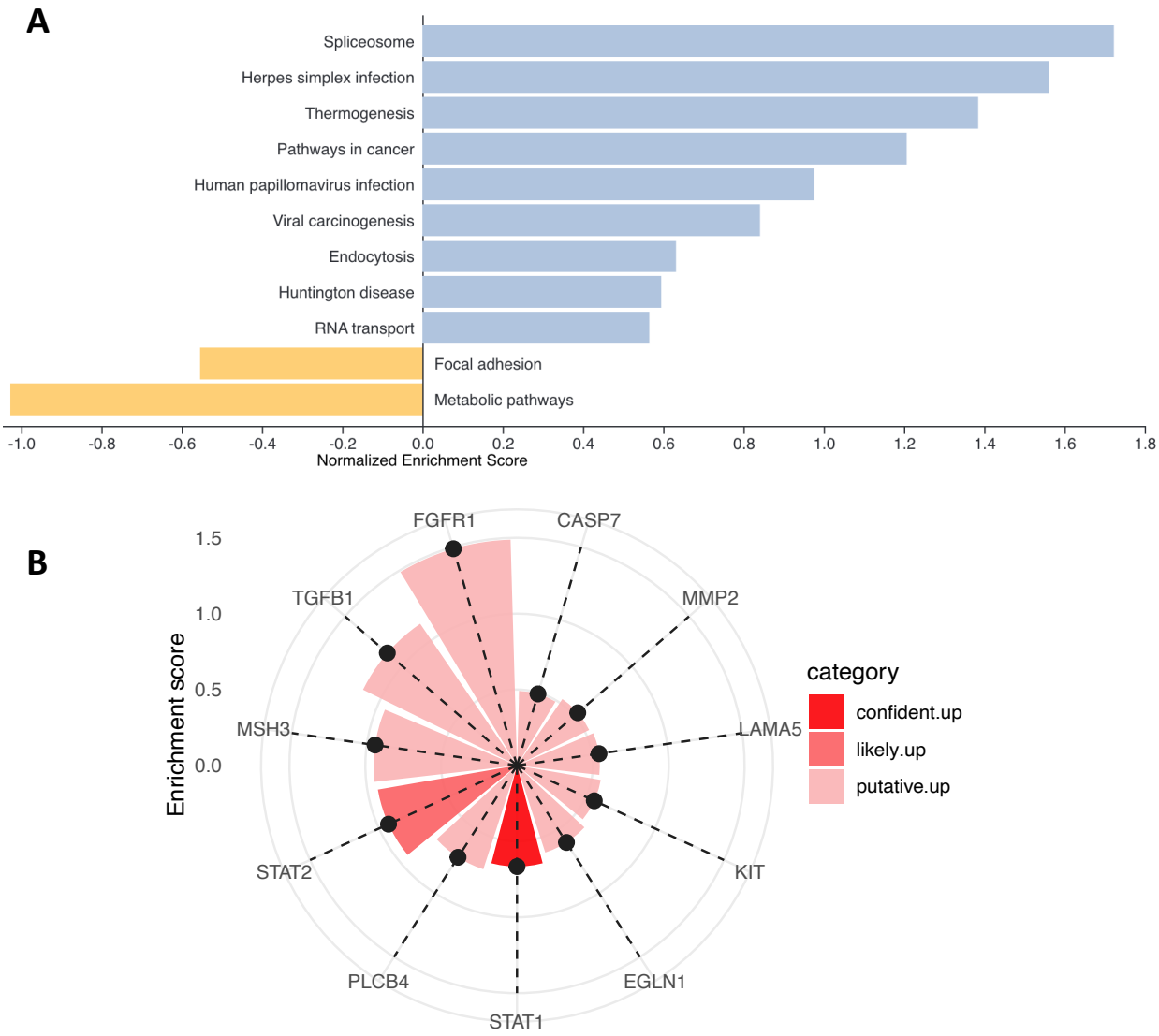

Figure 21. Protein set enrichment analysis (PSEA) in GIST.

GIST-T1 and GIST-T1/670 after 48 hours of PI3K/mTOR suppression. Horizontal bar-plot represent the enriched pathways (A). The circular bar-plot represent the proteins involved in the enrichment score of the pathways in cancer (B). Different statistical scores where applied to establish the confidence of the change in phospho-proteomic levels (confident, likely and putative).

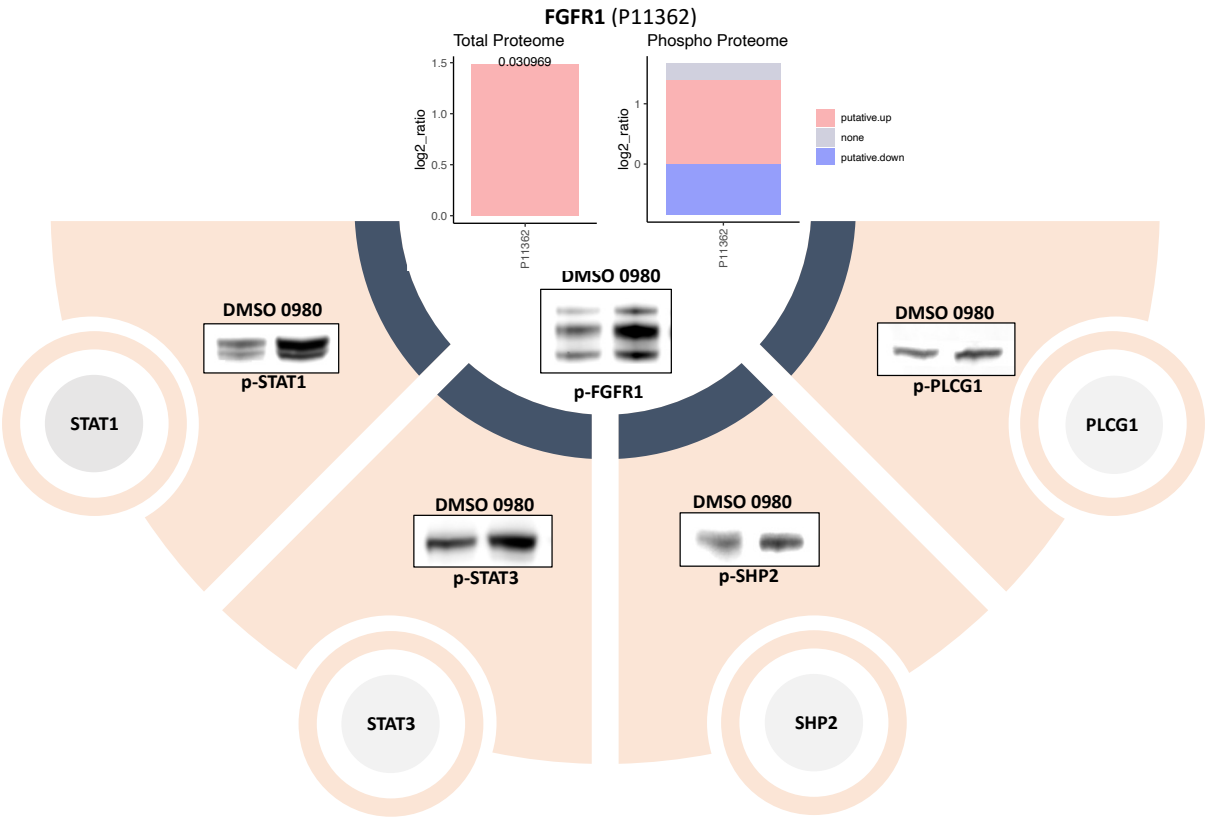

Figure 22. Total proteome and phosphor-proteome of FGFR1

Proteome/phospho-proteome (upper) and immunoblot representing the phosphorylated proteins of FGFR1 downstream pathway (lower) in GIST after PI3K/mTOR suppression

5.5. Therapeutic strategy to maximize the response to PI3K inhibition in GIST.

We have shown that the therapeutic adaptation to PI3K/mTOR pathway inhibition results from FGFR1-dependent JAK/STAT pathway activation. In the absence of available targeted STAT1 inhibitors, the documented FGFR1 crosstalk emerges as a promising approach to uncovering a new therapeutic strategy in GIST.

Therefore, we next asked whether we could maximize the therapeutic effect of PI3K/mTOR pathway inhibition with GDC-0980 treatment by co-targeting the

compensatory activation of STAT1 and STAT3 through FGFR1 inhibition. Interestingly, and as shown in Figure 23, low concentration of a pan-FGFR inhibitor (LY2874455) achieved an additive effect with GCD-0980 500nM. This effect was mediated by decreasing the phosphorylation of STAT1 and STAT3 in all three GIST models, leading to a reduction in the protein levels of the proliferative markers Cyclin A and PCNA, together with an increased in the apoptotic marker Cleaved PARP (Figure 23). This synergistic effect was further confirmed in cell viability assays (Figure 24). In addition, we observed an apoptosis induction increasing the Caspase 3/7 activity (Figure 25) and a significant decrease in cell proliferation in all studied GIST models (Figure 26). Together, these data provide strong evidence that FGFR1 is a critical upstream target for the suppression of the compensatory activation of JAK/STAT signaling, and therefore it emerges as a potential novel combination strategy for the treatment of GIST based the combined inhibition of PI3K/mTOR and JAK/STAT pathways in GIST regardless the type of primary or secondary KIT mutation.

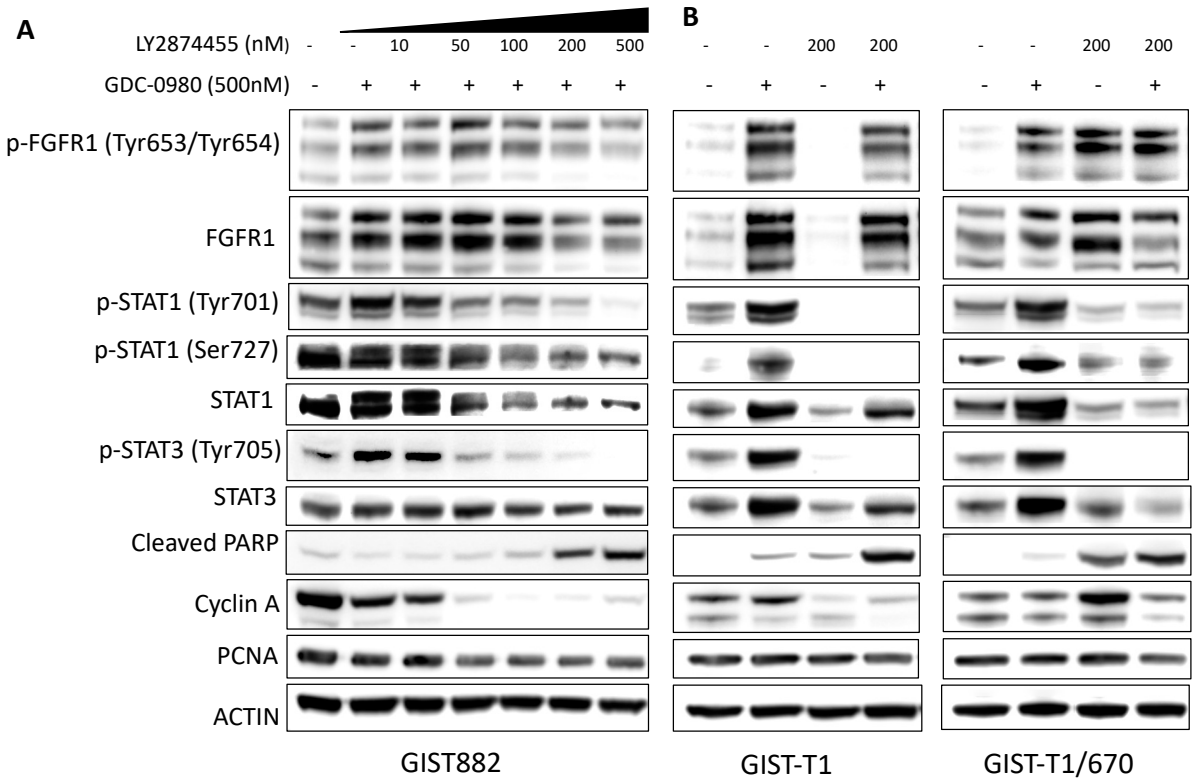

Figure 23. Immunoblot of GIST cell lines.

A GIST882 treated with GDC-0980 and LY2874455 (Pan FGFRi) for 48H in increasing concentration. B GIST-T1 and GIST-T1/670 treated with GDC-0980 and 200nM of LY2874455 for 48H.

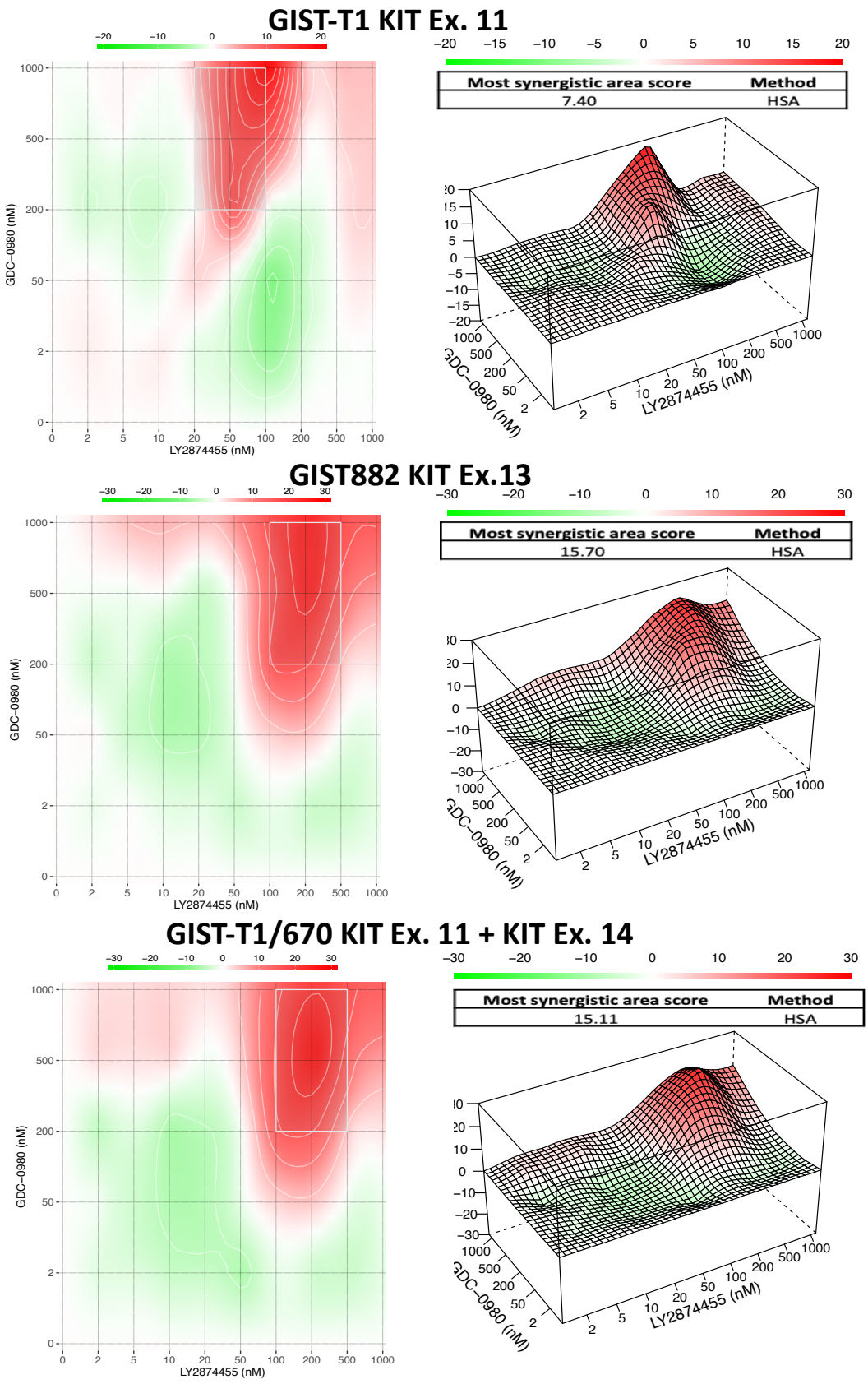

Figure 24. Cell Viability assay in GIST cell lines

Heatmap and Surface plots for drug combinations of LY2874455 and GDC-0980 in a range 1 to 1000 nM. HSA synergy score was applied in all three GIST cell lines.

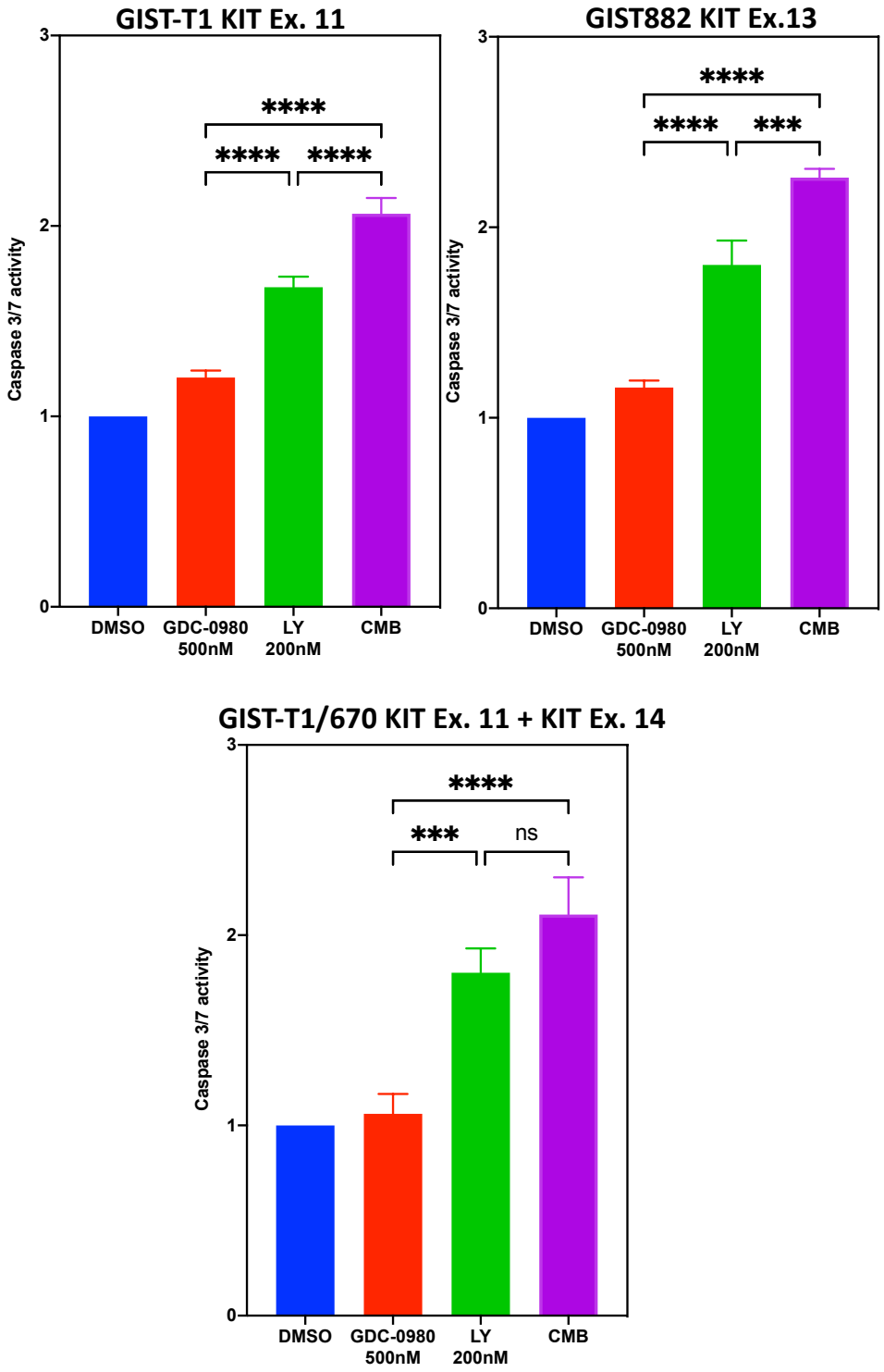

Figure 25. Apoptosis assay in GITS.

Bar-plot representing the suppression of FGFR1 with LY2874455 and the GDC-0980 in GIST cell lines. Doses are expressed in the figure. Differences between treatments were considered to be significant with a p-value, * ≤ 0.05; ** ≤ 0.005; *** ≤ 0.001; **** ≤ 0.0001.

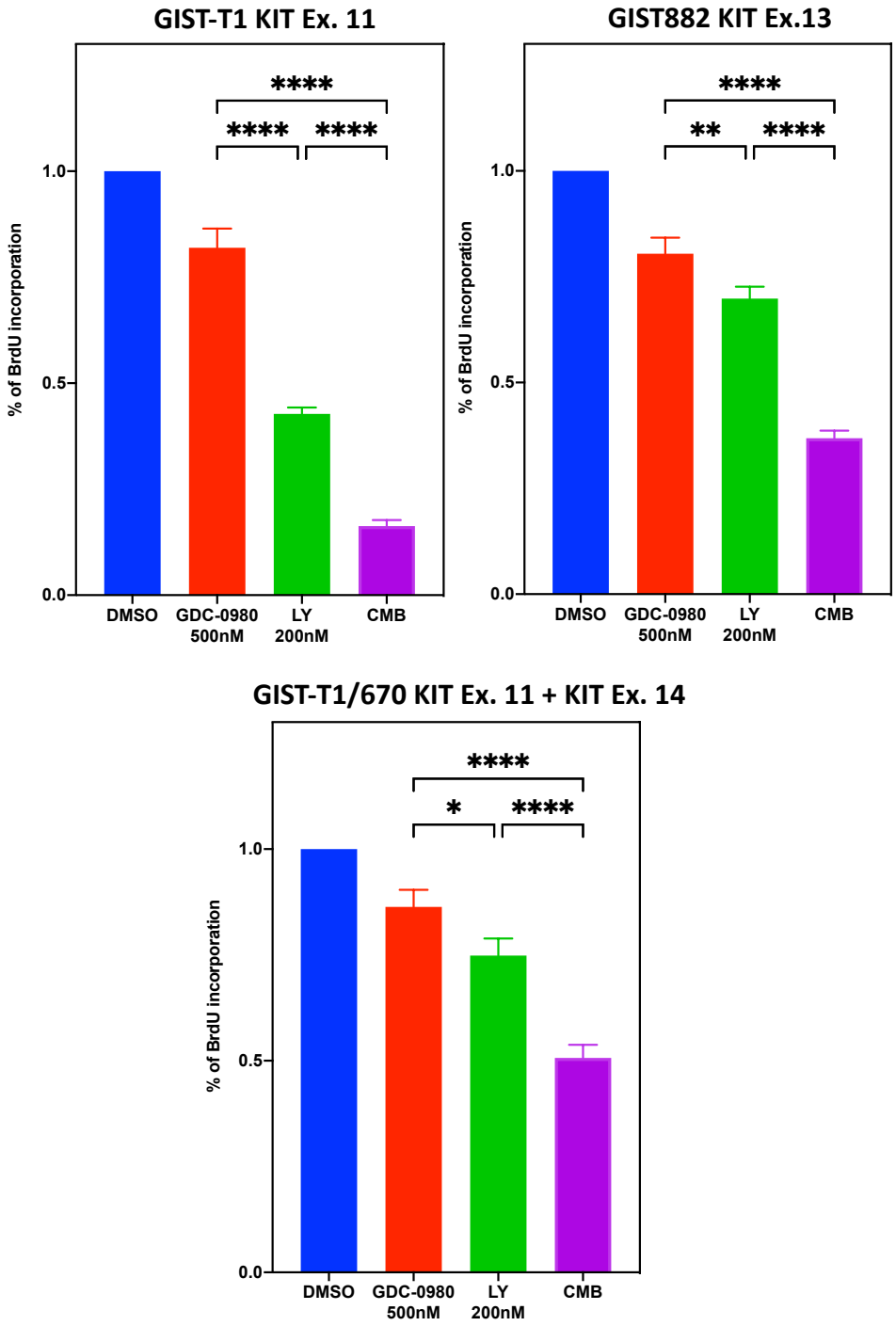

Figure 26. Proliferation assay in GIST

Bar-plot of the antiproliferative effect suppressing with LY2874455 and GDC-0980 in GIST cell lines. Doses are expressed in the figure. Differences between treatments were considered to be significant with a p-value, * ≤ 0.05; ** ≤ 0.005; *** ≤ 0.001; **** ≤ 0.0001.

DISCUSSION

6. DISCUSSION

Targeted therapy is the only efficient therapeutic strategy in the treatment of GIST. The inhibitors for KIT and PDGFRA have grown exponentially in the last two decades, revolutionizing and transforming GIST as an excellent model of genomically-driven disease. Considering that KIT or PDGFRA activation occurs in up to 85% of all GISTs, their inhibition by TKIs has become the primary therapeutic modality for the treatment of metastatic disease. The TKIs currently approved in GIST are imatinib, sunitinib, regorafenib, avapritinib and ripretinib. Unfortunately, the benefit obtained with KIT inhibitors after progression to imatinib is relatively modest, and the prognosis for these patients is ominous after successive lines of treatment. Therefore, it is essential to better understand the mechanisms responsible for adaptation and resistance to KIT inhibition in order to be able to design new therapeutic strategies in multiresistant GISTs.

PI3K/mTOR is an essential signaling pathway downstream of oncogenic KIT, regardless of the type of primary or secondary KIT mutation, because it regulates GIST cell survival, protein synthesis, and translation control (69,87). Despite the relevance of PI3K/mTOR signaling in GIST and the promising results of preclinical studies assessing targeting agents against the PI3K/mTOR pathway (78,87,127), the activity observed in clinical trials with these inhibitors has been limited (88–90). Therefore, therapeutic inhibition of PI3K/mTOR in GIST patients appears to produce a more modest clinical benefit than initially expected. Herein, we aimed to investigate whether alternative biological mechanisms collaborated in circumventing targeted PI3K/mTOR

blockade and that could also explain above clinical observations. To do so, we used in-depth transcriptomics and proteomics studies followed by subsequent functional validations to shed light on the adaptative mechanisms involved in the resistance to PI3K/mTOR inhibitors in GIST.

For this purpose, we used three clinically representative GIST cell models, two imatinib-sensitive and one imatinib-resistant. Our starting point was the *in-vitro* studies, where we observed a difference in the biological effect between the short-term versus long-term experiments (Figures 6 to 9). In the long-term assays, we identified that the suppression of the PI3K/mTOR pathway did not achieve a significant antiproliferative effect, which lead us to hypothesize that this lack of antiproliferative effect along the days could be a consequence of an adaptive mechanism emerging in the GIST cells triggered by PI3K/mTOR pathway inhibition. This, in turn, matches the clinical observations across clinical trials with such inhibitors in GIST. In order to elucidate this hypothesis, we generated RNA-seq data to evaluate which nodes or signaling pathways could be responsible for this potential mechanism of adaptation. In the first place, a GSEA was performed, involving in this analysis 40 signaling pathways; different alterations were found between the imatinib-sensitive and imatinib-resistant GIST cell lines. However, one single alteration was shared across the three models: the activation of the JAK/STAT signaling pathway (Figure 10). In the second place, we performed another bioinformatic analysis using HiPathia, which corroborated the activation of the JAK/STAT pathway through the overexpression of STAT1 and STAT3 (Figures 13 and 14). Interestingly, when this data was validated at the protein level,

we confirmed that this activation of the JAK/STAT pathway was fundamentally given by the activation of mainly pSTAT1, but also through pSTAT3, which indicates a new potential mechanism of resistance in GIST.

These results are consistent with reports in the literature describing the increased levels of phospho-STAT1 and phospho-STAT3 in other cancer models in the context of treatment resistance. In breast cancer models, different studies have demonstrated that increased STAT3 phosphorylation predicts intrinsic resistance to chemotherapeutic drugs due to the upregulation of antiapoptotic factors Mcl-1, Bcl-xL, Bcl-2, and survival (128–130). In addition, Fantin et al. showed that increased nuclear STAT1 and phospho-STAT3 staining in cutaneous T-cell lymphoma (CTCL) cells was associated with a lack of clinical response to vorinostat. Consequently, the authors proposed that inhibiting this pathway might result in a better response to the treatment with vorinostat for CTCL patients (131). The critical role of STAT1 and STAT3 proteins in KIT signaling has been extensively characterized in non-GIST models (132–134).

JAK/STAT pathway has been previously studied in GIST. Duensing et al. showed constitutive STAT1 and STAT3 activation in most primary GIST (70). Additionally, other research indicates that the activation of STAT1 and STAT3 in GIST is partially dependent on KIT (71). Finally, the inhibition of KIT with imatinib resulted in partial inhibition of STAT1 and STAT3 phosphorylation in both imatinib-sensitive and imatinib-resistant GIST models (69).

A recent study reported that constitutive activation of STAT1 from KIT is low in unstimulated GIST cell lines (135), which is consistent with our findings of low levels

of phosphorylated STAT1 in untreated GIST cell lines. On the contrary, after the suppression of the PI3K/mTOR pathway, we observed an increase in the phosphorylation of STAT1 and STAT3; this effect could be due to compensatory mechanism.

In tumorigenesis, STAT1 and STAT3 may play diverse oncogenic roles. STAT1 is involved in a complex series of signaling pathways related to the evasion of apoptosis and facilitating sustained tumor growth, survival, and resistance to therapies (136–138), while the activation of STAT3 is associated with tumor progression and nearly 70% of all solid and hematologic tumors have been reported to be associated with constitutive activation of STAT3 (139–142).

The activation of STAT1 and STAT3 proteins is an important biological process that in cancer can be triggered by extracellular, intracellular or transcriptional proteins. Extracellular upstream RTKs such as EGFR, FGFR, HER2 and KIT can activate STAT1 and STAT3 directly (134,143–145), or indirectly mediating this activation by other intracellular non-receptor tyrosine kinases like JAK families or Src (146,147). This activation also can be related by the interaction with other transcriptional factors like other STATs members, IRF9 or JUN (148,149). Considering this wide variety of proteins related to STAT1 and STAT3 activation, we chose proteomics due to its ability to analyze multiple proteins in a high-throughput manner in order to evaluate our hypothesis that compensatory mechanisms could mediate resistance to GDC-0980. Consequently, we carried out an in-depth proteomic characterization in two GIST models, one imatinib-sensitive and the other imatinib-resistant, treated with GDC-0980

(Figure 20), aiming to explore new mechanisms of acquired resistance through STAT1 and STAT3 that would allow us to identify potential new targets in GIST. For this purpose, we analyzed the total proteome data; performing a PSEA we showed the activation of pathways in cancer and the enrichment of this activation was predominantly due to FGFR1 increase (Figure 21). Different studies suggested that drug resistance is usually attributed to mutations in the drug-targeted genes (150,151); however, additional mechanisms of drug resistance have also gradually been discovered. For example, a recent study demonstrated that cell lineage alterations accompany drug resistance in prostate cancer. The findings revealed that the lineage transformation present in prostate cancer originates from epithelial cells as defined by a mixed lumen–basal phenotype. Additionally, JAK/STAT and FGFR signaling pathways were determined to be the core elements in inducing castration-tolerant or castration-resistant traits in prostate cancer. Subsequently, dual strategies comprising of targeting both pathways have shown potential in reprogramming tumor cells to be more responsive to AR-targeted therapies (152). Among the proteins potentially regulated by FGFR1 are STAT1, STAT3, SHP2, and PLCG1 (144,153,154), and all of them were increased after the suppression of the PI3K/mTOR pathway (Figure 22).

In this context, and given the potential crosstalk PI3K/mTOR > FGFR1 > JAK/STAT, we evaluated the effect of a pan-FGFR inhibitor in GIST cell lines. A dramatic reduction in STAT1, and STAT3 phosphorylation was achieved at low concentrations of this pan-FGFR inhibitor, achieving a synergistic effect in combination with PI3K/mTOR

inhibition (Figure 23), with an impact on the reduction of cell viability, proliferation and induction of apoptosis (Figures 24 to 26).

FGFR1 has been described as an oncogene in many types of cancer, and FGFR1 overexpression is involved in drug resistance in different tumors, including lung cancer, breast cancer, and bladder cancer (155–159).Various preclinical and clinical studies have evaluated the role of FGFR inhibitors in solid tumors (160–163). In the majority of these trials, the most widespread selection biomarker has been FGFR1 amplification. Likewise, there are preclinical studies with a rationale to target both: FGFR and the PI3K/mTOR pathway by combining selective inhibitors of both signaling pathways, demonstrating a synergistic effect with drugs directed at FGFR to counteract the resistance to the PI3K/mTOR pathway (164,165). These findings are similar to the results presented in this thesis since the activation of pSTAT1 and pSTAT3 after treatment with GDC-0980 was suppressed with the combination of a pan-FGFR inhibitor in our GIST models.

Collectively, we identified a novel mechanism that explain the resistance to PI3K/mTOR pathway suppression in GIST: PI3K/mTOR pathway inhibition is followed by specific transcriptomic and proteomic changes that trigger an alternative adaptive mechanism involving activation of FGFR1 and the JAK/STAT pathway. Target suppression of this compensatory mechanism could represent a new treatment strategy for GIST patients.

CONCLUSIONS

7. CONCLUSIONS

- Our results point to the compensatory activation of the JAK/STAT pathway as the main oncogenic mechanism responsible for the therapeutic adaptation to the inhibition of PI3K/mTOR in GIST. Its relation in GIST is fundamentally given by STAT1 and, to a lesser extent, STAT3.

- Our studies highlight the crucial role of FGFR1 oncogenic signaling and its impact through the JAK/STAT pathway on cell viability, cell proliferation, and apoptosis in GIST cell lines.

- The expression of FGFR1 in GIST cell lines after PI3K/mTOR suppression has a pro-oncogenic effect due to the activation of FGFR1, which leads to the downstream activation of the JAK/STAT pathway.

- A new strategy of combination therapy with PI3K/mTOR inhibitor and anti-FGFR could represent a new therapeutic approach for patients with GIST, thus hindering the emergence of the FGFR/JAK/STAT scape mechanism.

FUTURE LINES

8. FUTURE LINES

These results obtained as part of this doctoral thesis, have allowed us to present these preclinical evidence where we have shown that the JAK/STAT pathway plays an essential role in the adaptative resistance mechanism interacting with the PI3K/mTOR pathway in GIST, in both models sensitive and resistant to imatinib. However, further validation and further studies are required for them to be relevant from a translational perspective. In this sense, we will continue validating these discoveries with *in-vivo* studies in different models of GIST, both sensitive and resistant to imatinib. In addition, we will explore how suppression of the PI3K/mTOR and JAK/STAT pathways may affect other factors of GIST cell biology, such as migration and invasion. We will also investigate how the critical dysregulated proteins identified in this study can be used as biomarkers to predict response to therapy directed against the PI3K/mTOR pathway in GIST patients. Finally, we hope these studies will enable us to develop new, more effective, and personalized therapies for treating GIST, thereby improving clinical outcomes for patients with this disease.

BIBLIOGRAPHIC REFERENCES

9. BIBLIOGRAPHIC REFERENCES

1. Helman LJ, Meltzer P. Mechanisms of sarcoma development. Nat Rev Cancer. 2003 Sep;3(9):685–94.

2. Mazur MT, Clark HB. Gastric stromal tumors. Reappraisal of histogenesis. Am J Surg Pathol. 1983 Sep;7(6):507–19.

3. Schaldenbrand JD, Appelman HD. Solitary solid stromal gastrointestinal tumors in von Recklinghausen's disease with minimal smooth muscle differentiation. Hum Pathol. 1984 Mar;15(3):229–32.

4. Hirota S, Isozaki K, Moriyama Y, Hashimoto K, Nishida T, Ishiguro S, et al. Gain-of-function mutations of c-kit in human gastrointestinal stromal tumors. Science. 1998 Jan 23;279(5350):577–80.

5. Hirota S, Ohashi A, Nishida T, Isozaki K, Kinoshita K, Shinomura Y, et al. Gain-of-function mutations of platelet-derived growth factor receptor alpha gene in gastrointestinal stromal tumors. Gastroenterology. 2003 Sep;125(3):660–7.

6. Heinrich MC, Corless CL, Duensing A, McGreevey L, Chen CJ, Joseph N, et al. PDGFRA activating mutations in gastrointestinal stromal tumors. Science. 2003 Jan 31;299(5607):708–10.

7. Joensuu H, Roberts PJ, Sarlomo-Rikala M, Andersson LC, Tervahartiala P, Tuveson D, et al. Effect of the tyrosine kinase inhibitor STI571 in a patient with a metastatic gastrointestinal stromal tumor. N Engl J Med. 2001 Apr 5;344(14):1052–6.

8. Buchdunger E, Cioffi CL, Law N, Stover D, Ohno-Jones S, Druker BJ, et al. Abl protein-tyrosine kinase inhibitor STI571 inhibits in vitro signal transduction mediated by c-kit and platelet-derived growth factor receptors. J Pharmacol Exp Ther. 2000 Oct;295(1):139–45.

9. Heinrich MC, Griffith DJ, Druker BJ, Wait CL, Ott KA, Zigler AJ. Inhibition of c-kit receptor tyrosine kinase activity by STI 571, a selective tyrosine kinase inhibitor. Blood. 2000 Aug 1;96(3):925–32.

10. Demetri GD, von Mehren M, Blanke CD, Van den Abbeele AD, Eisenberg B, Roberts PJ, et al. Efficacy and safety of imatinib mesylate in advanced gastrointestinal stromal tumors. N Engl J Med. 2002 Aug 15;347(7):472–80.

11. Verweij J, Casali PG, Zalcberg J, LeCesne A, Reichardt P, Blay JY, et al. Progression-free survival in gastrointestinal stromal tumours with high-dose imatinib: randomised trial. Lancet. 2004 Oct 25;364(9440):1127–34.

12. Blanke CD, Demetri GD, von Mehren M, Heinrich MC, Eisenberg B, Fletcher JA, et al. Long-term results from a randomized phase II trial of standard- versus higher-dose imatinib mesylate for patients with unresectable or metastatic gastrointestinal stromal tumors expressing KIT. J Clin Oncol. 2008 Feb 1;26(4):620–5.

13. Demetri GD, van Oosterom AT, Garrett CR, Blackstein ME, Shah MH, Verweij J, et al. Efficacy and safety of sunitinib in patients with advanced gastrointestinal stromal tumour after failure of imatinib: a randomised controlled trial. Lancet. 2006 Oct 14;368(9544):1329–38.

14. Demetri GD, Reichardt P, Kang YK, Blay JY, Rutkowski P, Gelderblom H, et al. Efficacy and safety of regorafenib for advanced gastrointestinal stromal tumours after failure of imatinib and sunitinib (GRID): an international, multicentre, randomised, placebo-controlled, phase 3 trial. Lancet. 2013 Jan 26;381(9863):295–302.

15. Blay JY, Serrano C, Heinrich MC, Zalcberg J, Bauer S, Gelderblom H, et al. Ripretinib in patients with advanced gastrointestinal stromal tumours (INVICTUS): a double-blind, randomised, placebo-controlled, phase 3 trial. The Lancet Oncology. 2020 Jul;21(7):923–34.

16. Heinrich MC, Jones RL, von Mehren M, Schöffski P, Serrano C, Kang YK, et al. Avapritinib in advanced PDGFRA D842V-mutant gastrointestinal stromal tumour (NAVIGATOR): a multicentre, open-label, phase 1 trial. Lancet Oncol. 2020;21(7):935–46.

17. Miettinen M, Lasota J. Gastrointestinal stromal tumors--definition, clinical, histological, immunohistochemical, and molecular genetic features and differential diagnosis. Virchows Arch. 2001 Jan;438(1):1–12.

18. Murphy JD, Ma GL, Baumgartner JM, Madlensky L, Burgoyne AM, Tang CM, et al. Increased risk of additional cancers among patients with gastrointestinal stromal tumors: A population-based study: Increased Cancer Risk in GIST Patients. Cancer. 2015 Sep 1;121(17):2960–7.

19. Ducimetière F, Lurkin A, Ranchère-Vince D, Decouvelaere AV, Péoc'h M, Istier L, et al. Incidence of sarcoma histotypes and molecular subtypes in a prospective epidemiological study with central pathology review and molecular testing. PLoS ONE. 2011;6(8):e20294.

20. Nilsson B, Bümming P, Meis-Kindblom JM, Odén A, Dortok A, Gustavsson B, et al. Gastrointestinal stromal tumors: The incidence, prevalence, clinical course, and prognostication in the preimatinib mesylate era: A population-based study in Western Sweden. Cancer. 2005 Feb 15;103(4):821–9.

21. van der Graaf WTA, Tielen R, Bonenkamp JJ, Lemmens V, Verhoeven RHA, de Wilt JHW. Nationwide trends in the incidence and outcome of patients with gastrointestinal stromal tumour in the imatinib era. Br J Surg. 2018 Jul;105(8):1020–7.

22. Corless CL, Heinrich MC. Molecular Pathobiology of Gastrointestinal Stromal Sarcomas. Annual Review of Pathology: Mechanisms of Disease. 2008;3(1):557–86.

23. Rubió-Casadevall J, Borràs JL, Carmona C, Ameijide A, Osca G, Vilardell L, et al. Temporal trends of incidence and survival of sarcoma of digestive tract including Gastrointestinal Stromal Tumours (GIST) in two areas of the north-east of Spain in the period 1981-2005: a population-based study. Clin Transl Oncol. 2014 Jul;16(7):660–7.

24. Nowain A, Bhakta H, Pais S, Kanel G, Verma S. Gastrointestinal stromal tumors: clinical profile, pathogenesis, treatment strategies and prognosis. J Gastroenterol Hepatol. 2005 Jun;20(6):818–24.

25. DeMatteo RP, Lewis JJ, Leung D, Mudan SS, Woodruff JM, Brennan MF. Two hundred gastrointestinal stromal tumors: recurrence patterns and prognostic factors for survival. Ann Surg. 2000 Jan;231(1):51–8.

26. Amin MB, Edge S, Greene F, Byrd DR, Brookland RK, Washington MK, et al., editors. AJCC Cancer Staging Manual [Internet]. 8th ed. Springer International Publishing; 2017 [cited 2019 May 12]. Available from: https://www.springer.com/us/book/9783319406176

27. Edge SB, Compton CC. The American Joint Committee on Cancer: the 7th Edition of the AJCC Cancer Staging Manual and the Future of TNM. Annals of Surgical Oncology. 2010 Jun;17(6):1471–4.

28. Rammohan A, Sathyanesan J, Rajendran K, Pitchaimuthu A, Perumal SK, Srinivasan U, et al. A gist of gastrointestinal stromal tumors: A review. World J Gastrointest Oncol. 2013 Jun 15;5(6):102–12.

29. Miettinen M, Lasota J. Gastrointestinal stromal tumors: review on morphology, molecular pathology, prognosis, and differential diagnosis. Arch Pathol Lab Med. 2006 Oct;130(10):1466–78.

30. Foo WC, Liegl-Atzwanger B, Lazar AJ. Pathology of Gastrointestinal Stromal Tumors. Clin Med Insights Pathol. 2012 Jul 17;5:23–33.

31. Sepe PS, Moparty B, Pitman MB, Saltzman JR, Brugge WR. EUS-guided FNA for the diagnosis of GI stromal cell tumors: sensitivity and cytologic yield. Gastrointest Endosc. 2009 Aug;70(2):254–61.

32. Rubin BP, Blanke CD, Demetri GD, Dematteo RP, Fletcher CDM, Goldblum JR, et al. Protocol for the examination of specimens from patients with gastrointestinal stromal tumor. Arch Pathol Lab Med. 2010 Feb;134(2):165–70.

33. Eisenberg BL, Harris J, Blanke CD, Demetri GD, Heinrich MC, Watson JC, et al. Phase II trial of neoadjuvant/adjuvant imatinib mesylate (IM) for advanced primary and metastatic/recurrent operable gastrointestinal stromal tumor (GIST): early results of RTOG 0132/ACRIN 6665. J Surg Oncol. 2009 Jan 1;99(1):42–7.

34. Miettinen M, Lasota J. Gastrointestinal stromal tumors: pathology and prognosis at different sites. Semin Diagn Pathol. 2006 May;23(2):70–83.

35. Castelguidone E de L di, Messina A. GISTs - Gastrointestinal Stromal Tumors [Internet]. Mailand: Springer-Verlag; 2011 [cited 2020 Apr 20]. Available from: https://www.springer.com/gp/book/9788847018686

36. Fletcher CDM, Berman JJ, Corless C, Gorstein F, Lasota J, Longley BJ, et al. Diagnosis of gastrointestinal stromal tumors: A consensus approach. Hum Pathol. 2002 May;33(5):459–65.

37. Robinson TL, Sircar K, Hewlett BR, Chorneyko K, Riddell RH, Huizinga JD. Gastrointestinal stromal tumors may originate from a subset of CD34-positive interstitial cells of Cajal. American Journal of Pathology. 2000;

38. Miettinen M, Makhlouf H, Sobin LH, Lasota J. Gastrointestinal stromal tumors of the jejunum and ileum: A clinicopathologic, immunohistochemical, and molecular genetic study of 906 cases before imatinib with long-term follow-up. American Journal of Surgical Pathology. 2006;30(4):477–89.

39. Miettinen M, Wang ZF, Lasota J. DOG1 antibody in the differential diagnosis of gastrointestinal stromal tumors: a study of 1840 cases. Am J Surg Pathol. 2009 Sep;33(9):1401–8.

40. Liegl B, Hornick JL, Corless CL, Fletcher CDM. Monoclonal antibody DOG1.1 shows higher sensitivity than KIT in the diagnosis of gastrointestinal stromal tumors, including unusual subtypes. Am J Surg Pathol. 2009 Mar;33(3):437–46.

41. Kang GH, Srivastava A, Kim YE, Park HJ, Park CK, Sohn TS, et al. DOG1 and PKC-θ are useful in the diagnosis of KIT-negative gastrointestinal stromal tumors. Mod Pathol. 2011 Jun;24(6):866–75.

42. National Comprehensive Cancer Network. Soft Tissue Sarcoma (Version 2.2019). www.nccn.org/professionals/physician_gls/pdf/sarcoma.pdf.

43. Szucs Z, Thway K, Fisher C, Bulusu R, Constantinidou A, Benson C, et al. Molecular subtypes of gastrointestinal stromal tumors and their prognostic and therapeutic implications. Future Oncol. 2017 Jan;13(1):93–107.

44. Schaefer IM, DeMatteo RP, Serrano C. The GIST of Advances in Treatment of Advanced Gastrointestinal Stromal Tumor. Am Soc Clin Oncol Educ Book. 2022 Apr;42:1–15.

45. Zalcberg JR, Verweij J, Casali PG, Le Cesne A, Reichardt P, Blay JY, et al. Outcome of patients with advanced gastro-intestinal stromal tumours crossing over to a daily imatinib dose of 800 mg after progression on 400 mg. Eur J Cancer. 2005 Aug;41(12):1751–7.

46. Demetri GD, Benjamin RS, Blanke CD, Blay JY, Casali P, Choi H, et al. NCCN Task Force report: management of patients with gastrointestinal stromal tumor (GIST)--update of the NCCN clinical practice guidelines. J Natl Compr Canc Netw. 2007 Jul;5 Suppl 2:S1-29; quiz S30.

47. George S, Blay JY, Casali PG, Le Cesne A, Stephenson P, Deprimo SE, et al. Clinical evaluation of continuous daily dosing of sunitinib malate in patients with advanced gastrointestinal stromal tumour after imatinib failure. Eur J Cancer. 2009 Jul;45(11):1959–68.

48. Jones RL, Serrano C, von Mehren M, George S, Heinrich MC, Kang YK, et al. Avapritinib in unresectable or metastatic PDGFRA D842V-mutant gastrointestinal stromal tumours: Long-term efficacy and safety data from the NAVIGATOR phase I trial. Eur J Cancer. 2021 Mar;145:132–42.

49. Kindblom LG, Remotti HE, Aldenborg F, Meis-Kindblom JM. Gastrointestinal pacemaker cell tumor (GIPACT): gastrointestinal stromal tumors show phenotypic characteristics of the interstitial cells of Cajal. Am J Pathol. 1998 May;152(5):1259–69.

50. Maeda H, Yamagata A, Nishikawa S, Yoshinaga K, Kobayashi S, Nishi K, et al. Requirement of c-kit for development of intestinal pacemaker system. Development. 1992 Oct;116(2):369–75.

51. Torihashi S, Nishi K, Tokutomi Y, Nishi T, Ward S, Sanders KM. Blockade of kit signaling induces transdifferentiation of interstitial cells of cajal to a smooth muscle phenotype. Gastroenterology. 1999 Jul;117(1):140–8.

52. Lasota J, Miettinen M. Clinical significance of oncogenic KIT and PDGFRA mutations in gastrointestinal stromal tumours. Histopathology. 2008 Sep;53(3):245–66.

53. Lasota J, Corless CL, Heinrich MC, Debiec-Rychter M, Sciot R, Wardelmann E, et al. Clinicopathologic profile of gastrointestinal stromal tumors (GISTs) with primary KIT exon 13 or exon 17 mutations: a multicenter study on 54 cases. Mod Pathol. 2008 Apr;21(4):476–84.

54. Corless CL, Schroeder A, Griffith D, Town A, McGreevey L, Harrell P, et al. PDGFRA mutations in gastrointestinal stromal tumors: frequency, spectrum and in vitro sensitivity to imatinib. J Clin Oncol. 2005 Aug 10;23(23):5357–64.

55. Joensuu H, Hohenberger P, Corless CL. Gastrointestinal stromal tumour. The Lancet. 2013 Sep;382(9896):973–83.

56. Judson I, Demetri G. Advances in the treatment of gastrointestinal stromal tumours. Ann Oncol. 2007 Sep;18 Suppl 10:x20-24.

57. Heinrich MC, Corless CL, Demetri GD, Blanke CD, von Mehren M, Joensuu H, et al. Kinase mutations and imatinib response in patients with metastatic gastrointestinal stromal tumor. J Clin Oncol. 2003 Dec 1;21(23):4342–9.

58. Corless CL, Barnett CM, Heinrich MC. Gastrointestinal stromal tumours: origin and molecular oncology. Nat Rev Cancer. 2011 Dec;11(12):865–78.

59. Demetri GD, von Mehren M, Antonescu CR, DeMatteo RP, Ganjoo KN, Maki RG, et al. NCCN Task Force Report: Update on the Management of Patients with

Gastrointestinal Stromal Tumors. J Natl Compr Canc Netw. 2010 Apr;8(Suppl 2):S-1-S-41.

60. Rubin BP, Heinrich MC, Corless CL. Gastrointestinal stromal tumour. Lancet. 2007 May 19;369(9574):1731–41.

61. Antonescu CR, Besmer P, Guo T, Arkun K, Hom G, Koryotowski B, et al. Acquired resistance to imatinib in gastrointestinal stromal tumor occurs through secondary gene mutation. Clin Cancer Res. 2005 Jun 1;11(11):4182–90.

62. Chen LL, Trent JC, Wu EF, Fuller GN, Ramdas L, Zhang W, et al. A missense mutation in KIT kinase domain 1 correlates with imatinib resistance in gastrointestinal stromal tumors. Cancer Res. 2004 Sep 1;64(17):5913–9.

63. Wardelmann E, Thomas N, Merkelbach-Bruse S, Pauls K, Speidel N, Büttner R, et al. Acquired resistance to imatinib in gastrointestinal stromal tumours caused by multiple KIT mutations. Lancet Oncol. 2005 Apr;6(4):249–51.

64. Serrano C, George S, Valverde C, Olivares D, García-Valverde A, Suárez C, et al. Novel Insights into the Treatment of Imatinib-Resistant Gastrointestinal Stromal Tumors. Targ Oncol. 2017 Jun;12(3):277–88.

65. Liegl B, Kepten I, Le C, Zhu M, Demetri GD, Heinrich MC, et al. Heterogeneity of kinase inhibitor resistance mechanisms in GIST. J Pathol. 2008 Sep;216(1):64–74.

66. Napolitano A, Ostler AE, Jones RL, Huang PH. Fibroblast Growth Factor Receptor (FGFR) Signaling in GIST and Soft Tissue Sarcomas. Cells. 2021 Jun 17;10(6):1533.

67. Javidi-Sharifi N, Traer E, Martinez J, Gupta A, Taguchi T, Dunlap J, et al. Crosstalk between KIT and FGFR3 Promotes Gastrointestinal Stromal Tumor Cell Growth and Drug Resistance. Cancer Research. 2015 Mar 1;75(5):880–91.

68. Li F, Huynh H, Li X, Ruddy DA, Wang Y, Ong R, et al. FGFR-Mediated Reactivation of MAPK Signaling Attenuates Antitumor Effects of Imatinib in Gastrointestinal Stromal Tumors. Cancer Discovery. 2015 Apr 1;5(4):438–51.

69. Bauer S, Duensing A, Demetri GD, Fletcher JA. KIT oncogenic signaling mechanisms in imatinib-resistant gastrointestinal stromal tumor: PI3-kinase/AKT is a crucial survival pathway. Oncogene. 2007 Nov;26(54):7560–8.

70. Duensing A, Medeiros F, McConarty B, Joseph NE, Panigrahy D, Singer S, et al. Mechanisms of oncogenic KIT signal transduction in primary gastrointestinal stromal tumors (GISTs). Oncogene. 2004 May 13;23(22):3999–4006.

71. Zhu MJ, Ou WB, Fletcher CDM, Cohen PS, Demetri GD, Fletcher JA. KIT oncoprotein interactions in gastrointestinal stromal tumors: therapeutic relevance. Oncogene. 2007 Sep 27;26(44):6386–95.

72. Brems H, Beert E, Ravel TD, Legius E. Mechanisms in the pathogenesis of malignant tumours in neurofi bromatosis type 1. Lancet Oncology. 2009;10(5):508–15.

73. Serrano C, Wang Y, Mariño-Enríquez A, Lee JC, Ravegnini G, Morgan JA, et al. KRAS and KIT Gatekeeper Mutations Confer Polyclonal Primary Imatinib Resistance in GI Stromal Tumors: Relevance of Concomitant Phosphatidylinositol 3-Kinase/AKT Dysregulation. J Clin Oncol. 2015 Aug 1;33(22):e93–6.

74. Agaram NP, Wong GC, Guo T, Maki RG, Singer S, Dematteo RP, et al. Novel V600E BRAF mutations in imatinib-naive and imatinib-resistant gastrointestinal stromal tumors. Genes Chromosomes Cancer. 2008 Oct;47(10):853–9.

75. He Y, Sun MM, Zhang GG, Yang J, Chen KS, Xu WW, et al. Targeting PI3K/Akt signal transduction for cancer therapy. Sig Transduct Target Ther. 2021 Dec 16;6(1):1–17.

76. LoRusso PM. Inhibition of the PI3K/AKT/mTOR Pathway in Solid Tumors. J Clin Oncol. 2016 Nov 1;34(31):3803–15.

77. Peng Y, Wang Y, Zhou C, Mei W, Zeng C. PI3K/Akt/mTOR Pathway and Its Role in Cancer Therapeutics: Are We Making Headway? Frontiers in Oncology [Internet]. 2022 [cited 2023 Jan 29];12. Available from: https://www.frontiersin.org/articles/10.3389/fonc.2022.819128

78. Van Looy T, Wozniak A, Floris G, Sciot R, Li H, Wellens J, et al. Phosphoinositide 3-Kinase Inhibitors Combined with Imatinib in Patient-Derived Xenograft Models of Gastrointestinal Stromal Tumors: Rationale and Efficacy. Clinical Cancer Research. 2014 Dec 1;20(23):6071–82.

79. García-Valverde A, Rosell J, Serna G, Valverde C, Carles J, Nuciforo P, et al. Preclinical Activity of PI3K Inhibitor Copanlisib in Gastrointestinal Stromal Tumor. Mol Cancer Ther. 2020 Jun;19(6):1289–97.

80. Narayan P, Prowell TM, Gao JJ, Fernandes LL, Li E, Jiang X, et al. FDA Approval Summary: Alpelisib Plus Fulvestrant for Patients with HR-positive, HER2-negative, PIK3CA-mutated, Advanced or Metastatic Breast Cancer. Clinical Cancer Research. 2021 Apr 1;27(7):1842–9.

81. Yang Q, Modi P, Newcomb T, Quéva C, Gandhi V. Idelalisib: First-in-Class PI3K Delta Inhibitor for the Treatment of Chronic Lymphocytic Leukemia, Small Lymphocytic Leukemia, and Follicular Lymphoma. Clinical Cancer Research. 2015 Mar 31;21(7):1537–42.

82. Bird ST, Tian F, Flowers N, Przepiorka D, Wang R, Jung TH, et al. Idelalisib for Treatment of Relapsed Follicular Lymphoma and Chronic Lymphocytic Leukemia: A Comparison of Treatment Outcomes in Clinical Trial Participants vs Medicare Beneficiaries. JAMA Oncology. 2020 Feb 1;6(2):248–54.

83. Dreyling M, Santoro A, Mollica L, Leppä S, Follows GA, Lenz G, et al. Phosphatidylinositol 3-Kinase Inhibition by Copanlisib in Relapsed or Refractory Indolent Lymphoma. Journal of Clinical Oncology. 2017 Diciembre;35(35):3898–905.

84. Magagnoli M, Carlo-Stella C, Santoro A. Copanlisib for the treatment of adults with relapsed follicular lymphoma. Expert Rev Clin Pharmacol. 2020 Aug;13(8):813–23.

85. Flinn IW, O'Brien S, Kahl B, Patel M, Oki Y, Foss FF, et al. Duvelisib, a novel oral dual inhibitor of PI3K-δ,γ, is clinically active in advanced hematologic malignancies. Blood. 2018 Feb 22;131(8):877–87.

86. Frustaci AM, Tedeschi A, Deodato M, Zamprogna G, Cairoli R, Montillo M. Duvelisib for the treatment of chronic lymphocytic leukemia. Expert Opin Pharmacother. 2020 Aug;21(11):1299–309.

87. Bosbach B, Rossi F, Yozgat Y, Loo J, Zhang JQ, Berrozpe G, et al. Direct engagement of the PI3K pathway by mutant KIT dominates oncogenic signaling in gastrointestinal stromal tumor. Proc Natl Acad Sci USA. 2017 Oct 3;114(40):E8448–57.

88. Dolly SO, Wagner AJ, Bendell JC, Kindler HL, Krug LM, Seiwert TY, et al. Phase I Study of Apitolisib (GDC-0980), Dual Phosphatidylinositol-3-Kinase and Mammalian Target of Rapamycin Kinase Inhibitor, in Patients with Advanced Solid Tumors. Clinical Cancer Research. 2016 Jun 15;22(12):2874–84.

89. Schöffski P, Reichardt P, Blay JY, Dumez H, Morgan JA, Ray-Coquard I, et al. A phase I-II study of everolimus (RAD001) in combination with imatinib in patients with imatinib-resistant gastrointestinal stromal tumors. Ann Oncol. 2010 Oct;21(10):1990–8.

90. Gelderblom H, Jones RL, George S, Valverde Morales C, Benson C, Jean-Yves Blay null, et al. Imatinib in combination with phosphoinositol kinase inhibitor buparlisib in patients with gastrointestinal stromal tumour who failed prior therapy with imatinib and sunitinib: a Phase 1b, multicentre study. Br J Cancer. 2020 Apr;122(8):1158–65.

91. Chakrabarty A, Sánchez V, Kuba MG, Rinehart C, Arteaga CL. Feedback upregulation of HER3 (ErbB3) expression and activity attenuates antitumor effect of PI3K inhibitors. Proc Natl Acad Sci U S A. 2012 Feb 21;109(8):2718–23.

92. Serra V, Scaltriti M, Prudkin L, Eichhorn PJA, Ibrahim YH, Chandarlapaty S, et al. PI3K inhibition results in enhanced HER signaling and acquired ERK dependency in HER2-overexpressing breast cancer. Oncogene. 2011 Jun 2;30(22):2547–57.

93. Muranen T, Selfors LM, Worster DT, Iwanicki MP, Song L, Morales FC, et al. Inhibition of PI3K/mTOR Leads to Adaptive Resistance in Matrix-Attached Cancer Cells. Cancer Cell. 2012 Feb 14;21(2):227–39.

94. Britschgi A, Andraos R, Brinkhaus H, Klebba I, Romanet V, Müller U, et al. JAK2/STAT5 inhibition circumvents resistance to PI3K/mTOR blockade: a rationale for cotargeting these pathways in metastatic breast cancer. Cancer Cell. 2012 Dec 11;22(6):796–811.

95. Alves R, Gonçalves AC, Rutella S, Almeida AM, De Las Rivas J, Trougakos IP, et al. Resistance to Tyrosine Kinase Inhibitors in Chronic Myeloid Leukemia—From Molecular Mechanisms to Clinical Relevance. Cancers (Basel). 2021 Sep 26;13(19):4820.

96. Yaghmaie M, Yeung CC. Molecular Mechanisms of Resistance to Tyrosine Kinase Inhibitors. Curr Hematol Malig Rep. 2019 Oct 1;14(5):395–404.

97. Thomas SJ, Snowden JA, Zeidler MP, Danson SJ. The role of JAK/STAT signalling in the pathogenesis, prognosis and treatment of solid tumours. Br J Cancer. 2015 Jul 28;113(3):365–71.

98. Pencik J, Pham HTT, Schmoellerl J, Javaheri T, Schlederer M, Culig Z, et al. JAK-STAT signaling in cancer: From cytokines to non-coding genome. Cytokine. 2016 Nov;87:26–36.

99. Bar-Natan M, Nelson EA, Xiang M, Frank DA. STAT signaling in the pathogenesis and treatment of myeloid malignancies. JAKSTAT. 2012 Apr 1;1(2):55–64.

100. Kumar H, Tichkule S, Raj U, Gupta S, Srivastava S, Varadwaj PK. Effect of STAT3 inhibitor in chronic myeloid leukemia associated signaling pathway: a mathematical modeling, simulation and systems biology study. 3 Biotech [Internet]. 2016 Jun [cited 2019 Jul 6];6(1). Available from: https://www.ncbi.nlm.nih.gov/pmc/articles/PMC4729759/

101. Valent P. Targeting the JAK2-STAT5 pathway in CML. Blood. 2014 Aug 28;124(9):1386–8.

102. Velazquez L, Fellous M, Stark GR, Pellegrini S. A protein tyrosine kinase in the interferon alpha/beta signaling pathway. Cell. 1992 Jul 24;70(2):313–22.

103. Wilks AF, Harpur AG, Kurban RR, Ralph SJ, Zürcher G, Ziemiecki A. Two novel protein-tyrosine kinases, each with a second phosphotransferase-related catalytic domain, define a new class of protein kinase. Mol Cell Biol. 1991 Apr;11(4):2057–65.

104. Thomas SJ, Snowden JA, Zeidler MP, Danson SJ. The role of JAK/STAT signalling in the pathogenesis, prognosis and treatment of solid tumours. Br J Cancer. 2015 Jul 28;113(3):365–71.

105. Hu X, Li J, Fu M, Zhao X, Wang W. The JAK/STAT signaling pathway: from bench to clinic. Sig Transduct Target Ther. 2021 Nov 26;6(1):1–33.

106. Levy DE, Darnell JE. Stats: transcriptional control and biological impact. Nat Rev Mol Cell Biol. 2002 Sep;3(9):651–62.

107. Morris R, Kershaw NJ, Babon JJ. The molecular details of cytokine signaling via the JAK/STAT pathway. Protein Sci. 2018 Dec;27(12):1984–2009.

108. Yoshimura A, Nishinakamura H, Matsumura Y, Hanada T. Negative regulation of cytokine signaling and immune responses by SOCS proteins. Arthritis Res Ther. 2005 Mar;7(3):1–11.

109. Jn I. Janus kinases in cytokine signalling. Philosophical transactions of the Royal Society of London Series B, Biological sciences [Internet]. 1996 Feb 29 [cited 2023 Jan 31];351(1336). Available from: https://pubmed.ncbi.nlm.nih.gov/8650262/

110. Starr R, Hilton DJ. Negative regulation of the JAK/STAT pathway. Bioessays. 1999 Jan;21(1):47–52.

111. Shuai K, Liu B. Regulation of JAK-STAT signalling in the immune system. Nat Rev Immunol. 2003 Nov;3(11):900–11.

112. Cieślik M, Chinnaiyan AM. Cancer transcriptome profiling at the juncture of clinical translation. Nat Rev Genet. 2018 Feb;19(2):93–109.

113. Cui M, Cheng C, Zhang L. High-throughput proteomics: a methodological mini-review. Lab Invest. 2022 Nov;102(11):1170–81.

114. Wu C, Zheng L. Proteomics promises a new era of precision cancer medicine. Sig Transduct Target Ther. 2019 May 3;4(1):1–2.

115. Legrain P, Aebersold R, Archakov A, Bairoch A, Bala K, Beretta L, et al. The Human Proteome Project: Current State and Future Direction. Molecular & Cellular Proteomics [Internet]. 2011 Jul 1 [cited 2023 Jan 31];10(7). Available from: https://www.mcponline.org/article/S1535-9476(20)30201-2/abstract

116. Karczewski KJ, Snyder MP. Integrative omics for health and disease. Nat Rev Genet. 2018 May;19(5):299–310.

117. Zhu B, Song N, Shen R, Arora A, Machiela MJ, Song L, et al. Integrating Clinical and Multiple Omics Data for Prognostic Assessment across Human Cancers. Sci Rep. 2017 Dec 5;7(1):16954.

118. García-Valverde A, Rosell J, Sayols S, Gómez-Peregrina D, Pilco-Janeta DF, Olivares-Rivas I, et al. E3 ubiquitin ligase Atrogin-1 mediates adaptive resistance to KIT-targeted inhibition in gastrointestinal stromal tumor. Oncogene. 2021 Dec;40(48):6614–26.

119. Taguchi T, Sonobe H, Toyonaga S ichi, Yamasaki I, Shuin T, Takano A, et al. Conventional and molecular cytogenetic characterization of a new human cell line, GIST-T1, established from gastrointestinal stromal tumor. Lab Invest. 2002 May;82(5):663–5.

120. Bauer S, Yu LK, Demetri GD, Fletcher JA. Heat shock protein 90 inhibition in imatinib-resistant gastrointestinal stromal tumor. Cancer Res. 2006 Sep 15;66(18):9153–61.

121. Garner AP, Gozgit JM, Anjum R, Vodala S, Schrock A, Zhou T, et al. Ponatinib Inhibits Polyclonal Drug-Resistant KIT Oncoproteins and Shows Therapeutic Potential in Heavily Pretreated Gastrointestinal Stromal Tumor (GIST) Patients. Clinical Cancer Research. 2014 Nov 15;20(22):5745–55.

122. Serrano C, Mariño-Enríquez A, Tao DL, Ketzer J, Eilers G, Zhu M, et al. Complementary activity of tyrosine kinase inhibitors against secondary kit mutations in imatinib-resistant gastrointestinal stromal tumours. Br J Cancer. 2019;120(6):612–20.

123. Thingholm TE, Jørgensen TJD, Jensen ON, Larsen MR. Highly selective enrichment of phosphorylated peptides using titanium dioxide. Nat Protoc. 2006;1(4):1929–35.

124. Subramanian A, Tamayo P, Mootha VK, Mukherjee S, Ebert BL, Gillette MA, et al. Gene set enrichment analysis: A knowledge-based approach for interpreting genome-wide expression profiles. Proc Natl Acad Sci U S A. 2005 Oct 25;102(43):15545–50.

125. Hidalgo MR, Cubuk C, Amadoz A, Salavert F, Carbonell-Caballero J, Dopazo J. High throughput estimation of functional cell activities reveals disease mechanisms and predicts relevant clinical outcomes. Oncotarget. 2016 Dec 22;8(3):5160–78.

126. Wang J, Vasaikar S, Shi Z, Greer M, Zhang B. WebGestalt 2017: a more comprehensive, powerful, flexible and interactive gene set enrichment analysis toolkit. Nucleic Acids Research. 2017 Jul 3;45(W1):W130–7.

127. Floris G, Wozniak A, Sciot R, Li H, Friedman L, Van Looy T, et al. A Potent Combination of the Novel PI3K Inhibitor, GDC-0941, with Imatinib in Gastrointestinal Stromal Tumor Xenografts: Long-Lasting Responses after Treatment Withdrawal. Clinical Cancer Research. 2013 Feb 1;19(3):620–30.

128. Barré B, Vigneron A, Perkins N, Roninson IB, Gamelin E, Coqueret O. The STAT3 oncogene as a predictive marker of drug resistance. Trends Mol Med. 2007 Jan;13(1):4–11.

129. Gariboldi MB, Ravizza R, Molteni R, Osella D, Gabano E, Monti E. Inhibition of Stat3 increases doxorubicin sensitivity in a human metastatic breast cancer cell line. Cancer Letters. 2007 Dec 18;258(2):181–8.

130. Gritsko T, Williams A, Turkson J, Kaneko S, Bowman T, Huang M, et al. Persistent activation of stat3 signaling induces survivin gene expression and confers resistance to apoptosis in human breast cancer cells. Clin Cancer Res. 2006 Jan 1;12(1):11–9.

131. Fantin VR, Loboda A, Paweletz CP, Hendrickson RC, Pierce JW, Roth JA, et al. Constitutive Activation of Signal Transducers and Activators of Transcription Predicts Vorinostat Resistance in Cutaneous T-Cell Lymphoma. Cancer Research. 2008 May 15;68(10):3785–94.

132. Ning ZQ, Li J, McGuinness M, Arceci RJ. STAT3 activation is required for Asp(816) mutant c-Kit induced tumorigenicity. Oncogene. 2001 Jul 27;20(33):4528–36.

133. Corbacioglu S, Kilic M, Westhoff MA, Reinhardt D, Fulda S, Debatin KM. Newly identified c-KIT receptor tyrosine kinase ITD in childhood AML induces ligand-independent growth and is responsive to a synergistic effect of imatinib and rapamycin. Blood. 2006 Nov 15;108(10):3504–13.

134. Chaix A, Lopez S, Voisset E, Gros L, Dubreuil P, De Sepulveda P. Mechanisms of STAT Protein Activation by Oncogenic KIT Mutants in Neoplastic Mast Cells. J Biol Chem. 2011 Feb 25;286(8):5956–66.

135. Liu M, Etherington MS, Hanna A, Medina BD, Vitiello GA, Bowler TG, et al. Oncogenic KIT Modulates Type I IFN–Mediated Antitumor Immunity in GIST. Cancer Immunology Research. 2021 May 1;9(5):542–53.

136. Sanda T, Tyner JW, Gutierrez A, Ngo VN, Glover J, Chang BH, et al. TYK2-STAT1-BCL2 Pathway Dependence in T-Cell Acute Lymphoblastic Leukemia. Cancer Discov. 2013 May;3(5):564–77.

137. Camicia R, Bachmann SB, Winkler HC, Beer M, Tinguely M, Haralambieva E, et al. BAL1/ARTD9 represses the anti-proliferative and pro-apoptotic IFNγ-STAT1-IRF1-p53 axis in diffuse large B-cell lymphoma. J Cell Sci. 2013 May 1;126(Pt 9):1969–80.

138. Khodarev NN, Beckett M, Labay E, Darga T, Roizman B, Weichselbaum RR. STAT1 is overexpressed in tumors selected for radioresistance and confers protection from radiation in transduced sensitive cells. Proc Natl Acad Sci U S A. 2004 Feb 10;101(6):1714–9.

139. Horiguchi A, Oya M, Shimada T, Uchida A, Marumo K, Murai M. Activation of Signal Transducer and Activator of Transcription 3 in Renal Cell Carcinoma: A Study of Incidence and Its Association With Pathological Features and Clinical Outcome. Journal of Urology. 2002 Aug;168(2):762–5.

140. Pan Y, Wang S, Su B, Zhou F, Zhang R, Xu T, et al. Stat3 contributes to cancer progression by regulating Jab1/Csn5 expression. Oncogene. 2017 Feb 23;36(8):1069–79.

141. Bromberg JF, Wrzeszczynska MH, Devgan G, Zhao Y, Pestell RG, Albanese C, et al. Stat3 as an Oncogene. Cell. 1999 Aug 6;98(3):295–303.

142. Taniguchi K, Tsugane M, Asai A. A Brief Update on STAT3 Signaling: Current Challenges and Future Directions in Cancer Treatment. Journal of Cellular Signaling. 2021 Sep 6;2(3):181–94.

143. Ferluga S, Baiz D, Hilton DA, Adams CL, Ercolano E, Dunn J, et al. Constitutive activation of the EGFR–STAT1 axis increases proliferation of meningioma tumor cells. Neurooncol Adv. 2020 Jan 21;2(1):vdaa008.

144. Hart KC, Robertson SC, Kanemitsu MY, Meyer AN, Tynan JA, Donoghue DJ. Transformation and Stat activation by derivatives of FGFR1, FGFR3, and FGFR4. Oncogene. 2000 Jul 6;19(29):3309–20.

145. Chung SS, Giehl N, Wu Y, Vadgama JV. STAT3 activation in HER2-overexpressing breast cancer promotes epithelial-mesenchymal transition and cancer stem cell traits. Int J Oncol. 2014 Feb;44(2):403–11.

146. Andl CD, Mizushima T, Oyama K, Bowser M, Nakagawa H, Rustgi AK. EGFR-induced cell migration is mediated predominantly by the JAK-STAT pathway in

primary esophageal keratinocytes. American Journal of Physiology-Gastrointestinal and Liver Physiology. 2004 Dec;287(6):G1227–37.

147. Quesnelle KM, Boehm AL, Grandis JR. STAT-mediated EGFR signaling in cancer. Journal of Cellular Biochemistry. 2007;102(2):311–9.

148. Edsbäcker E, Serviss JT, Kolosenko I, Palm-Apergi C, De Milito A, Tamm KP. STAT3 is activated in multicellular spheroids of colon carcinoma cells and mediates expression of IRF9 and interferon stimulated genes. Sci Rep. 2019 Jan 24;9:536.

149. Platanias LC. Mechanisms of type-I- and type-II-interferon-mediated signalling. Nat Rev Immunol. 2005 May;5(5):375–86.

150. Vo JN, Wu YM, Mishler J, Hall S, Mannan R, Wang L, et al. The genetic heterogeneity and drug resistance mechanisms of relapsed refractory multiple myeloma. Nat Commun. 2022 Jun 29;13(1):3750.

151. Levatić J, Salvadores M, Fuster-Tormo F, Supek F. Mutational signatures are markers of drug sensitivity of cancer cells. Nat Commun. 2022 May 25;13(1):2926.

152. Chan JM, Zaidi S, Love JR, Zhao JL, Setty M, Wadosky KM, et al. Lineage plasticity in prostate cancer depends on JAK/STAT inflammatory signaling. Science. 2022 Sep 9;377(6611):1180–91.

153. Matalkah F, Martin E, Zhao H, Agazie YM. SHP2 acts both upstream and downstream of multiple receptor tyrosine kinases to promote basal-like and triple-negative breast cancer. Breast Cancer Research. 2016 Jan 4;18(1):2.

154. Brewer JR, Molotkov A, Mazot P, Hoch RV, Soriano P. Fgfr1 regulates development through the combinatorial use of signaling proteins. Genes Dev. 2015 Sep 1;29(17):1863–74.

155. Sánchez-Guixé M, Hierro C, Jiménez J, Viaplana C, Villacampa G, Monelli E, et al. High FGFR1–4 mRNA Expression Levels Correlate with Response to Selective FGFR Inhibitors in Breast Cancer. Clinical Cancer Research. 2022 Jan 5;28(1):137–49.

156. Cihoric N, Savic S, Schneider S, Ackermann I, Bichsel-Naef M, Schmid RA, et al. Prognostic role of FGFR1 amplification in early-stage non-small cell lung cancer. Br J Cancer. 2014 Jun;110(12):2914–22.

157. Drago JZ, Formisano L, Juric D, Niemierko A, Servetto A, Wander SA, et al. FGFR1 Amplification Mediates Endocrine Resistance but Retains TORC Sensitivity in Metastatic Hormone Receptor-Positive (HR+) Breast Cancer. Clin Cancer Res. 2019 Nov 1;25(21):6443–51.

158. Formisano L, Stauffer KM, Young CD, Bhola NE, Guerrero-Zotano AL, Jansen VM, et al. Association of FGFR1 with ERα Maintains Ligand-Independent ER Transcription and Mediates Resistance to Estrogen Deprivation in ER+ Breast Cancer. Clin Cancer Res. 2017 Oct 15;23(20):6138–50.

159. Tomlinson DC, Lamont FR, Shnyder SD, Knowles MA. Fibroblast growth factor receptor 1 promotes proliferation and survival via activation of the mitogen-activated protein kinase pathway in bladder cancer. Cancer Res. 2009 Jun 1;69(11):4613–20.

160. Grünewald S, Politz O, Bender S, Héroult M, Lustig K, Thuss U, et al. Rogaratinib: A potent and selective pan-FGFR inhibitor with broad antitumor activity in FGFR-overexpressing preclinical cancer models. Int J Cancer. 2019 Sep 1;145(5):1346–57.

161. Aggarwal C, Redman MW, Lara PN, Borghaei H, Hoffman P, Bradley JD, et al. SWOG S1400D (NCT02965378), a Phase II Study of the Fibroblast Growth Factor Receptor Inhibitor AZD4547 in Previously Treated Patients With Fibroblast Growth Factor Pathway–Activated Stage IV Squamous Cell Lung Cancer (Lung-MAP Substudy). Journal of Thoracic Oncology. 2019 Oct 1;14(10):1847–52.

162. Hall TG, Yu Y, Eathiraj S, Wang Y, Savage RE, Lapierre JM, et al. Preclinical Activity of ARQ 087, a Novel Inhibitor Targeting FGFR Dysregulation. PLoS One. 2016;11(9):e0162594.

163. Papadopoulos KP, El-Rayes BF, Tolcher AW, Patnaik A, Rasco DW, Harvey RD, et al. A Phase 1 study of ARQ 087, an oral pan-FGFR inhibitor in patients with advanced solid tumours. Br J Cancer. 2017 Nov 21;117(11):1592–9.

164. Krook MA, Lenyo A, Wilberding M, Barker H, Dantuono M, Bailey KM, et al. Efficacy of FGFR Inhibitors and Combination Therapies for Acquired Resistance in FGFR2-Fusion Cholangiocarcinoma. Mol Cancer Ther. 2020 Mar;19(3):847–57.

165. Cowell JK, Qin H, Hu T, Wu Q, Bhole A, Ren M. Mutation in the FGFR1 tyrosine kinase domain or inactivation of PTEN is associated with acquired resistance to FGFR inhibitors in FGFR1-driven leukemia/lymphomas. Int J Cancer. 2017 Nov 1;141(9):1822–9.

Universitat Autònoma de Barcelona

VHIO VALL D'HEBRON Instituto de Oncología

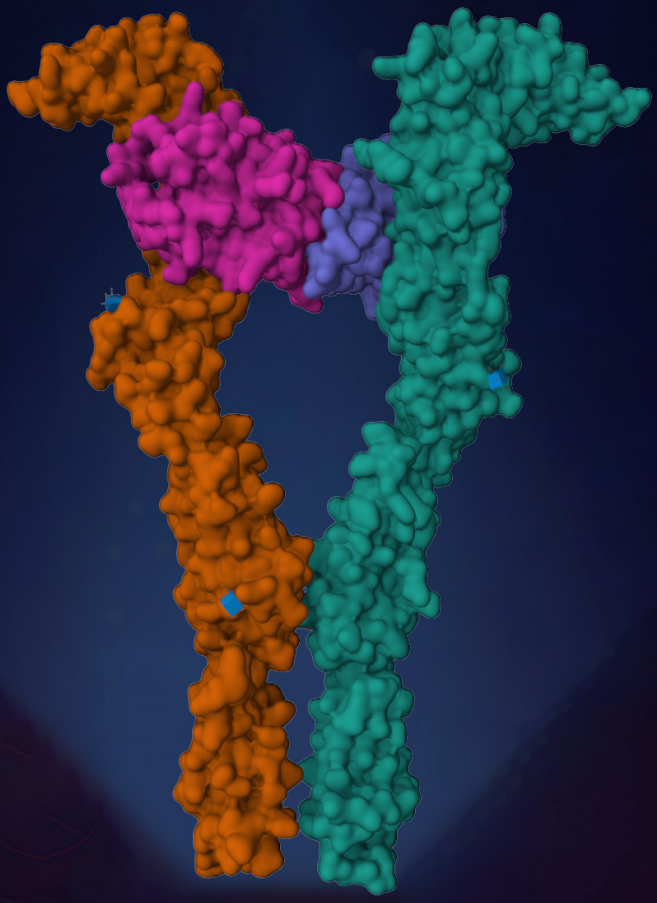

Doctoral program in Medicine

2023